

DEVELOPMENT OF A NEW MANUFACTURING METHOD OF ELECTRODES
FOR SOLID OXIDE FUEL CELLS

BY WILLIAM WAUGH

A Thesis submitted in partial fulfilment of the requirements of Edinburgh Napier
University for the Degree of Philosophy.

November 2009

DECLARATION

I hereby declare that the work presented in this thesis was solely carried out by myself at Edinburgh Napier University, Edinburgh, except where acknowledgements are made, and that it has not been submitted for any other degree.

William Waugh (candidate)

1st August 2009

Acknowledgements

The author wishes to acknowledge the support and understanding of Aerospace Machining Technology Ltd who have continually provided encouragement throughout my career and my desire to advance both within the company and academically.

I wish to acknowledge Mr Alan Davidson in his role as my academic supervisor and also as a colleague during the Proof of Concept application and project work. Additional thanks go to the members of the Edinburgh Napier Business Management Team, including Dr Brendan McGuckin, Dr Neil Bowering and Dr Ian McEwan.

My thanks also to Mr William Brownlee and Dimitrius Tsiligiannis, who provided technical support and expertise during the experimentation and characterisation work.

Additionally I would like to thank in particular Mrs Nor Bahiyah Baba and also research students at Edinburgh Napier for their assistance and support.

My thanks also to Dr Gordon Lindsay and Dr Callum Wilson for their invaluable assistance and experience in planar SOFC designs. Thanks also to Mr Gordon Bennett of Unitec Ceramics and Mr Brian Reid of Schloetter Company Ltd who provided samples of the YSZ and plating chemistry respectively.

Part of the project has received financial assistance from the Proof of Concept Programme managed by Scottish Enterprise and from the European Regional Development Fund. The Proof of Concept Programme supports the pre-commercialisation of leading-edge technologies emerging from Scotland's Universities, Research Institutes and NHS Trusts.

Finally thanks to my wife, Lisa, and children, Kathryn, Jonathan and Jamie, who supported me through the years whilst I was carrying out this work and helped spur me on to complete the thesis.

ABSTRACT.

It is well established that anodes for solid oxide fuel cells (SOFCs) can be manufactured by processes involving final sintering. This research investigated a novel alternative method which relies on the electroless co-deposition of yttria-stabilised zirconia (YSZ) or ceria-stabilised zirconia (CeSZ) and nickel onto a YSZ substrate. This process allows complex or simple shaped substrates to be coated, thereby replacing the high temperature sintering and reduction stages with a single plating operation, which is substantially more cost effective and greatly simplifies the manufacture of any cell design. The technique also eliminates the production of larger nickel grains (which occurs during sintering), thus improving cell performance.

Through a series of multifactoral experiments, a successful method was established and optimised for the deposition of the metal-ceramic composite which was successfully used in Solid Oxide Fuel Cell stack. The typical process involves degreasing and chemical pre-treatment of the substrates, followed by electroless co-deposition of the cermet coating, using either proprietary based chemicals or standard analytical reagents which have been specially formulated.

Through the metallurgical examination of the experimental samples it has been shown that the ratio of the metal to ceramic can be varied, thus catering to a potentially large customer base, and that a composition gradient can be achieved through the coating. Additional parameters such as porosity and electrical conductivity have also been evaluated and the results have been so encouraging that there has been significant commercial interest in the process.

Further work is continuing as part of a Proof of Concept (POC) project, with funding generously provided by Scottish Enterprise. Intellectual Property has been secured initially through funding supplied by Edinburgh Napier University, then subsequently through the POC project, with the aim that on completion of the project a spin-out company from Edinburgh Napier University is established.

CONTENTS

	<u>Page</u>	
Declaration	2	
Acknowledgements	3	
Abstract	4	
<u>Chapter</u>	<u>Title</u>	<u>Page</u>
1.	Introduction	12
	1.1 Background	12
	1.2 Solid Oxide Fuel Cell Technology	14
	1.2.1 Cathodes	20
	1.2.2 Electrolytes	20
	1.2.3 Anodes	21
	1.2.4 Interconnect	21
	1.3 Current Manufacturing Techniques	22
	1.3.1 Silk Screening	22
	1.3.2 Tape Casting	24
	1.3.3 Tape Calendaring	25
	1.3.4 Slurry Spraying	26
	1.3.5 Thermal Spraying	26
	1.3.6 Chemical Vapour Deposition	27
	1.3.7 Physical Vapour Deposition	27
	1.4 Impact of Cell Design on SOFC Costs	28
	1.5 Applications	31
2.	Current Research Review	37
3.	Electroless Plating	40
	3.1 Electroless Nickel	42
	3.2 Alloy Deposition	45
	3.3 Composite Deposition	46
	3.4 Deposition Rate, Coating Thickness and Deposit Morphology	48
	3.4.1 Agitation Effects	50

	3.4.2	Bath Loading with Particles	51
	3.4.3	Substrate Orientation	53
	3.5	Properties of Electroless Nickel	54
	3.5.1	Physical Properties	54
4		Project Aims	56
5		Experimental	57
	5.1	Characterisation Techniques	57
	5.1.1	Composition	57
	5.1.1.1	ICP-AES	58
	5.1.2	Surface Topography	59
	5.1.3	Electrical Resistivity	60
	5.1.4	X-Ray Fluorescence	64
	5.1.5	Porosity	64
	5.1.5.1	Mercury Porosimetry	65
	5.1.6	Surface Mapping	67
	5.1.7	Microscopy	67
	5.1.8	Dilatometry	67
	5.1.9	UV-Vis Spectrophotometry	69
	5.1.10	Scanning Electron Microscopy	70
	5.2	Fuel Cell Testing	71
	5.2.1	Wetting and Drying Gases	72
	5.2.2	Standard Hydrogen Mixture	72
	5.2.3	Standard Cathode Gas Compositions	72
	5.2.4	Standard Mixtures for Conductivity Measurements	73
	5.2.5	Temperature and Duration	73
	5.2.6	Conductivity Measurements	73
	5.2.7	Cell Testing	74
	5.2.7.1	Half Cell Measurements	75
	5.2.7.2	Divided and Undivided Cells	75
	5.2.7.3	Symmetric and Asymmetric Cells	75
	5.2.7.4	Thermal Cycling	75
	5.2.7.5	Ageing	76
	5.2.8	Electrochemical Impedance Spectroscopy	76

5.2.8.1	Cathode Testing By EIS	80
5.2.8.2	Anode Testing By EIS	81
5.3	Experimental Materials	82
5.4	Initial Pre-Treatment and Plating	83
5.5	Surface Roughness Experiments	87
5.6	Bath Loading Experiments	92
5.7	Spectrophotometer Experiments	105
5.8	Experiments with Polystyrene	107
5.9	Flocculant Experiments	111
5.10	Electrical Experiments	113
5.11	Cathode Manufacturing Experiments	116
6	Discussion	118
7	Conclusions	123
8	Commercial Implications	125
9	Future Work	127
	APPENDIX A	132
	APPENDIX B	141
	APPENDIX C	154
	APPENDIX D	181

Tables

1	Commonly Used Commercial SOFC Materials	19
2a	Manufacturing Costs	29
2b	Cell Material and Fabrication Costs	29
2c	Raw Material Costs	30
3	Metal Deposits Which Can Be Produced Electrolessly	41
4	Ceramic Particles and Their Properties	52
5	Details on Substrates Used in Experiments	82
6	Process Procedure for Pre-Treatment of YSZ Samples	83
7	Results of Etching Experiments	88
8	Surface roughness results for sample prepared by abrasive blasting and chemical etching.	91
9	YSZ Bath Loading Sample Data	93

10	Spectrophotometer samples	105
11	Polystyrene Additions in Electroless Nickel Plating Solutions	108
12	EDXA Compositional Analysis of Floquat Samples	111
13	Initial Electrical Property Results at 20°C	113

Figures

1	Planar SOFC design.	15
2	Tubular SOFC design.	15
3	Illustration of Reactions in a Fuel Cell	16
4a	Screen Printing Press	22
4b	Screen Printing Principle	22
5	Tape casting schematic and the drying and sintering effects on slip material.	24
6	Tape Casting Set-up	25
7	Tape Calendaring Fabrication Process	25
8a	Principle of Thermal Spraying	26
8b	Example of Anode Manufacture	27
9	Schematic of physical vapour deposition process.	28
10	Stack Cost Breakdown for \$110 / kW System	30
11a	Main Players in the SOFC Supply Chain	33
11b	SOFC Supply Chain, Additional Players	34
12a	An Application Map Versus Power Range Shows Some Trends for Different Fuel Cell Types	35
12b	A Map of Power Range vs Estimated Time to Competitive Products	36
13	Schematic Layout of a Typical ICP Instrument	59
14	Example of a Roughness Profile	60
15	Schematic of Four Point Probe Set-Up	61
16	Effect on an Atom When Bombarded by X-Ray Radiation	64
17	An Overview of Dilatometry	68
18	Energy Level States	70
19	Diagram of Basic Layout of a SEM	71

20	Impedance Analyser Set-Up	77
21	Equivalence Circuit for Ionic Conductivity of SOFC's	78
22	Model for Interpretation of EIS Results	79
23	Example of Multi-Step Oxygen Reduction at the Cathode	81
24	SEM Image of Uncoated YSZ Powder	84
25	Nickel Coated YSZ Substrate	85
26	EDX Spectra for Typical Electroless Nickel Coating	86
27	SEM Image of Ni/YSZ Coating on Napier YSZ Substrate	86
28	EDX Spectra for Ni/YSZ Coating on Napier YSZ Substrate	87
29	SEM Image of Ni/YSZ Coating on Etched YSZ Substrate	89
30	EDX Spectra for Ni/YSZ Coating on Etched YSZ Substrate	90
31a	Abrasive blasted sample	91
31b	Chemically etched sample	91
32a	Sample 1 SEM Image	94
32b	Sample 2 SEM Image	94
32c	Sample 3 SEM Image	94
32d	Sample 4 SEM Image	94
32e	Example of Area Where Typical Compositional Data Taken	94
33	Typical Composition of Deposits Produced from 1g/l YSZ Solution	95
34	Typical EDX Analysis of Deposits Produced from 1g/l YSZ Solution	95
35a	Sample 5 SEM Image	96
35b	Sample 6 SEM Image	96
35c	Sample 7 SEM Image	96
35d	Sample 8 SEM Image	96
35e	Example of Area Where Typical Compositional Data Obtained for 2g/l Solution	96
36	Typical Composition of Deposits Produced from 2g/l YSZ Solution	97
37	Typical EDX Analysis of Deposits Produced from 2g/l YSZ Solution	97
38a	Sample 9 SEM Image	98

38b	Sample 10 SEM Image	98
38c	Sample 11 SEM Image	98
38d	Sample 12 SEM Image	98
38e	Example of Area Where Typical Compositional Data Obtained for 5g/l Solution	98
39	Typical Composition of Deposits Produced from 5g/l YSZ Solution	99
40	Typical EDX Analysis of Deposits Produced from 5g/l YSZ Solution	99
41a	Sample 13 SEM Image	100
41b	Sample 14 SEM Image	100
41c	Sample 15 SEM Image	100
41d	Sample 16 SEM Image	100
41e	Example of Area Where Typical Compositional Taken for 10g/l Deposit	100
42	Typical Composition of Deposits Produced from 10g/l YSZ Solution	101
43	Typical EDX Analysis of Deposits Produced from 10g/l YSZ Solution	101
44	Effect of Solution pH on the Ceramic Reinforcement Content of the Deposit	102
45	Effect of Agitation Method on the Co-Deposition of Ceramic Particles	103
46	Typical Area of 7.5g/l Deposit Examined Under SEM and EDXA	104
47	Compositional Analysis of Area Shown in Figure 45	104
48	Area of Porosity	104
49	Mapped Area of Porosity (Porosity Indicated in Red)	104
50	Precipitation Rate of YSZ From Electroless Nickel Solution	106
51	Precipitation Rate of LSM From Electroless Nickel Solution	106
52	Precipitation Rate of LSM & YSZ From Electroless Nickel Solution	107

53	SEM Image of Deposit Plated with 0.1 μ m Polystyrene Particles	109
54	SEM Image of Deposit Plated with 0.1 μ m Polystyrene Particles Post Heat Treat	109
55	SEM Image of Deposit Plated with 0.5 μ m Polystyrene Particles	109
56	SEM Image of Deposit Plated with 0.5 μ m Polystyrene Particles Post Heat Treat	109
57	SEM Image of Deposit Plated with 1.0 μ m Polystyrene Particles	109
58	SEM Image of Deposit Plated with 1.0 μ m Polystyrene Particles Post Heat Treat	109
59	EDXA Spectra of Deposit Plated with 0.1 μ m Polystyrene Particles	110
60	EDXA Spectra of Deposit Plated with 0.5 μ m Polystyrene Particles	110
61	EDXA Spectra of Deposit Plated with 1.0 μ m Polystyrene Particles	110
62	Typical EDXA Spectra of Deposit with Flocculant	112
63a	Bath 1 with 2 Drops of Floquat	112
63b	Bath 2 with 2 Drops of Floquat	112
63c	Bath 3 with 2 Drops of Floquat	112
63d	Bath 4 with 2 Drops of Floquat	112
64	Temperature vs Resistivity for Deposited Sample	114
65	Temperature vs Conductivity for Deposited Sample	114
66a&b	Example of Published Electrical Conductivity Data	115
67	Conventionally Produced Cathode	116
68	Cathode Produced by Electroless Deposition	116
69	Composition of Cathode Produced by Electroless Deposition	117

CHAPTER 1 - Introduction

1.1 *Background*

The global drive for environmentally friendly power generation has initiated research in numerous diverse fields, ranging from solar panels, to wind or tidal farms. While these are effective sources of electrical energy, they have productivity issues, for example on a cloudy or windless day, energy production would be greatly reduced. Additionally the size and position of these farms are critical and has come under close scrutiny due to their impact on rural communities and their own environmental impact on the countryside. Ideally a power generation system is required which would efficiently produce significant energy levels and which could be either portable, e.g. in a vehicle, or a fixed system, e.g. within a factory, home, etc.

Swiss scientist Emil Baur and his colleague H. Preis, experimented with solid oxide electrolytes in the late 1930s, using such materials as zirconium, yttrium, cerium, lanthanum, and tungsten. Their designs were not as electrically conductive as expected and reportedly experienced unwanted chemical reactions between the electrolytes and various gases, including carbon monoxide. In the 1940s, the Russian O. K. Davtyan added monazite sand to a mix of sodium carbonate, tungsten trioxide, and soda glass "in order to increase the conductivity and mechanical strength." Davtyan's designs, however, also experienced unwanted chemical reactions and short life ratings.

By the late 1950s, research into solid oxide technology began to accelerate at the Central Technical Institute in The Hague, Netherlands, Consolidation Coal Company, in Pennsylvania, and General Electric, in Schenectady, New York. A 1959 discussion of fuel cells noted that problems with solid electrolytes included relatively high internal electrical resistance, melting, and short-circuiting due to semi-conductivity. It seemed that many researchers began to believe that molten carbonate fuel cells showed more short-term promise. Not all gave up on solid oxide, however. The promise of a high-temperature cell that would be tolerant of carbon monoxide and use a stable solid electrolyte continued to draw modest attention. Researchers at

Westinghouse, for example, experimented with a cell using zirconium oxide and calcium oxide in 1962.

In 1962 researchers at Westinghouse Electric Corporation demonstrated the feasibility of producing electricity from a solid oxide fuel cell. This has led to intensive research and development in that field but as yet has not made the impact on energy production that was first envisioned. More recently, climbing energy prices and advances in materials technology have reinvigorated work on SOFCs, and numerous countries are investing heavily in research programmes.

1.2 Solid Oxide Fuel Cell Technology

Solid oxide fuel cell (SOFC) technology varies slightly from manufacturer to manufacturer as each company is developing units for subtly different applications. In most instances these companies are still developing their products and few production models are available on the market. The compromise between cost, functional performance and materials availability is still the overwhelming constraint hindering the widespread breakthrough into the marketplace.

Any processing method, materials development, increase in performance or cost reduction which brings the technology within the budget of the prospective market clients will be eagerly accepted by the manufacturers, provided that they have not heavily invested in existing manufacturing processes.

The current technology is based on ceramic materials for fuel cell operating temperatures between 500 and 1100°C. SOFC's are highly efficient, capable of efficiencies of 60-80%, and are very flexible in their operational fuels. Typical fuels used to date include hydrogen^[49], natural gas, synthesis gas, reformat gas, coal gas^[76,77,90], LPG, methane^[2] and bio-gas^[28]. Another important advantage is that they can use a variety of non-precious metal catalysts which can make them competitive against other fuel cell types.

SOFC's can be categorised into different types and this is typically done by operating temperature, cell design and cell materials. If we initially consider temperature categories we see that they can be split as follows,

Lower temperature	LTSOFC	500 - 700°C
Intermediate temperature ^[63]	ITSOFC	700 - 850°C
High temperature ^[64]	HTSOFC	850 - 1100°C

The low and intermediate temperature designs have better thermal shock resistance, reduced start-up times and lower cost of materials (through the use of cheaper, lower grade stainless steel alloys) than their higher temperature counterparts. On the other hand HTSOFC's have greater power densities which makes them more efficient.

Four distinct fuel cell stack configurations have been considered including the monolithic, planar, tubular^[92,107] and the segmented cell-in-series design. To date the most commonly used designs are the planar and tubular which are depicted below in figures 1 and 2.

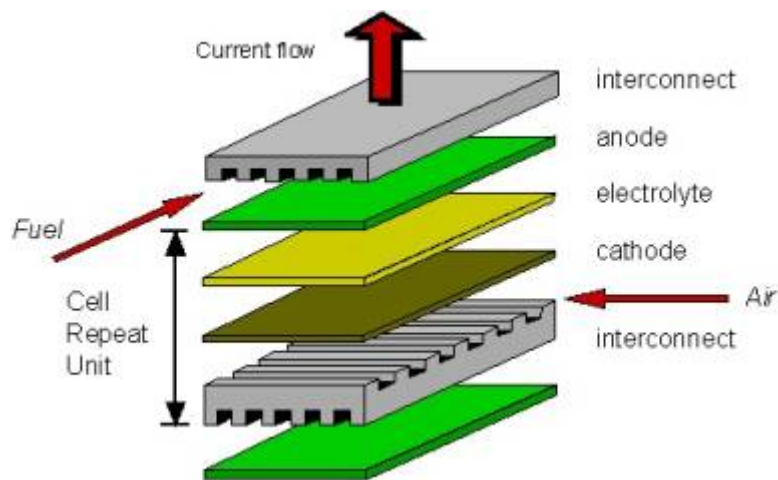


Figure 1 – Planar SOFC design.

(Image from Bath University (C. Fisher 2001))

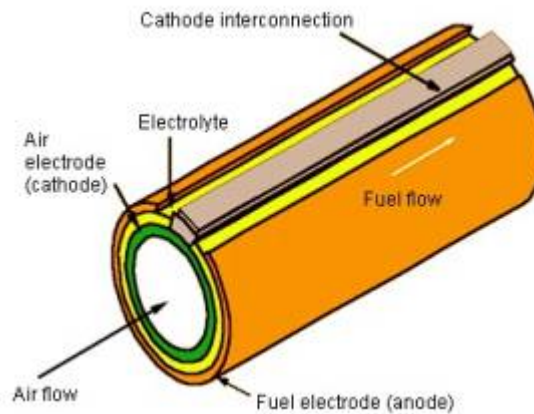


Figure 2 – Tubular SOFC design (Westinghouse).

(Image from US National Energy Technology Laboratory)

Planar designs are simpler to manufacture, which makes them more cost effective. There are major concerns, however, with safety issues due to difficulties in sealing each cell, which can lead to the release of explosive or flammable gases. The tubular

design avoids these problems but it can be difficult to manufacture and its higher intrinsic electrical resistance reduces its efficiency.

Basically a fuel cell is an electrochemical device which converts chemical energy from fuels such as hydrogen, methane, butane, etc; into electrical energy by exploiting the natural tendency for hydrogen and oxygen to react,



and it can be illustrated as detailed in figure 3.

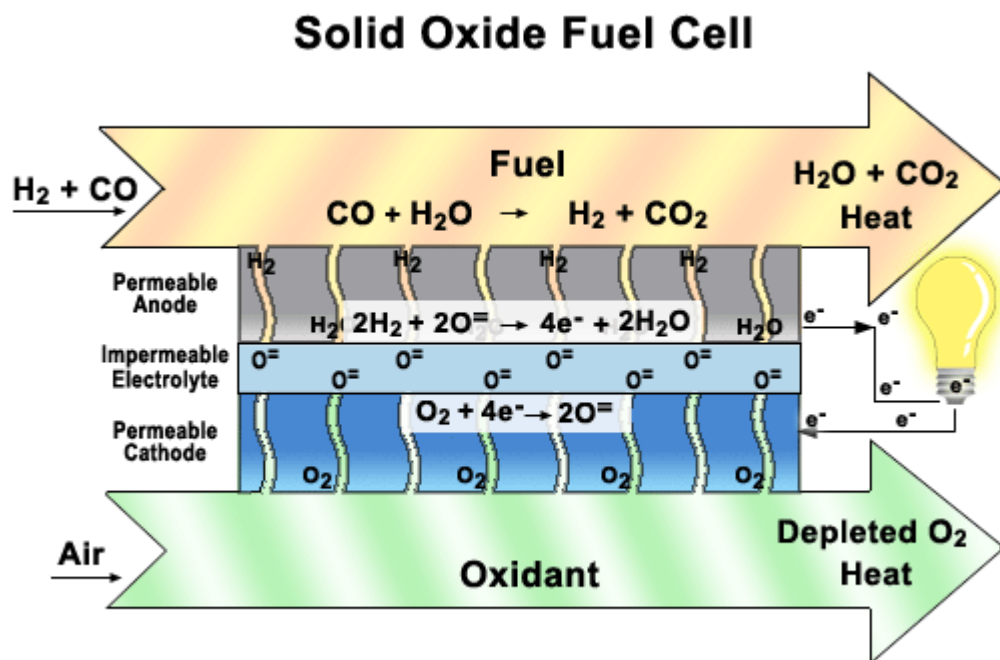


Figure 3 – illustration of reactions in an internally reformed fuel cell.

(Image from NASA TcSAM project)

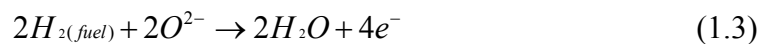
Fuel cells are simple devices, containing no moving parts and only four functional component elements, those being,

- i. Cathode,
- ii. Anode,
- iii. Electrolyte
- iv. Interconnect

A cell is typically constructed where two porous electrodes sandwich an electrolyte with hydrogen as the basic fuel, but cells also require oxygen, hence a flow of air passes along and over the cathode where oxygen molecules contact with the cathode / electrolyte interface and they catalytically acquire four electrons from the cathode and splits into two oxygen ions,



These oxygen ions diffuse into the electrolyte material and migrate to the other side of the cell where they meet the anode. At the anode / electrolyte interface the oxygen ions catalytically react with the hydrogen fuel producing electrons and water,



The electrons transport through the anode to the external circuit via the interconnect. If alternating current (AC) is required, the direct current (DC) output of the fuel cell can be routed through an inverter.

The electrolyte plays a key role whereby it permits only the appropriate ions to pass between the anode and the cathode. If free electrons or other chemical substances were to pass through the electrolyte, they would disrupt the chemical reaction. Additionally in the electrolyte supported design it provided the structural support for the cell.

From the equations it can be seen that the hydrogen and oxygen react to form only water, which drains from the cell. As long as a fuel cell is supplied with hydrogen and oxygen, it will generate electricity. In some applications, the waste water would be considered as a valuable commodity.

As fuel cells generate electricity chemically, rather than by combustion, they are not subject to the thermodynamic laws that limit a conventional power plant. Fuel cells are therefore more efficient in extracting energy from a fuel. Some cell designs also

produce waste heat which can be extracted and utilised by other systems, e.g. internal heating systems. In such systems designed to capture and utilise the systems waste heat (co-generation), overall fuel efficiencies could be 80-85% efficient.

The selection of materials for SOFC's present enormous challenges to meet the properties required for each individual component. Each component must have the required electrical properties as well as the chemical and mechanical stability to endure fabrication and operational conditions. SOFC's operate at very high temperatures, 500-1,000°C in order to achieve sufficiently high current densities and power output required. They also remove the need to use precious-metal catalysts which also reduces costs. Operation up to 1,000°C is possible using the most common electrolyte material, Yttria-Stabilised Zirconia (YSZ). Reaction and interdiffusion between the components must be minimised and the coefficients of thermal expansion^[57,86] of the materials must be matched as closely as possible to prevent thermal mismatch which would produce mechanical failure. The airside of the cell must be capable of operating in an oxidising environment whilst the fuel side must operate in a reducing environment. The temperature, environmental conditions and mechanical properties dictate the selection criteria for all the fuel cell components. Additionally for a SOFC to be commercially viable, the materials, processing and fabrication must be cost-effective. A selection of the commercially used SOFC materials are listed in Table 1, and the required properties for each component are detailed in the following sections.

Table 1. Commonly Used Commercial SOFC Materials [9, 27, 37, 43, 44, 50, 52,70,79,103]

	Electrolyte	Cathode	Anode	Interconnect
Materials	<ul style="list-style-type: none"> • YSZ (yttria-stabilized-zirconia) • ZrO₂ • Bi₂O₃ • Sr-and Mg-doped LaGaO₃ • YDC (Y-doped CeO₂) • SDC (Sm-doped CeO₂) • GDC (Gd-doped CeO₂) • LSGMC ((La,Sr) (Ga, Mg, Co) O₃) • ScSZ 	<ul style="list-style-type: none"> • LSM • LSM/ZrO₂ • LSN (Sr-doped La₂NiO₄) • LSCF (lanthanum strontium cobaltite ferrite) • LaMnO₃ • LaCoO₃ • SSc ((Sm, Sr)CoO₃) • LSM-YSZ 	<ul style="list-style-type: none"> • Ni-YSZ • LSCF • Ni/ZrO₂ • NiSDC (Ni-(Ce, Sm) O₂) • NiO/CeO₂ • Ce₂O₃ (Copper with ceria) • CeGdO 	<ul style="list-style-type: none"> • LaCrO₃ (HT SOFC) • Metallic interconnect materials: • Ferritic stainless steels • Austenitic stainless steels • Ni-based superalloys • Sintered metal powders (e.g. ODS (Cr5FeY))

1.2.1 Cathodes

The cathode provides reaction sites for the electrochemical reduction of the oxidant and thus must be stable in oxidising environments. Main requirements for the cathode include chemical and mechanical stability, sufficient electrical conductivity and it must be compatible with other cell components. Additionally the cathode must also be porous to allow oxygen molecules to reach the electrode/electrolyte interface. The cathode in some designs contribute as much as 90% of the cell's weight and can also provide structural support to the cell. The most commonly used cathode material is Lanthanum Manganite (La Mn O_3), a p-Type Perovskite; which is doped with strontium and called LSM ($\text{La}_{1-x} \text{Sr}_x \text{Ma O}_3$)^[48]. There is no ionic conductivity with these perovskites as they only exhibit electrical conductivity. As well as being compatible with YSZ electrolytes it also functions at intermediate temperatures ($\sim 700^\circ\text{C}$) which allow it to be used with alternative electrolyte compositions. Any reduction in operating temperature reduces operating costs and allows more varied materials selection, which in turn further reduces costs.

1.2.2 Electrolytes

The electrolytes main function is to conduct ions between the anode and the cathode and to separate the fuel from the oxidant gas. Electrolyte must therefore possess a high ionic conductivity and no electrical conductivity to allow migration of the oxygen ions. It must also be fully dense to prevent short circuiting between the anode and cathode yet should be as thin as possible to minimise electrical resistance within the cell. It should also be chemically, thermally and structurally stable across a wide temperature range.

YSZ, doped cerium oxide and doped bismuth oxide are several materials which have been evaluated by other researchers. YSZ is the most commonly used material. Yttria stabilises the zirconia into the cubic structure at high temperatures and provides oxygen vacancies (rate of one vacancy / mole of dopant, with a typical dopant level of 10 mol% of Yttria).

A thin, dense film of electrolyte is applied to the cathode substrate; typically $\sim 40\mu\text{m}$ thick. Electrochemical vapour deposition can be used to deposit the electrolyte, but whilst effective, it is expensive and involves expensive capital investment. Alternative coating methods also include spray coating and dip coating followed by sintering.

1.2.3 *Anodes*

The anode's main function is to provide reaction sites for the electrochemical fuel oxidation. The anode must possess the required electrical conductivity compatible with other cell components, have a matched coefficient of thermal expansion (CTE) and adequate porosity, and must be capable of operating within a reducing atmosphere.

Most research to date has focused on nickel^[42] due to its availability and affordability. However in its pure state its CTE ($13.3\mu\text{m}\cdot\text{C}^{-1}$) is too high compared to that of YSZ ($10\mu\text{m}\cdot\text{C}^{-1}$) and would introduce thermal stresses during temperature cycling and operation. Additionally, its tendency to sinter and thus reduce its porosity hinders its efficiency as an anode material. By using a composite material of nickel and YSZ the CTE can be effectively matched with the YSZ electrolyte whilst minimising the tendency for the nickel to sinter^[56]. Finally, adhesion of the anode to the electrolyte can be significantly improved by producing a composite anode.

Utilising nickel as an anode material can be a disadvantage if hydrocarbons are used as a fuel as it catalyses the formation of graphite from the hydrocarbons. The deposited graphite on the internal surfaces of the anode reduce its efficiency^[2].

1.2.4 *Interconnect*

To generate sufficient power, multiple cells require to be connected together and to facilitate this, a means of collecting the electrical current is required. The interconnect functions as an electrical contact to the cathode whilst protecting it as a physical barrier from the reducing atmosphere at the anode.

The combination of the high operating temperatures and the severe atmospheres requires that the interconnects must be non-porous, have high electrical conductivity, be chemically inert and have a matched CTE.

For a YSZ SOFC operating at $\sim 1000^\circ\text{C}$, the interconnect material is usually La Cr O_3 doped with a rare earth element to improve its conductivity. Typically interconnects are plasma sprayed onto the anode and then sintered. The drive for lower temperature SOFC allows specific grades of stainless steel^[36,44] to be utilised.

Any reduction in component costs can be directly translated into improved energy affordability.

1.3 *Current manufacturing techniques*

Traditional fabrication routes for producing cells for solid oxide fuel cells can be split into two categories, wet routes and gaseous routes.

Wet ceramic processes generally require to be housed in a clean, air conditioned environment to ensure that consistent results are obtained. The four main wet manufacturing routes will each be considered in turn, but it is important to note that most cell manufacturers will use a combination of these techniques to produce the complete cell.

1.3.1 *Silk Screening*

Screen printing is a flexible fabrication process which first appeared in China in approximately 960-1279. It has been used for many large scale batch applications, for example in the graphic design of posters, displays and t-shirts, and is also ideally suited to small scale production and research.

The process can either be done manually, or automated as illustrated in figure 4a, depending on the scale of manufacture. The basic concept is that a mesh of woven fabric or metal wire-cloth (C&D) is stretched over a support frame (E). Areas of the mesh are masked off with a non-permeable material (C), which is a negative image of the design to be printed (F). The screen is placed over a substrate material and a reservoir of ink (A), placed at one side is smeared over the mesh using a rubber blade (B). The ink is forced by the rubber blade, down the areas of open mesh (C) by capillary action onto the substrate below as is depicted in figure 4b.

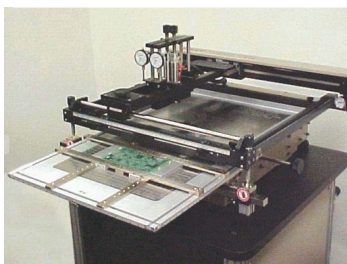


Figure 4a – Screen Printing Press
(Image from NFCRC, University of California)

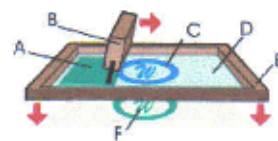


Figure 4b – Screen Printing Principle
(Image from Wikipedia)

In the manufacture of SOFC's the ink generally contains fine powders of YSZ, suitable binders and a solvent, although the composition will vary on the part of the cell being manufactured. Once the screen is removed the substrate is heated to dry the deposited film, removing the solvents, and then fired at high temperatures to form a dense deposit and burn off the binders. Whilst the technique is well understood and commonly used, the automated silk screening plant, plus the furnaces required for the sintering operations can make the process costly in terms of initial capital outlay. To fully appreciate the manufacturing process^[71] and the production timescales a typical silk screen printing procedure is detailed as follows :

1. Ball milling of NiO + YSZ powders in IPA, dried and reground for up to 24 hours.
2. Calcined in air for 5 hours @ 1400°C.
3. Pulverised into powder and mixed with polyethylene glycol.
4. Silk screened printed onto component.
5. Calcined (optional).
6. Sintered at 1400°C for 5 hours.

Alternatively

1. As above.
2. Powders dried in oven at 90°C for 6 hours.
3. Calcined in argon at 600°C.
4. Silk screening.
5. Sintered at 1200°C -1400°C for 4 hours.
6. Reduced at 900°C in hydrogen / argon atmosphere for 2 hours.

Traditionally anodes have been manufactured by applying a slurry of Ni and YSZ through silk screening techniques and the coating is then sintered, or a slurry of NiO – YSZ is applied and the NiO is reduced to particulate nickel in the sintering operation to ensure porosity. Addition agents such as starch, carbon or thermosetting resins can be added, which during

sintering, burn out, leaving pores behind. However this technique forms inefficient pathways of porosity^[58], which reduces the transport efficiency of the reaction gases through the electrode, and which can also increase the likelihood of cracking during sintering due to the reduced structural integrity.

1.3.2 Tape Casting

With tape casting^[5,55,59,74,78], a manufactured ceramic slurry is placed in the initial dosing chamber. The chamber has a small gap controlled by a doctor blade. Underneath this gap passes a polymer tape and the slurry is deposited onto the surface of the passing polymer tape to the thickness of the doctor (casting) blade gap, as shown in figure 5. The slurry and tape pass through an oven where the liquid is evaporated forming a solid ceramic tape on a polymer backing. The tape then exits the oven and is wound onto a spool. Films are cut by stamping, before being sintered. Figure 5 also illustrates the effects of drying and sintering on the original slip material. An example of an industrial tape casting machine is shown in Figure 6.

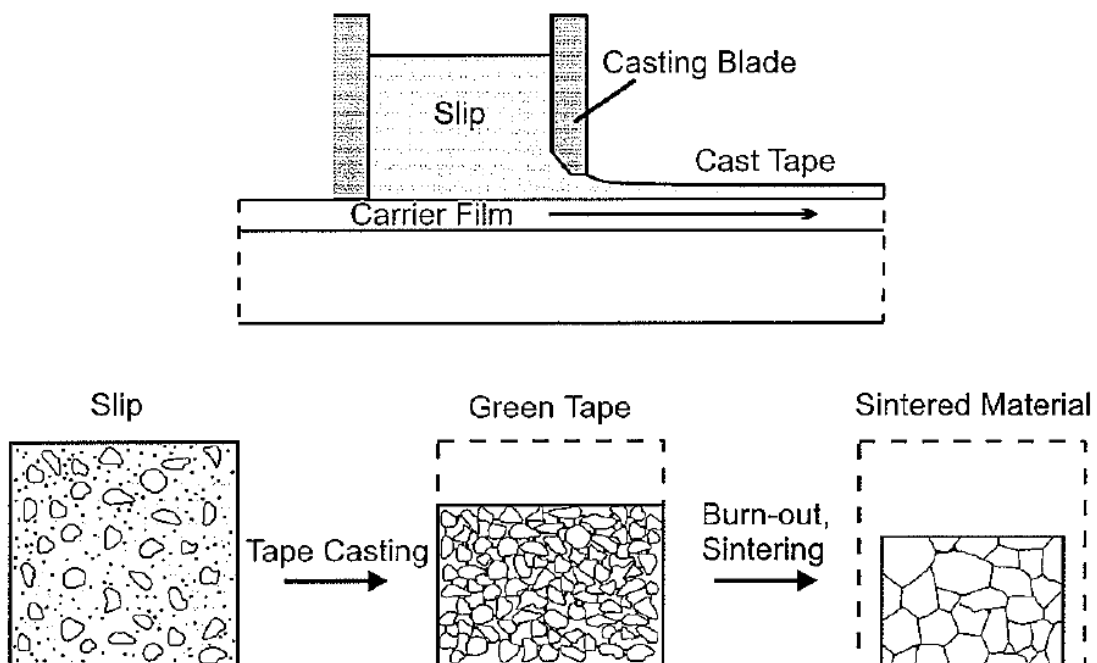


Figure 5 – Tape casting schematic and the drying and sintering effects on slip material.

(Image from the Swedish Ceramic Institute)

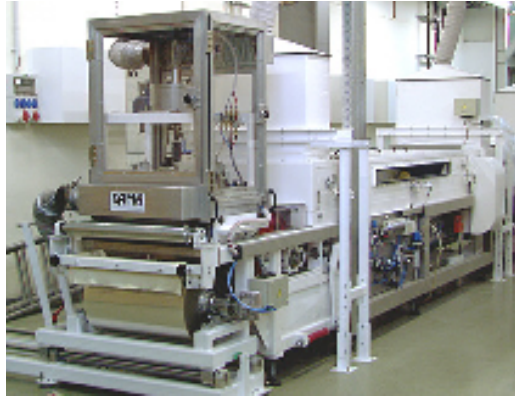


Figure 6 – tape casting set-up.

(Image from SAMA Maschinebau GmbH, Model FGA500)

1.3.3 Tape Calendaring

Tape calendaring involves squeezing a softened thermoplastic / ceramic mix between two rollers producing a continuous sheet of material.

YSZ powder is blended with plasticisers and binders and once a solvent is added, the mixture is extruded to form a homogenous plastic mass. It is then passed through rollers. The solvent is then evaporated off and the films are cut by stamping, before being sintered as shown in figure 7.

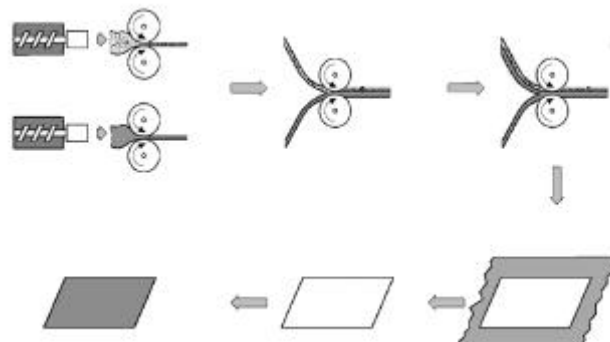


Figure 7 – Tape calendaring fabrication process

(Image from Allied Signal Aerospace presentation M-06129)

1.3.4 Slurry Spraying

In slurry spraying,^[54] a YSZ powder is mixed with additional materials depending on the component being fabricated and then ball-milled. This compound is used as the slurry which is forced through a small nozzle using compressed air onto the substrate. It is then dried before high temperature sintering.

1.3.5 Thermal Spraying

Thermal spraying is a generic term for a group of commonly used processes which are used to deposit metallic, non-metallic and cermet coatings. Coatings can be sprayed from powder, wire or rod feedstock depending on the technique used, which includes flame or plasma-arc^[6] spraying. Each cell developer may have a preferred technique depending on the composition of the electrode and the properties required of the deposit in terms of thickness, porosity, etc. As with all coating techniques substrate cleanliness and sufficient surface roughness are vital to ensure adequate adhesion. An example of the principle involved in spraying is shown in figure 8a.

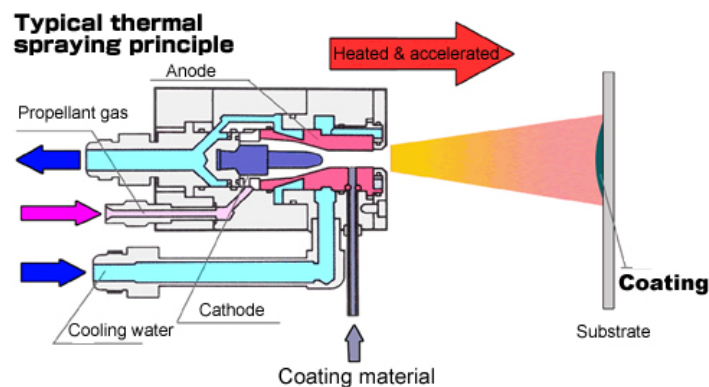


Figure 8a – principle of thermal spraying.

(Image from Plasma Giken Kogyo Co. Ltd)

Typically in SOFC manufacture, a powder is introduced via a hopper or feeder, into a compressed air or gas stream which delivers the powder to the flame where it is heated to a semi-molten or molten state and propelled onto the substrate, to which it adheres upon impact. An example of the production route in manufacturing an anode by thermal spraying is shown in figure 8b.

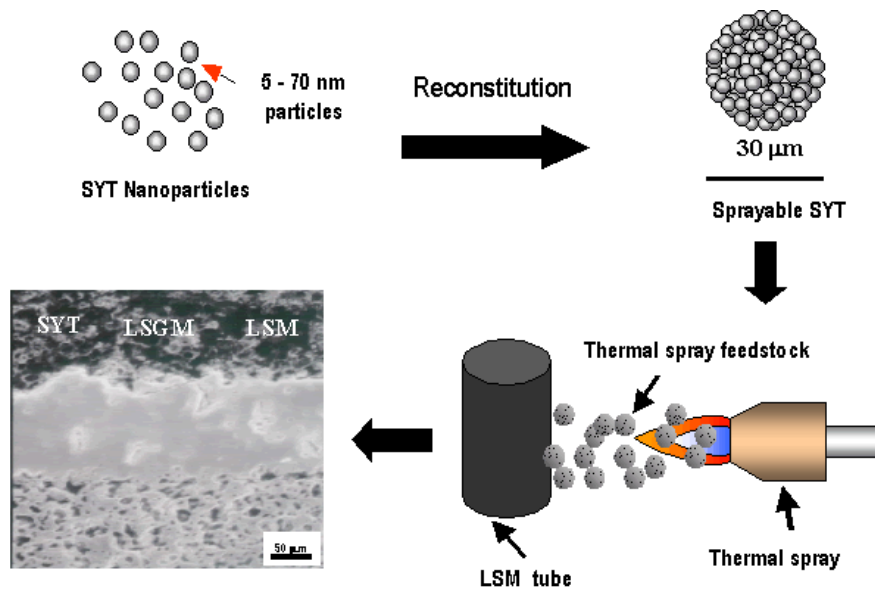


Figure 8b – Example of anode manufacture (NB, SYT is Strontium Yttria Titanate)

(Image from US Nanocorp Inc.)

1.3.6 Chemical Vapour Deposition

In chemical vapour deposition a reactant gas or precursor is fed into a processing chamber, where it decomposes at the substrate's surface. One of the decomposition products will be absorbed onto or deposited onto the substrate, while the other decomposition products are removed from the chamber along with any excess of the reactant gas. Whilst the technique is flexible in the variety and reproducibility of deposits which can be produced, the operating and initial capital costs can be very high.

1.3.7 Physical Vapour Deposition (PVD)

Physical vapour deposition is similar to chemical vapour deposition except that the precursors are in the solid form. The process is performed in a vacuum chamber and involves four main steps. During the evaporation stage, a target composed of the material to be deposited, is bombarded by a high energy beam of electrons or ions. This vaporises the atoms on the

target, which migrate from the target to the substrate in a ‘line of sight’ direction. In some cases the vaporised atoms may react with the transport gas to form a new compound. The deposition of the vaporised ions on the substrate continues until the required thickness is achieved.

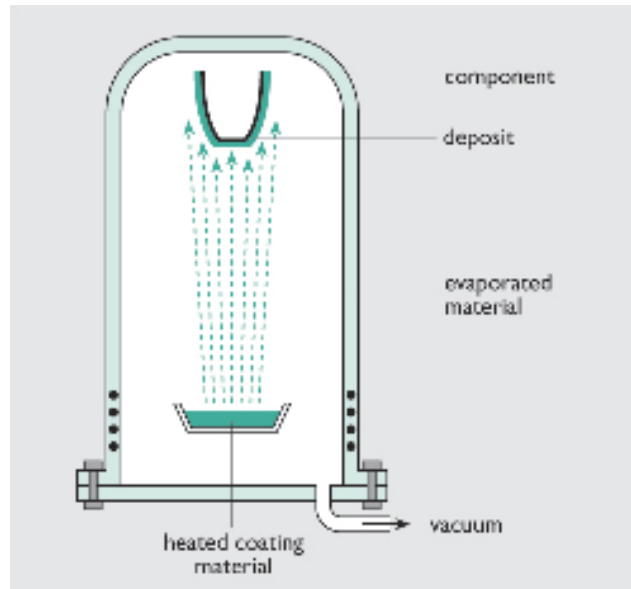


Figure 9 – Schematic of physical vapour deposition process.

(Image from Open University, Unit T173)

The majority of the processes described previously require that the layers be sintered or co-fired to obtain their final properties. Cell thicknesses vary in design but are typically between 0.25 and 0.55mm; and the different layers can be as thin as 10 – 50 μ m; which again depends on the design and choice of materials used.

1.4 Impact of Cell Design on SOFC Costs

The cell and stack manufacturing processes are influenced by, and also dictate the design of the cell. Cell types can be further sub-divided into another three types as detailed:

Electrolyte Supported Cells

In this case the electrolyte is typically thick to provide suitable mechanical strength to the cell. It is primarily used in high temperature conditions.

Anode Supported Cells

Thick anode used to provide the mechanical strength and is used in intermediate temperature fuel cells.

Metal Supported Cells

Used in low temperature designs.

Different SOFC cost models suggest different proportions of final cost due to fabrication techniques, as the cell design has a large impact on the overall stack costs. Stacks with planar rectangular cell designs are estimated to cost \$90/kW whereas tubular anode supported are estimated to cost \$140/kW.

Anode material, capital costs, labour and utilities are the primary factors which influence cell manufacturing costs. Typically for 140cm² cells with 400mW.cm⁻², cell costs are approximately \$90/kW. It should be noted that cost models depend considerably on model assumptions, including amount and cost of raw materials. SOFC designs and production routes have significantly different costs associated with them, and multi-step manufacturing process can be especially difficult to breakdown. However some estimated costings are detailed in tables 2a, 2b and 2c based on market research for the Proof Of Concept 9-ENR-003 project.

Cell cost	\$.m ⁻²
Maintenance	50
Labour and utilities	110
Capital charge	160
Other materials	10
Anode support material	30
TOTAL	360

Table 2a – manufacturing costs

Cell cost	\$.m ⁻² (material only)	\$.m ⁻² (material and fabrication)
Anode	126	136
Cathode	15	22
Electrolyte	6	12
Interconnects	119	138
Fabrication		126
TOTAL	266	434

Table 2b – Cell material and fabrication costs.

Material	\$. kg ⁻¹
Ni-YSZ	14
YSZ (>1µm particle size)	12
YSZ (<1µm particle size)	25
LSM	25
LSCO/LSCF	36
Ferritic stainless steel	5

Table 2c – Raw material costs.

A more detailed cost breakdown for a Delphi system is shown in Figure 9 which clearly shows that fabrication costs are the largest percentages of the overall stack costs.

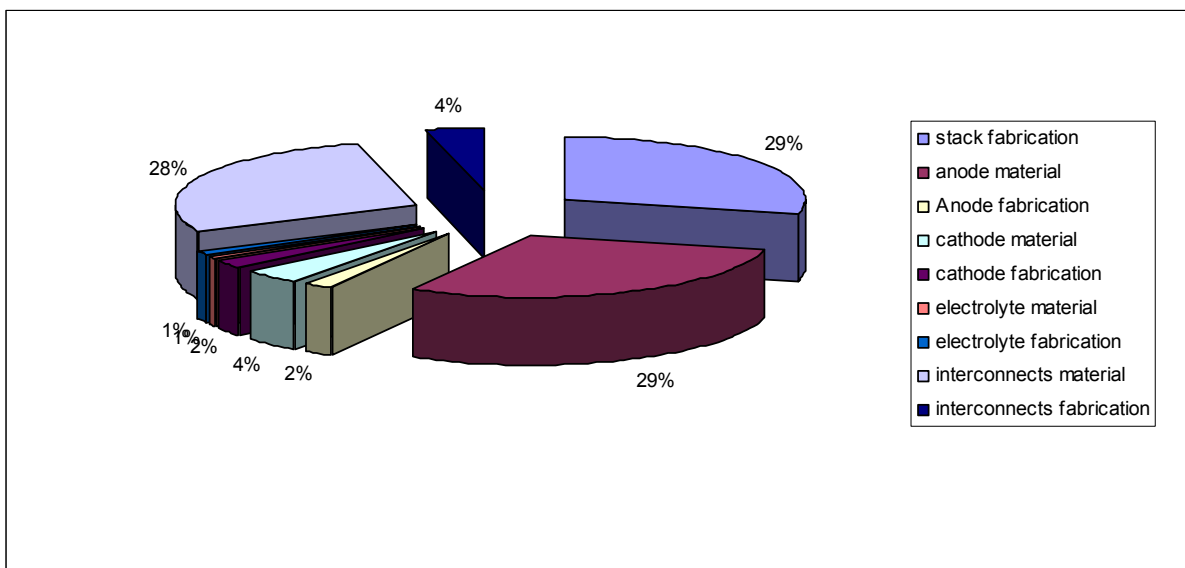


Figure 10 – Stack cost breakdown for \$110/kW system

(Image based on market research for the Proof Of Concept 9-ENR-003 project.)

It is envisioned that cell cost reductions will follow three routes over the coming years,

- i. Increasing production volumes
- ii. Technology improvement (less material, increased power density, etc)
- iii. Stack scale up

As is apparent from other industries, if the production volumes can be increased there can be a dramatic reduction in unit costs. At low volumes, fixed costs are high due to poor utilisation of capital and labour. SOFC total system costs were reviewed by the US SECA

Program which targeted manufacturing costs of \$400/kW by 2010, and they estimated that installation costs to be 2-3 times greater. They have also assumed that successful market introduction by a single manufacturer would require production volumes of approximately 500,000 units per annum.

The electrical efficiencies in solid oxide fuel cells typically range from 20–50% depending on the design, operating parameters, fuel type and application. In combined heat and power configurations, where the waste heat energy can be utilised for producing hot water and heat, then the total efficiency for electrical and thermal can be as high as 90%. The power density of a cell is a function of the current density ($A.cm^{-2}$) and the voltage level a cell can sustain at that load level. Or alternatively, the power density is normally expressed in electrical power per active fuel cell area. The balancing act occurs in trying to maintain a high power density as operation at high levels reduces cell lifetimes.

If power density can be increased then costs can be further reduced, as it has been estimated that an increase in power density from approximately $400mW.cm^{-2}$ to $515mW.cm^{-2}$ would reduce the costs from \$120/kW to approximately \$85/kW.

Cell size tends to be limited to a certain size due to the difficulty in handling and assembly of the brittle cells. At present the largest cell size manufactured to date is 50cm x 50cm, but typical sizes are 10cm x 10cm and 15cm x 15cm.

The existing supply chain has extensive cross over, from materials to component, into stacks and complete systems. A summary of the primary and secondary companies in this sector are detailed in figures 10a and 10b along with their supplier / customer relationships.

1.5 Applications

SOFC's are targeted for use in three energy applications; stationary energy sources such as homes, office buildings, industrial sites, etc; Transportation in both trucks and automobiles; and finally military markets, due to their flexibility at being used in remote locations, being quiet and non-polluting. Moreover, using fuel cells in military applications could reduce deployment costs, as 70% by weight of the material that the military transports is fuel. A

breakdown of potential market areas and the estimated timeline to commercial breakthrough are shown in figures 11a and 11b.

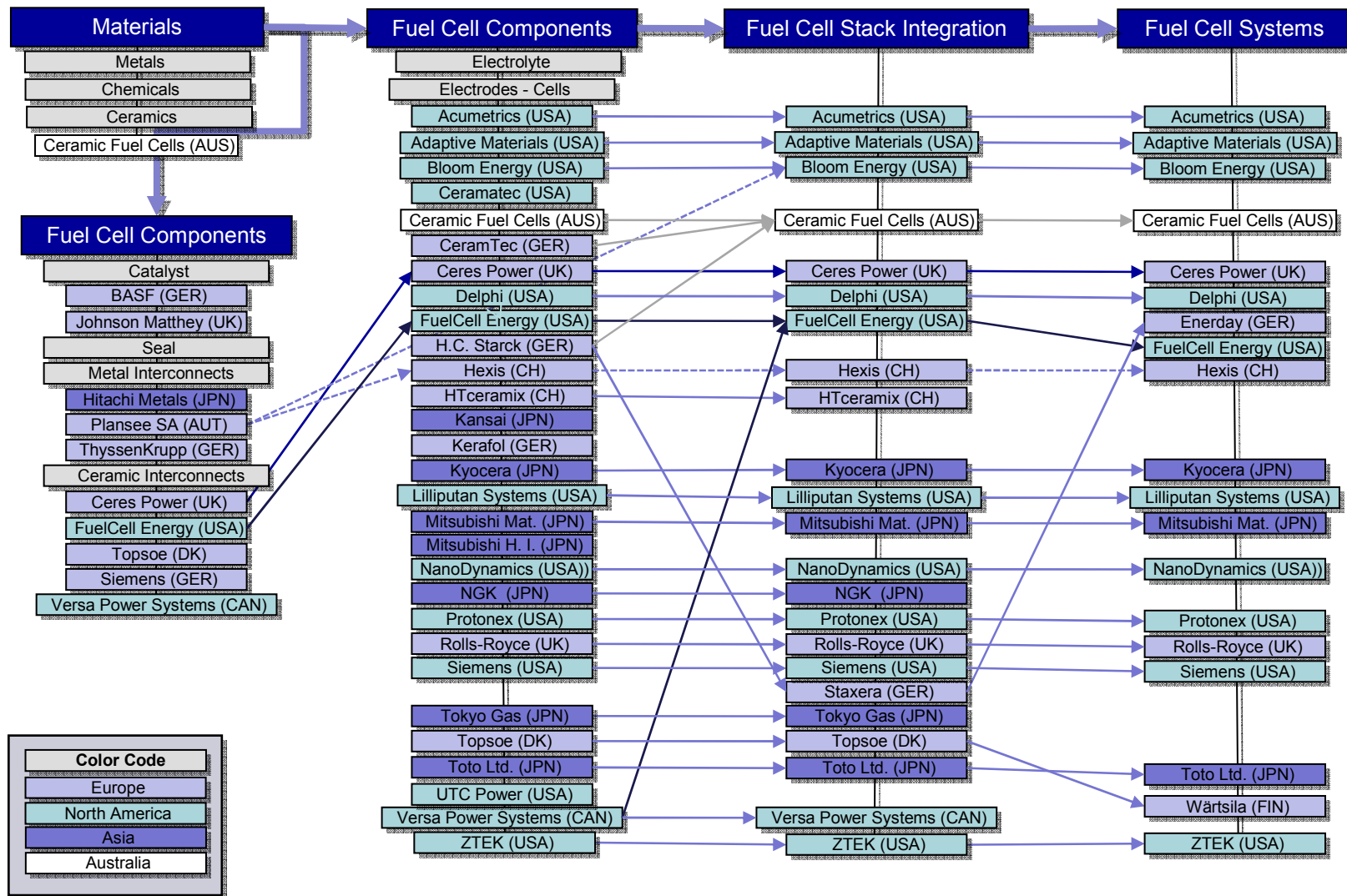


Figure 11a – Main players in the SOFC supply chain.
 (Image based on market research for the Proof Of Concept 9-ENR-003 project.)

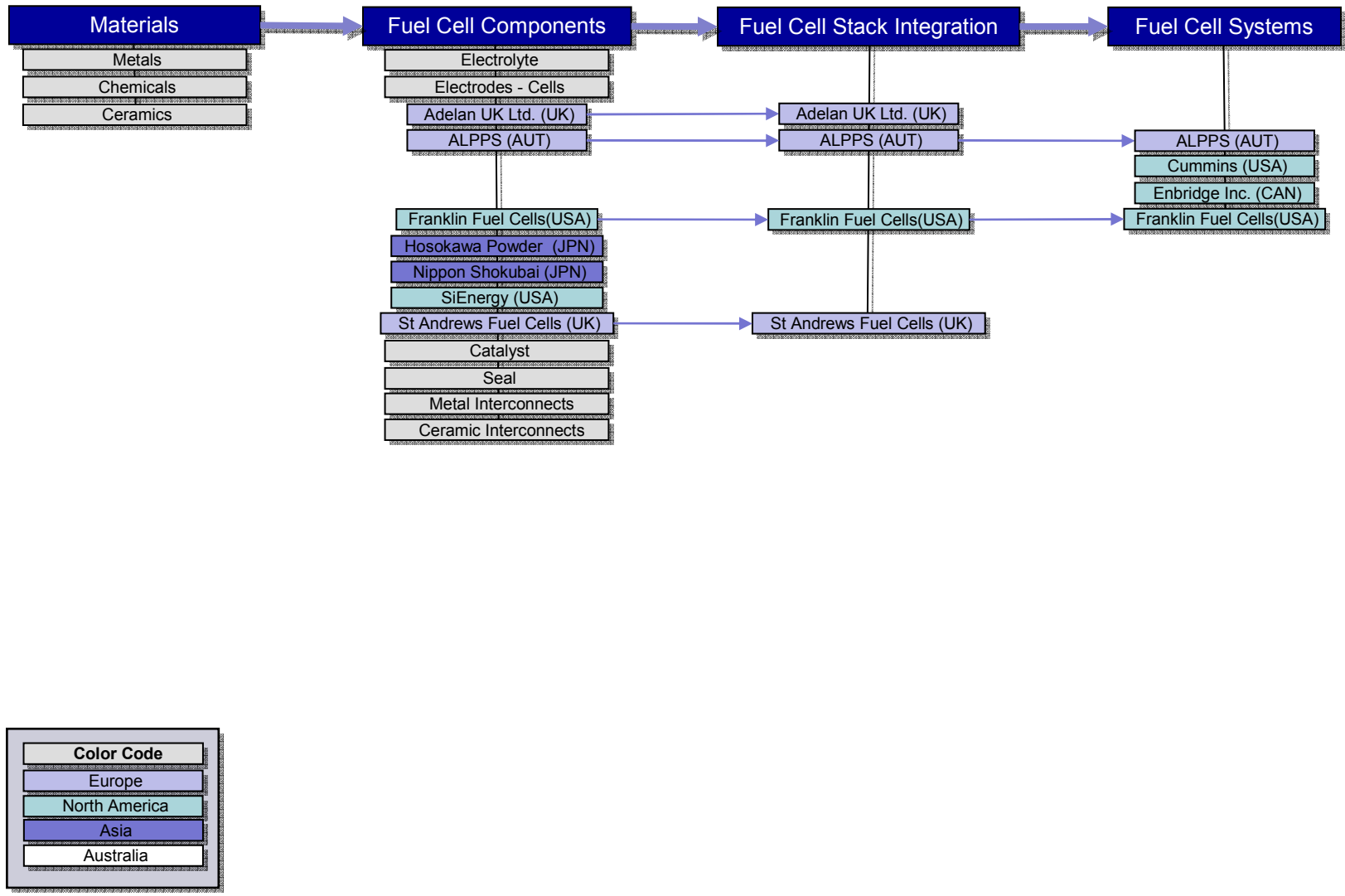


Figure 11b – SOFC supply chain, additional players
(Image based on market research for the Proof Of Concept 9-ENR-003 project.)

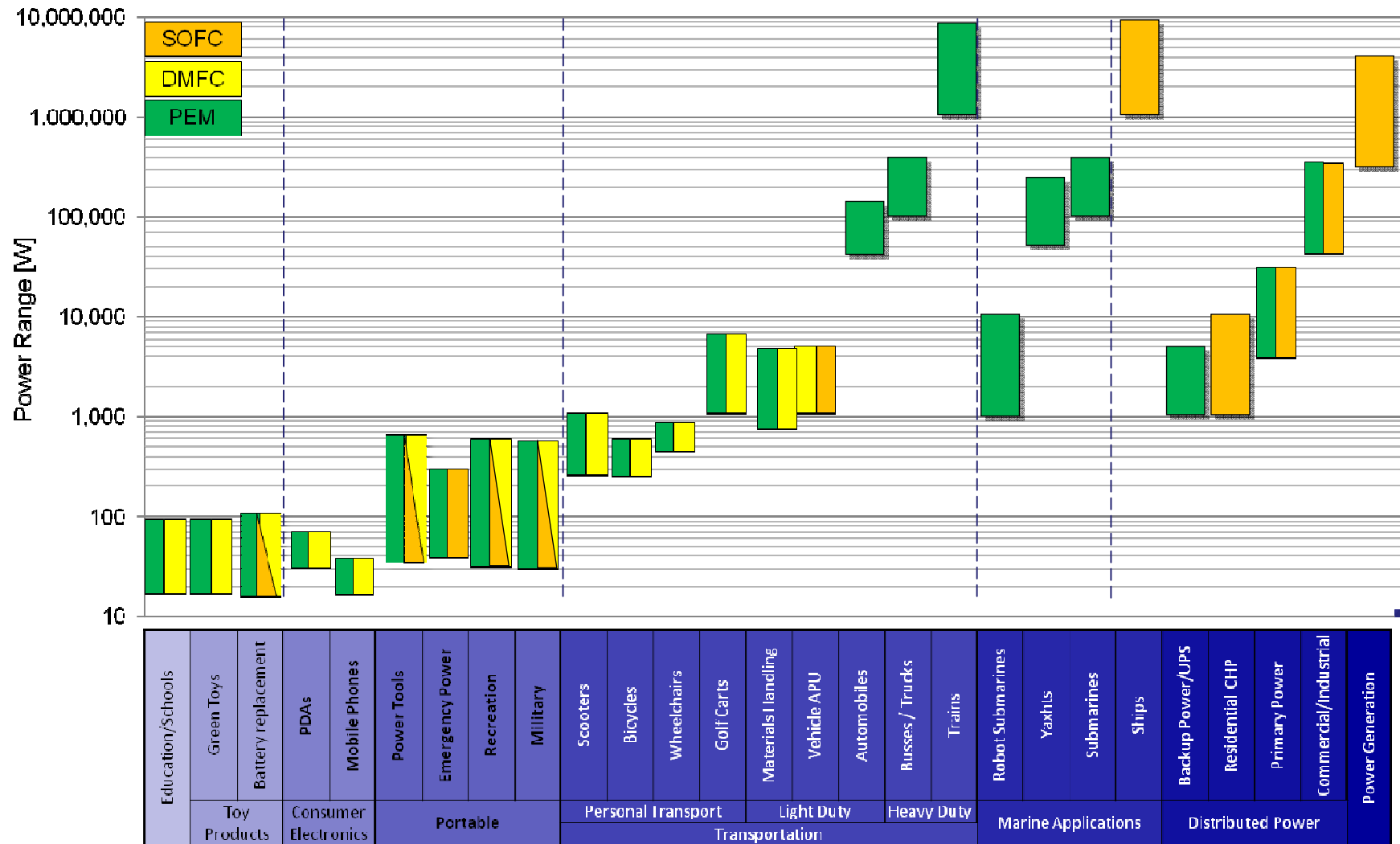


Figure 12a - An application map versus power range shows some trends for different fuel cell types
(Image based on market research for the Proof Of Concept 9-ENR-003 project.)

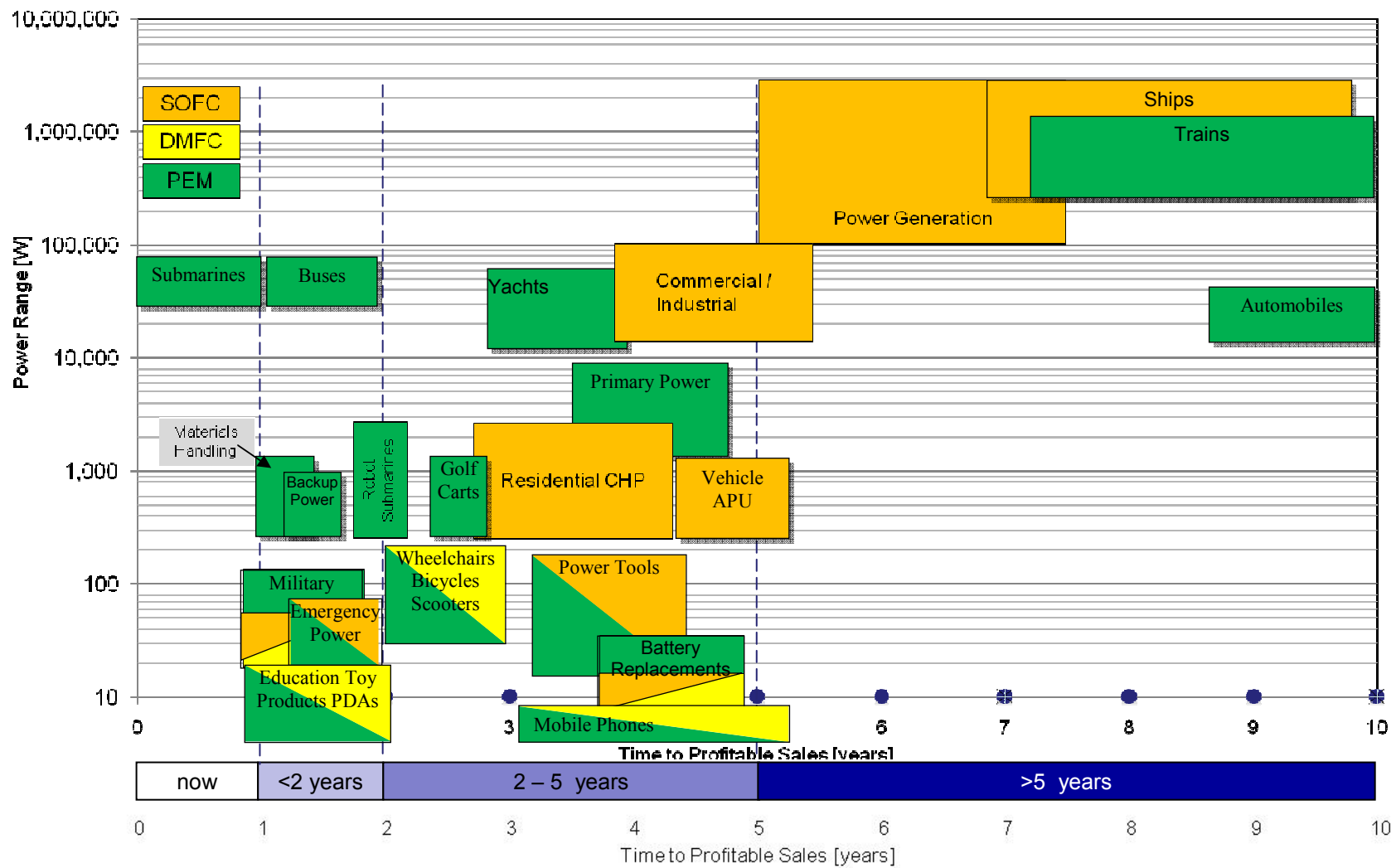


Figure 12b - A map of power range vs. estimated time to competitive products.
(Image based on market research for the Proof Of Concept 9-ENR-003 project.)

CHAPTER 2 - *Current Research Review*

SOFC's offer advantages in higher efficiency and lower emissions over conventional power generation methods ^[29]. The research on anode manufacture has in recent years revolved around the nickel-yttria stabilised zirconia (YSZ) cermet ^[4], and the fabrication techniques have primarily centred on traditional techniques such as silk screen printing and subsequent sintering.

Ni / YSZ cermet anodes^[7] are the most commonly used anode materials due to their excellent electro-catalytic activity for,

- i. Hydrogen oxidation reduction.
- ii. Electrical conductivity.
- iii. High compatibility and stability with YSZ electrolyte.

The electrical activity^[53] of the nickel anodes is directly proportional to the length of the three-phase boundary where Ni, H₂ and YSZ meet. Therefore increasing the grain boundary length of the Ni / YSZ anode will improve activity and cell performance.

However, high temperature sintering (at approximately 1400°C) and the reducing steps (at approximately 1000°C) associated with these traditional techniques causes significant grain growth in both the nickel and YSZ phase^[56]. This subsequently causes a reduction in length of the grain boundaries.

The only research involving electroless nickel plating in anode manufacture involved uniformly depositing the nickel-phosphorous coating onto the YSZ powder^[3,51] or alternatively as a top layer on the anode^[65] or as the anode itself^[106]. The coated YSZ powder was pressed into bar-shaped samples which were sintered. The samples manufactured in this way were better suited for SOFC anode applications as they had increased conductivity with lower nickel content, which would help to match the CTE of the electrolyte.

Other fabrication techniques which have been investigated include Polarised Electrochemical Vapour Deposition (PEVD) ^[27], which showed some promise as a 'higher' temperature anode material and which could also possibly allow the use of fuels which would normally 'poison' the fuel cell.

Literature reviews revealed extensive research and articles on fuel cell integration, hydrogen storage, safety, components, materials development and economics. It was abundantly apparent that well established knowledge transfer networks (KTN) were in operation in the United Kingdom. These KTN's help to establish relationships between academia and industry by focusing research in key areas. One example is the Supergen consortium (www.supergenfuelcells.org.uk), which has been established between the following partners,

University of Nottingham	Imperial College London
Ceres Power	Rolls Royce
DSTL	Johnson Matthey
University of St Andrews	University of Newcastle Upon Tyne
EaST Chem (joint chemistry research school of Edinburgh & St Andrews Universities)	

Additionally, this review revealed that research groups specialising in SOFC's were concentrated in the following universities.

Birmingham	Newcastle
Cranfield	Nottingham
Imperial	St Andrews
Keele	Surrey
Leeds	University College London
Loughborough	Warwick

These universities appear to be concentrating their research activities into developing new materials and evaluating fuel performance. Further work between these universities and privately owned companies is focused at integration and development of commercial SOFC stacks. What is also apparent is that the fabrication methods being used by these institutes is based on the traditional manufacturing techniques previously discussed.

Information from the UK ERC (www.ukerc.ac.uk) and the Knowledge Transfer Network for Low Carbon and Fuel Cell Technology (www.lowcarbonktn.org.uk) clearly showed that no research had been carried out on co-depositing an electroless nickel / YSZ deposit as an anode material, utilising the proposed electroless plating technique (See Appendix D, Section

8, Marketing Information). This technique would make fabrication simpler and would potentially remove a number of technical problems associated with traditionally used fabrication techniques. Possible advantages of the technology include;

- Overcoming the grain growth issues normally associated with the sintering process.
- Ability to offer a wider range of nickel : ceramic ratios for the anode and to have a ratio gradient through the deposit.
- Much less labour intensive process
- Less expensive capital equipment with lower operational costs

Further investigation revealed that there were no patents currently filed or pending on this area of research (see appendix D, section 2). This could therefore be a viable research topic which could have commercial implications for the University and any Small To Medium Enterprise (SME).

CHAPTER 3. - *Electroless Plating*

The term electroless plating involves the production of coatings from solutions of metal ions without the use of an external source of electrical energy. As such this definition can include each of the three following techniques:

- i) Immersion plating
- ii) Homogenous chemical reduction
- iii) Autocatalytic deposition

Immersion plating involves the deposition of a more noble metal in the electrochemical series onto the surface of a less noble metal. The best example of this is when steel (iron) is immersed into a solution of copper ions, and the copper is deposited onto the steel substrate. This technique has few applications due to the thin, non-adherent coatings that are typically produced.

In the case of homogenous chemical reduction, a chemical reagent provides electrons for reduction of metal ions, which deposit onto the substrate as the metal. Thicker coatings can be deposited by this method, but there are still adhesion issues. Another disadvantage of this process is that the metal ion solution and the chemical reducer must be kept separate otherwise they immediately react.

Autocatalytical deposition utilises chemical reducing agents to provide the electrons for plating, but the treatment solutions are formulated to deposit onto naturally catalytic surfaces, or ones which can be rendered catalytic. The deposit is itself catalytic thus the reaction is self-perpetuating. The coating can thus be built up to significant thickness, and is highly adherent.

Most autocatalytic plating solutions are proprietary in nature and the full composition of such solutions are rarely disclosed but the composition of a number of processes which have been accumulated over 20 years are attached in appendix C, section 4.

In general terms each of these solutions contain a

- i) Source of metal

- ii) Chemical reducing agent
- iii) Complexants (which promote homogenous deposition of metal hydroxides or other precipitates)
- iv) Buffers (as stabilisers to prevent spontaneous decomposition of the solution)
- v) Accelerators to increase plating rate
- vi) Others eg wetting agents, brighteners, etc

Possible candidate coatings available via electroless deposition techniques are detailed in Table 3.

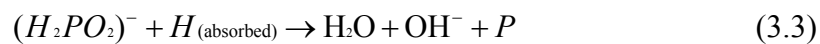
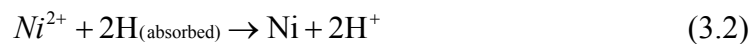
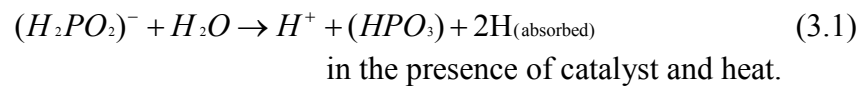
METAL	MELTING POINT °C	ELECTRICAL RESISTIVITY Ω.cm	COEFFICIENT OF THERMAL EXPANSION μm.°C ⁻¹
Ruthenium	2310	7.2×10^{-6}	9.6
Rhodium	1960	4.3×10^{-6}	8.5
Tungsten	3370	5.65×10^{-6}	4.4
Molybdenum	2617	5.7×10^{-6}	6.5
Vanadium	1735	24.8×10^{-6}	10.9
Chromium	1860	13×10^{-6}	6.2
Platinum	1769	10.6×10^{-6}	9.1
Cobalt	1493	6.24×10^{-6}	14.2
Nickel	1455	6.4×10^{-6}	13.1
Palladium	1552	9.93×10^{-6}	13.9

Table 3 – Metal deposits which could be produced electrolessly

3.1 *Electroless Nickel*

Electroless nickel plating^[8,10,11,12, 31,32,33,35,40,41,95,96] is used extensively within industry and in fact is the most prevalent electroless coating used for engineering purposes. It has some unique physical properties, including excellent corrosion^[20], wear and abrasion resistance, ductility, lubricity, electrical properties, high hardness, (especially when heat treated) and good solderability. The deposits typically contain 2 – 14% by weight of phosphorous^[14], depending on the plating solution type, and the plating is carried out by means of an autocatalytic reaction which does not require an external electrical current source.

The process relies on a reaction proceeding at a specific temperature, typically around 90°C, when a suitably activated substrate is immersed in the solution. The deposition rate for this process is approximately 16 to 20µm per hour depending on the condition of the bath chemistry. An advantage of this process is that both metallic and non-metallic substrates can be coated provided they have been suitably pretreated. The process follows the chemical reactions for electroless nickel deposition as detailed in equations 1 to 4 as shown below. The Ni²⁺ and the (H₂PO₂)⁻ come from the nickel salts and the sodium hypophosphite respectively in the plating solution.



(Equations from ASM Handbook, 9th Edition, Vol. 5)

The deposited nickel coating has an even, uniform thickness even down deep bores and recesses, and at corners and edges. The uniformity of the deposit reproduces the substrate

surface finish, which can be roughened to increase its surface area. This also means that the coating can be applied as the final production operation and can meet stringent dimensional tolerances.

The bath constituents are detailed as follows,

i) Source of Metal

Most acid solutions use nickel sulphate whilst nickel chloride is used in alkaline solutions. Deposition rate increases with increase in nickel concentration but conversely solution stability decreases.

ii) Reducing Agent

Sodium hypophosphite is widely used due to its low cost and availability. As with nickel content we see the same effects with concentration on deposition rate and stability. Reducer is replenished at the same rate as the nickel ions to maintain the deposition rate. Most commercial suppliers sell the plating process in multiple pack systems to supply the nickel and reducer. Both nickel and reducer concentrations can be readily determined by volumetric analysis and some large scale commercial facilities have automated analysis and chemical dosing systems.

Hypophosphite consumption can be higher than expected with low surface area substrates compared to the total solution volume, and when air agitation is utilised. Approximately 30% of hypophosphite is used to produce Ni-P, whilst the remainder produces hydrogen.

iii) Complexants

The complexant used depends primarily on the nickel concentration. Some formulations may use a single complexant whilst others use combinations to maintain a low free nickel ion concentration. Commonly used complexants are glycolic or lactic acid for acid based solutions and ammonium hydroxide for alkaline solutions. These are contained in the nickel replenisher solution to make bath management simpler.

iv) Buffers

Hydrogen ions produced during plating causes the pH of the solution to decrease and since pH is a major factor in controlling deposition rate and the

phosphorus content of the deposit, it must be stabilized using buffers. Common buffers include acetic or propionic acids and their salts. These acids also increase the deposition rate. Even when using buffer agents there is a slow fall in pH as plating occurs which may be corrected with ammonium hydroxide or potassium carbonate or in commercial solutions is contained in the reducer replenisher.

v) Stabilisers / brighteners

Stabilisers are used to prevent spontaneous decomposition of the plating solutions. Traditionally these included heavy metals such as lead or cadmium at very low concentrations (<1ppm). To comply with new ROHS regulations (see Appendix B) the heavy metals have been substituted in most commercial formulations, with compounds such as molybdate or iodates.

Since most solutions used in industry are proprietary, the full formulation is never known, thus requiring the solution to be carefully controlled for optimum results. Factors to control include

- i) Nickel concentration of the solution
- ii) Reducer concentration of the solution
- iii) Uniform solution temperature
- iv) Solution pH
- v) Filtration

Typically for a solution operating at pH4.5 the following effects have been previously noted

Effect of Temperature

Temp, °C	Deposition Rate, $\mu\text{m}\cdot\text{hour}^{-1}$	Phosphorus content of deposit
85	6	13.5%
90	13	10.4%
95	20	10.2%

Effect of pH

pH	Phosphorus content
4.5	10.2%
5.0	9.0%
5.5	7.2%

The area of work in the plating bath should be at least $50\text{cm}^2.\text{l}^{-1}$, to avoid solution decomposition, random plating out and edge misplating. During plating several breakdown products may form^[15], including sodium orthophosphate, sodium sulphate, hydrogen gas and hydrogen ions. These products can reduce the plating rate^[16], alter the pH and produce rough and porous coatings. Typically the concentration of free nickel ions in the solution are kept at low levels, since the orthophosphate breakdown product can cause precipitation of nickel phosphate which in turn produces rough deposits and induces premature decomposition of the plating solution^[17]. Additionally hydrogen ion production causes the pH of the solution to fall, which reduces the deposition rate and increases the phosphorus content of the deposit. This is the reason a buffer salt is required to stabilise the pH of the solution.

3.2 *Alloy Deposition*^[18]

Tungsten can be readily codeposited with electroless nickel-phosphorus^[101] up to 20% by weight of the composition. Lowering the citrate concentration of the plating solution results in lower tungsten and phosphorus contents but increases the deposition rate. These deposits may find applications where resistance to high temperatures are required, as the melting point of the deposit is substantially increased by the addition of the tungsten, which also increases its corrosion resistance. An example formulation is :

Nickel sulphate.6H ₂ O	7 g.l ⁻¹
Sodium tungstate.2H ₂ O	35 g.l ⁻¹
Sodium hypophosphite	10 g.l ⁻¹
Temperature	98°C

20g.l ⁻¹ sodium citrate			40g.l ⁻¹ sodium citrate			solution pH
Ni	W	P	Ni	W	P	
-	-	-	87.5	2.9	9.5	5.5
87.5	6.7	4.8	74.6	16.6	8.6	7.0
83.8	12.7	4.4	73.5	20.5	6.5	8.2
-	-	-	72.0	18.2	9.8	9.5

Additions of potassium perrhenate to an ammoniacal-alkaline electroless nickel-phosphorus produces alloys containing more than 45% rhenium and 2.3% phosphorus. The deposit has a melting point of approximately 1700°C

NiSO ₄ .6H ₂ O	30 g.l ⁻¹
NH ₄ Cl	50 g.l ⁻¹
Na ₃ C ₆ H ₅ O ₇ .2H ₂ O	85 g.l ⁻¹
KReO ₄	1.5 g.l ⁻¹
NaH ₂ PO ₂ .2H ₂ O	10 g.l ⁻¹
pH adjusted with NH ₄ OH	9
Temperature	98°C

A tertiary alloy of 9%W and 30% rhenium can be achieved by the addition of 10 g.l⁻¹sodium tungstate and 0.8 g.l⁻¹ potassium perrhenate to a standard alkaline nickel plating solution at pH 8.9 and operated at 98°C.

These are only some of the examples of electroless deposits which can be obtained. A more comprehensive listing of some of the more common plating solutions is contained within Appendix C, section 4.

3.3 *Composite Deposition*

The inclusion of finely divided particles within an electrolessly deposited matrix involves the need to maintain a uniform dispersion of the particulate material during the metal deposition.

Specialised knowledge and equipment are required to achieve successful high quality deposits^[67,85,99,100,104].

With regard to nickel-phosphorus systems it has been found^[13] that the co-deposition of the dispersed phase reduces the phosphorus content in the coating. This is connected to the structure of the Ni-P coating, which is a supersaturated solution of phosphorus in the nickel matrix. The particulates seem to be competitors in occupying the active centres in the matrix to the exclusion of the phosphorus. This may be additionally advantageous in our application in further reducing the phosphorus content and thus increasing the melting point of the deposit. Furthermore, reduction of the phosphorus content increases the degree of crystallinity of the deposit and therefore a possible increase in grain boundary length.

Zeta potential is a measure of the magnitude of the repulsion or attraction between particles. Its measurement brings detailed insight into the dispersion mechanism and is the key to electrostatic dispersion control and is therefore vitally important when co-depositing reinforcement particles. When a new suspension or emulsion is formulated, one of the biggest consumers of time is the measurement of the stability of the candidate formulations in a variety of conditions. Zeta potential can be used to test candidate formulations to reject poor examples at an early stage; reducing the cost of the stability study. This can also lead to an understanding of the mechanisms of stability, and hence help with research into product quality improvements.

Simple experiments can be performed to quickly understand this effect especially with regard to successful co-deposition and these will be further developed in the experimental section of the project. It is reported that the reinforcement in deposited coatings is affected by the Zeta Potential on the surface of the particles and that the potential is determined by the selection and addition of surfactants^[93,105]. Most reinforcement particles readily coagulate and precipitate in the plating solution. This decreases the probability of co-deposition and therefore a means of retaining the particles in suspension is required. The suspension of the particles can be evaluated by changes of transmittance as measured by a spectrophotometer, immediately after stirring. This could therefore give suspension times, if time based measurements are made and could be used to give comparisons between different surfactants.

Another simple test^[81] involves mixing solutions with fixed volumes of particles and monitoring their rate of sedimentation by reading the volumes of sediment in a measuring cylinder over time. Effects of the addition of surfactants could be evaluated by this method.

Possible surfactants for evaluation

Type	Chemical Name	Clouding Point
Non-ionic	Polyoxy ethylene nonyl phenyl ether (HL B=14)	333K
Non-ionic	Polyoxy ethylene nonyl phenyl ether (HL B=15)	343K
Non-ionic	Polyoxy ethylene nonyl phenyl ether (HL B=16)	350K
Non-ionic	Polyoxy ethylene nonyl phenyl ether (HL B=17)	358K
Cationic	Perfluoro alkyl trimethyl ammonium salt	
Cationic	Perfluoro alkyl ammonium salt	
Cationic	Perfluoro alkyl ammonium iodide	
Anionic	Perfluoro alkyl carboxylic acid ammonium salt	
Anionic	Perfluoro alkyl phosphate	
Anionic	Perfluoro alkyl sulphonic acid	
Anionic	Sodium lauryl sulphate (99) 0.1g/l {Sodium dodecyl sulphate (99) (C ₁₂ H ₂₅ SO ₄ Na)}	

In general, non-ionic surfactants defenate and become ineffective above a certain temperature, the so called “clouding point”.

Sodium lauryl sulphate or sodium dodecyl sulphate is an anionic surfactant. The molecule has a tail of 12 carbon atoms, attached to a sulphate group, giving the molecule amphiphilic properties required of a detergent. An amphiphilic molecule contains both hydrophilic and hydrophobic properties.

3.4 Deposition Rate, Coating Thickness and Deposit Morphology

As has been previously stated the deposition rate^[30] of the plating process can be greatly influenced by the following parameters.

- i) Solution composition
- ii) Maintaining the solution chemicals at optimal concentrations
- iii) Bath loading of particles
- iv) Surface area of substrate
- v) Deposit thickness
- vi) Particle surface morphology
- vii) Agitation^[23,108]
- viii) Solution temperature^[21]
- ix) pH^[102]

It is therefore critical that stringent control is maintained over the plating process to ensure repeatability and reproducibility. To overcome this problem the bath solution is prepared in 25 litre batches which can be split and used over multiple experiments. Chemical analysis of the plating solution can also be performed during long term experiments. It had been reported^[97] that with increasing coating thickness there is an increase in the percentage of co-deposited particles. Also the surface roughness increases and the deposits have an “orange peel” appearance or with lower phosphorus contents a rough surface with spherical particles on the deposit surface up to “cauliflower-like” nodules on high phosphorus deposits^[87], of approximately 0.9-21 μm in size. It is also vital that the solution volume to substrate surface area be maintained at a certain ratio, especially in light of the very high surface area of the particles which can act as catalytic sites. It was therefore planned to maintain the ratio whenever possible at 16.

For plating processes which only produce thin deposits, in the 1-5 μm range, then nanoparticles would be required for the co-deposition process, eg ruthenium and rhodium.

3.4.1 *Agitation Effects*

The use of ultrasonics^[34] during deposition greatly influences the reaction kinetics by

- i) increasing the hydrogen degassing at the catalytic sites
- ii) assists in maintaining the suspension of YSZ particles in solution
- iii) causes local thermal effects at the catalytic sites by introducing additional energy which can lower the thermal input required.

The cavitation effect lowers the surface energy especially affecting the first coating layers which can lead to greater coverage, decreased porosity and less defects.

Typically ultrasonic units operate at 15W and 530 kHz. Although the possibility of improving YSZ particle suspension would be beneficial, it is unclear if the detrimental effects on the porosity could be offset. Ultrasonics plus additional agitation in the form of argon gas at 5 l.hour⁻¹ increase the mass transfer coefficient.

Traditional agitation methods usually involve mechanical agitation by pumping or stirring methods or air agitation by either compressed air or inert gas. In recent years, nickel salt mists produced from air agitation methods have been documented as posing a health and safety risk. To overcome this problem more efficient mechanical agitation systems have been introduced which do not generate these harmful mists. Eductor nozzle systems which operate on a venturi principle can easily be fitted to a conventional mechanical pumping system. This also negates the requirement for a compressor or gas bottles to be situated on site.

Agitation is a necessity when performing co-deposition as the particles must be kept in suspension. Efficient agitation is required^[89] to ensure that high deposition rates are maintained during plating, as the agitation replenishes the ionic species at the catalytic sites. If the agitation decreases then there will be lower concentrations of the ionic species and subsequently reaction kinetics decreases. However with electroless deposition and especially co-deposition excessive agitation can also be detrimental, and careful experimentation is required to determine optimal agitation levels.

For the initial experimental work, air, mechanical and ultrasonic agitation methods would be evaluated and the results compared against samples prepared under standard conditions.

3.4.2 Bath Loading with Particles

As bath loading increases, bath deposition rates decrease^[89], due to the increase surface area of particles which can act as catalytic sites for nickel deposition. One gram of powder-like particles having a 1 μ m diameter contains 10^{12} particles with a total surface area of 150m². For silicon carbide particles bath loadings in the range of 15 – 25 g.l⁻¹ resulted in optimal deposits. Further papers^[67,85,99,100,104] have published results for other particulates of polymers or ceramics and in each case the optimal bath loading for each particulate material had to be established experimentally.

The optimal loading concentration needs to be established in conjunction with the bath agitation as the increased physical collision of particles with the surface is directly related to the entrapment rate of the particles into the deposit.

Additional research^[97] has shown that chemicals known as surfactants can be added to the plating solution, which assist in keeping the particles in suspension. This in turn increases the probability of substrate surface contact.

Ceramic	Chemical Formula	Electrical conductivity, S.cm ⁻¹	Electrical resistivity, Ω.cm	Ionic conductivity, S.cm ⁻¹	Coefficient of thermal expansion μm. °C ⁻¹
SDC ¹⁾	(Ce _{0.8} Sm _{0.2})O _{1.9}	-	-	>0.015 @ 600°C	12.7
Al ₂ O ₃ ⁱⁱ⁾	Al ₂ O ₃	-	2×10 ⁷	-	8.2
YSZ ¹⁾	(ZrO ₂) _{0.92} (Sc ₂ O ₃) _{0.08}	-		>0.2 @ 800°C	10.5
GDC ¹⁾	(Ce _{0.8} Gd _{0.20})O _{1.9}	-	-	>0.015 @ 600°C	13.4
LSM ¹⁾	(La _{0.80} Sr _{0.20})MnO _{3-δ}	>200 @ 800°C	-	-	10 - 11

Table 4 – Ceramic particles and their properties.

Notes

- i) Data obtained from Fuel Cell Materials.com
- ii) Data from CoorsTek

3.4.3 *Substrate Orientation*

The orientation of the substrate in the plating solution can be critical to uniform deposition. Previous studies^[89] have showed that samples positioned vertically with optimal agitation produced nickel deposits with uniformly dispersed particles which exhibited good adhesion to the substrate.

Further work^[91] with diamond particles reported that substrates positioned in the vertical orientation at a bath loading of $>10 \text{ g.l}^{-1}$ incorporated less than 20% diamond and the deposits were noncoherent. The same research reported bath loading at 2 g.l^{-1} in the horizontal orientation produced deposits with greater than 20% vol of reinforcement, and the deposits were smooth, adherent and coherent.

Similar contradictions for other research, with different particulate materials, has also been experienced and it is necessary to evaluate any new material and particle size individually by experimentation.

3.5 *Properties of Electroless Nickel*

There are major differences between electrodeposited^[47] and electroless nickel deposits that are associated with their purity and structure. Electrodeposited nickel typically has a purity of 99% or greater, whereas when sodium hypophosphite is used as a reducing agent in electroless nickel plating, a typical composition for the resulting deposit is 92% nickel and 8% phosphorous. The phosphorous content has a great effect on deposit properties and can be varied over a wide range, typically 3 – 12%.

The structure of electroless nickel is responsible for some of its unique properties^[25]. It is normally described as having an amorphous structure or one consisting of ultra-fine crystallites. With increasing phosphorous content the amorphous nature of the deposits dominates and above 10% is considered truly amorphous. The absence of a well defined crystal structure eliminates the possibility of intergranular corrosion.

Heat treatment of nickel-phosphorous deposits^[19,24,39,60] results in significant changes in properties and structure. X-ray diffraction examination shows substantial crystallinity and segregation of the nickel into small crystallites of two distinct phases, nickel metal and nickel phosphide (Ni₃P). Some volume shrinkage is associated with recrystallisation which can result in cracking.

3.5.1 *Physical Properties*

Density – the density of pure nickel is 8.9g.cm⁻³ whilst a 9% phosphorous content deposit is typically around 8g.cm⁻³.

Melting point – pure nickel has a melting point of 1455°C, but the phosphorous content of electroless nickel has a significant effect on its melting point which declines almost linearly down to the eutectic at 880°C for an 11% phosphorous deposit.

Electrical properties – the resistivity of high purity nickel is 7.8×10⁻⁶ Ω.cm, but that of electroless nickel can be as much as ten times greater. Typically, values are in the range of 30 – 100 ×10⁻⁶ Ω.cm. Heat treatment of the deposit decreases the resistivity and is most

significant at temperatures which cause a structural change by precipitation of nickel phosphide, ie $>260^{\circ}\text{C}$.

Thermal properties – the coefficient of thermal expansion varies from $22.3\mu\text{m}\cdot^{\circ}\text{C}^{-1}$ at 3% phosphorous to $11.1\mu\text{m}\cdot^{\circ}\text{C}^{-1}$ at 11% phosphorous. By comparison a high-purity electrodeposited nickel is typically $14 - 17\mu\text{m}\cdot^{\circ}\text{C}^{-1}$.

Mechanical properties – hardness is strongly influenced by the phosphorous content of the deposit. The hardness of electrodeposited nickel decreases significantly on heat treatment due to recrystallisation and grain growth. However, when an electroless nickel deposit is heat treated an increase in hardness results from the formation of a nickel phosphide phase.

CHAPTER 4. - Project Aims

The initial aim of the project was to determine the feasibility of the co-deposition of an electroless nickel / YSZ deposit and to evaluate the deposit for basic plated quality criteria, such as,

- i.* Adhesion
- ii.* Plating thickness
- iii.* Dispersion of ceramic particles
- iv.* Porosity
- v.* Nickel content

The secondary aim was to characterise the samples produced to determine their properties for further research. The initial analytical techniques which would be used to evaluate the deposits included,

- i.* X-Ray Fluorescence (XRF)
- ii.* Scanning Electron Microscopy (SEM)
- iii.* EDXA (energy dispersive X-ray analysis)
- iv.* Talysurf surface profiling
- v.* Standard adhesion testing

However during the course of the project other techniques were developed, and test apparatus and equipment was purchased through funding obtained from Scottish Enterprise.

Further samples were then manufactured for experimentation in a fuel cell stack to determine their efficiency under actual operating conditions and compared against conventional manufactured anodes.

It was hoped that further areas for research would be highlighted for evaluation and project plans put in place to finalise the experiments which would be performed in subsequent years.

CHAPTER 5. - Experimental

In this study, the electroless deposition route was evaluated to produce a nickel / YSZ composite directly onto the ceramic substrate of the SOFC. The traditional techniques for producing anode materials for SOFC's involves producing cermets through silk screening and subsequent sintering. Cermets produced in this fashion typically have defects due to coefficient of thermal expansion (CTE) mismatch of the anode and the electrolyte in the fuel cell. Additionally the sintering technique and reduction of nickel oxide produces larger nickel grains which reduces the cells performance.

The deposition of an electroless nickel / YSZ composite on a YSZ substrate would dramatically reduce the CTE mismatch within the cell and allow complex or simple shapes to be coated. Replacement of the sintering and reduction stages with a single plating operation would also be more cost effective and greatly simplify manufacture of any cell design.

Electroless deposition would also give a continuous electrical circuit and could be deposited on specific areas thus aiding cell design.

5.1 *Characterisation Techniques*

A review of the techniques and the standards used during the course of the experimental work are detailed as follows, however a summary is retained in Appendix C, section 3, along with electronic copies of the respective standards.

5.1.1 *Composition*

Deposited coatings were weighed, chemically stripped and analysed against traceable national standards by inductively coupled plasma-atomic emission spectroscopy (ICP-AES) as per the method detailed in ASTM B733-97. ASTM E60 was used to determine the phosphorus content of the deposit. Gravimetric analysis techniques can be utilised to determine the percentage mass of codeposited ceramic particles.

Additional qualitative and semi-quantitative compositional analysis was performed using Energy Dispersive X-ray Analysis (EDXA) on a scanning electron microscope.

5.1.1.1 ICP-AES

Inductively Coupled Plasma-Atomic Emission Spectrometry (ICP-AES) is one of the most common techniques for elemental analysis. Its high specificity, multi-element capability and good detection limits result in the use of the technique in a large variety of applications (<http://las.perkinelmer.co.uk/TechnicalSupport/default.htm>). All kinds of dissolved samples can be analyzed, varying from solutions containing high salt concentrations to diluted acids. A plasma source is used to dissociate the sample into its constituent atoms or ions, exciting them to a higher energy level. They return to their ground state by emitting photons of a characteristic wavelength depending on the element present. This light is recorded by an optical spectrometer. When calibrated against standards the technique provides a quantitative analysis of the original sample.

The ICP-AES is composed of two parts: the ICP and the optical spectrometer, see Figure 12. The ICP torch consists of three concentric quartz glass tubes and a coil of the radio frequency (RF) generator which surrounds part of this torch. Argon gas is typically used to create the plasma. When the torch is turned on, an intense magnetic field from the RF generator is turned on. The argon gas flowing through is ignited with a Tesla unit (typically a copper strip on the outside of the tube). The argon gas is ionized in this field and flows in a particular rotationally symmetrical pattern towards the magnetic field of the RF coil. A stable, high temperature plasma of about 7000 K is then generated as the result of the inelastic collisions created between the neutral argon atoms and the charged particles. A peristaltic pump delivers an aqueous or organic sample into a nebuliser where it is atomized and introduced directly inside the plasma flame. The sample immediately collides with the electrons and other charged ions in the plasma and is broken down into charged ions. The various molecules break up into their respective atoms which then lose electrons and recombine repeatedly in the plasma, producing light with characteristic wavelengths of the elements involved. One or two transfer lenses are then used to focus the emitted light onto a diffraction grating where it is separated into its component radiation in the optical spectrometer. The light intensity is then measured with a photomultiplier tube at the specific wavelength for each element line involved. The intensity of each line is then compared to

previous measured intensities of known concentrations of the element and its concentration is then calculated by extrapolation from a calibration graph.

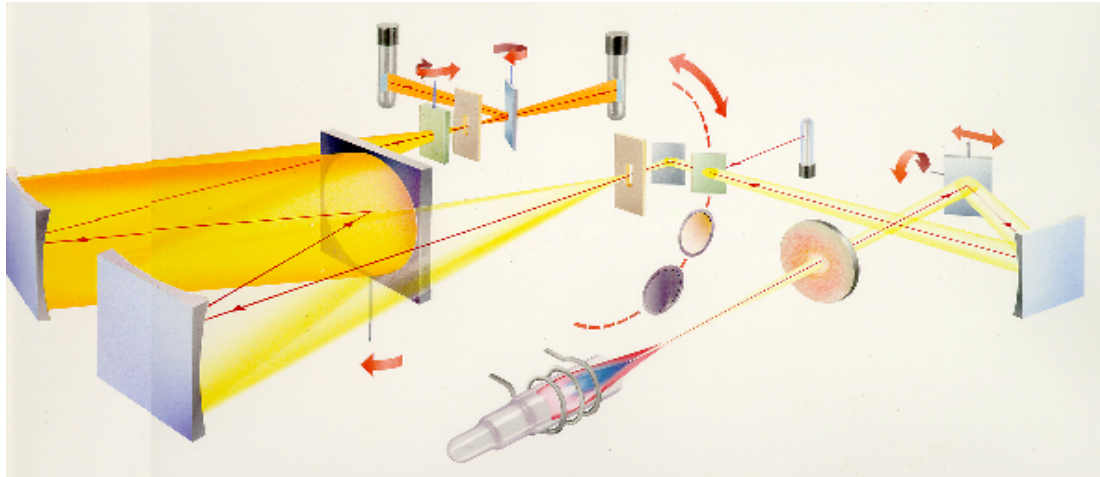


Figure 13 – Schematic layout of a typical ICP instrument.

(Image from Perkin Elmer instrument manual)

5.1.2 *Surface Topography* (roughness, Ra)

In many applications surface texture is closely related to function and this is certainly the case when applied to fuel cells. For the anode to be as efficient as possible it must have a significantly large surface area to increase the rate of reaction. One method of increasing surface area is to produce a rougher surface texture and another is by increasing its porosity. By combining both methods the maximum surface area can be achieved with hopefully the most efficient reaction kinetics.

Since individual roughness irregularities are too small to see with the naked eye, some form of magnifying device is required. First thought turns naturally to a microscope, but while this usually reveals the spacing of the horizontal pattern, it will not gauge the peaks and valleys as these are perpendicular to the surface and the relative heights are not revealed.

To achieve a ‘picture’ of the surface a very sharp stylus is drawn across the surface at a constant speed over a set distance. An electrical signal is obtained and amplified to produce a

much enlarged vertical image. This signal can be displayed on both graphical and screen outputs and the values of peaks and valleys, and roughness of the surface calculated.

The Ra (Roughness average) value of a surface is generated by averaging the roughness height of the surface profile. This parameter is most commonly used in surface texture analysis and has historically been called the centre line average (CLA) or arithmetic average (AA).

The figure 14 illustrates the derivation of Ra, in a typical surface profile where Ra is the mean height of the resulting profile. Mathematically Ra is the arithmetic average of the departure of the profile from the centre line throughout the sampling length.

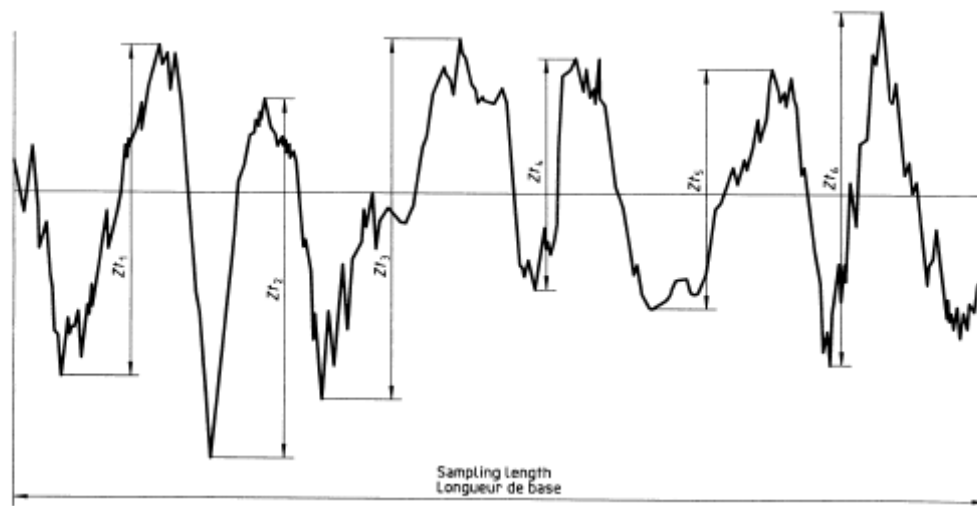


Figure 14 – Example of a roughness profile.

(Image from BS EN ISO 4287- 1997, Fig 9)

Additional comparative roughness evaluations were performed using a scanning electron microscope.

5.1.3 *Electrical Resistivity*

The four point electrical probe is a very versatile device used widely in physics and materials characterisation^[88,98] for the investigation of electrical phenomena. When a simple measurement of the electrical resistance of a test sample is performed by attaching two wires to it, the resistance of the contact point of the wires to the sample is also measured. Typically the resistance of the point of contact (called contact resistance) is far smaller than the

resistance of the sample, and can thus be ignored. However, when one is measuring a very small sample resistance, especially under variable temperature conditions, the contact resistance can dominate and completely obscure changes in the resistance of the sample itself. This is the situation that can exist when testing electrode deposits at fuel cell operating temperatures.

The effects of contact resistance can be eliminated with the use of a four point probe. A schematic of a four point probe is shown in Figure 15 below. In this diagram, four wires (or probes) have been attached to the test sample. A constant current is made to flow the length of the sample through probes labelled 1 and 4 in the figure. This can be done using a current source or a power supply as shown. Many power supplies have a current output readout built into them. If not, an ammeter in series with this circuit can be used to obtain the value of the current. If the sample has any resistance to the flow of electrical current, then there will be a drop of potential (or voltage) as the current flows along the sample, for example between the two wires (or probes) labelled 2 and 3 in the figure. The voltage drop between probes 2 and 3 can be measured by a digital voltmeter. The resistance of the sample between probes 2 and 3 is the ratio of the voltage registering on the digital voltmeter to the value of the output current of the power supply. The high impedance of the digital voltmeter minimizes the current flow through the portion of the circuit comprising the voltmeter. Thus, since there is no potential drop across the contact resistance associated with probes 2 and 3, only the resistance between probes 2 and 3 is measured.

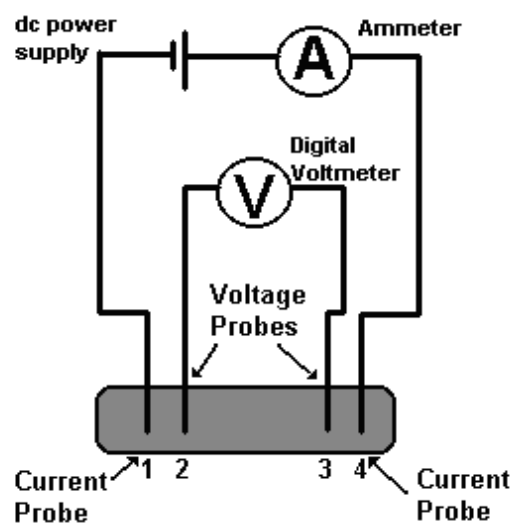


Figure 15 – schematic of four point probe set-up.

[Image from Images Scientific Instruments Inc]

According to four point probe theory,

The resistivity of a semi-infinite volume is given by;

$$\rho_0 = 2\pi s \frac{V}{I} \quad (3.5)$$

Where the interprobe spacing $s_1 = s_2 = s_3 = s$,

I is the current

V is the measured voltage

and ρ_0 is the measured value of the resistivity and is equal to the actual value, ρ , only if the sample is of semi-infinite volume.

However practical samples are of finite size, therefore ρ is not equal to ρ_0 and correction factors for different boundary configurations are required.

When the thickness, t , is $\leq 5s$ the true resistivity is expressed as;

$$\rho_0 = 2a\pi s \frac{V}{I} \quad (3.6)$$

Where a is a thickness correction factor and

$$a = K \left(\frac{t}{s} \right)^m \quad (3.7)$$

And K is the value of a at $(t/s)=1$, and m is the slope. Therefore

$$a = 0.72 \frac{t}{s} \quad (3.8)$$

When equation 5.4 is substituted into equation 5.2, it results in

$$\rho_0 = 2\pi sa \frac{V}{I} = 4.53t \frac{V}{I} \quad \text{for } t/s \leq 0.5 \quad (3.9)$$

This value of ρ is referred to as the bulk resistivity, R_s , with units of $\Omega \cdot \text{cm}$.

If both sides of equation 5.5 are divided by t , it produces

$$R_s = \frac{\rho}{t} = 4.53 \frac{V}{I} \quad \text{for } t/s \leq 0.5 \quad (3.10)$$

Which is referred to as the sheet resistance. When the thickness, t , is very small, then this is the preferred measurement parameter.

The sheet resistance measurements made on a typical button cell are not large compared to the probe spacing. A correction factor, C , for the geometry effects produces equation 5.7, and R_s is expressed in Ω .

$$R_s = C \frac{V}{I} \quad (3.11)$$

and when $d/s > 40$, then $C = 4.53$

Conductivity, σ , is expressed as:

$$\sigma = \frac{1}{\rho} \quad \text{with units } \text{S} \cdot \text{cm}^{-1} \quad (3.12)$$

Resistivity measurements at room temperature are relatively easy with commercially available equipment. However, high temperature measurements under fuel cell operating conditions can be extremely problematic. The lack of commercially available equipment which was capable of these high temperature measurements resulted in new apparatus having to be designed. Technical drawings and models were produced, see Appendix 1, and test apparatus is under construction which could be marketed by any spin out company.

5.1.4 X-Ray fluorescence

The principle of energy dispersive X-ray fluorescence involves the radiation from an x-ray tube exciting the sample to emit x-ray fluorescence radiation, which is characteristic for each element, as illustrated in Figure 16. The detector registers the energy spectrum and the elements contained in the sample can be identified from their characteristic energies of the peaks detected in the spectrum. The concentrations of the elements, or the coating thicknesses respectively, can be determined by the intensity of their radiation portions. A proportional counter tube or a semiconductor detector delivers the measured signal. Typically the technique conforms to ASTM B568 or BS EN ISO 3497.

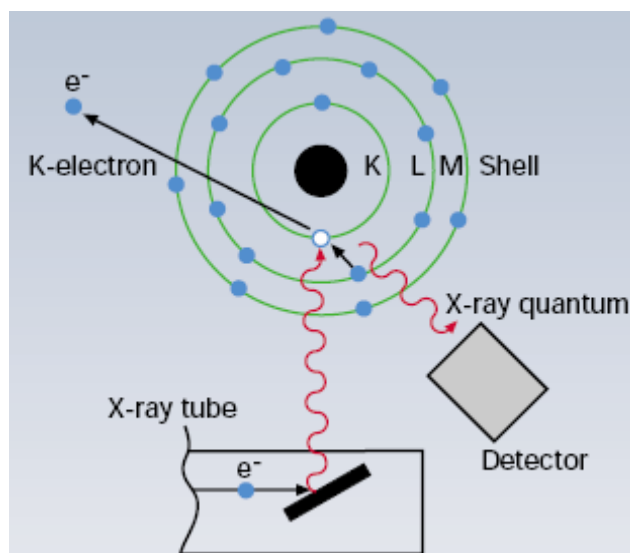


Figure 16 – Effect on an atom when bombarded by x-ray radiation.

[Image from Fischer Instrumentation GB, XRF instrumentation brochure]

5.1.5 Porosity

A porosity test expresses either the number of pores in a coating or the area of substrate exposed through pores in the coating. Typical surface coatings require there to be little or no porosity as this can affect the corrosion performance. However as has been previously stated porosity is an essential parameter for fuel cell applications.

For metallic substrates there are numerous testing methods⁽⁶⁸⁾ based on chamber testing with various aggressive corrosive mists which reveal the pores presence through reaction and discolouration of the substrate.

ASTM B920 and ASTM B809 are commonly used test specification, but unfortunately the vast majority of the methods described within them only work on metallic substrates.

5.1.5.1 *Mercury porosimetry*

Mercury porosimetry characterises a material's porosity by applying various levels of pressure to a sample immersed in mercury. The pressure required to intrude mercury into the sample's pores is inversely proportional to the size of the pores.

During an analysis, a sample is loaded into a penetrometer, which consists of a sample cup connected to a metal-clad, precision-bore, glass capillary stem. The penetrometer is sealed and placed in a low pressure port, where the sample is evacuated to remove air and moisture. As pressure on the filled penetrometer increases, mercury intrudes into the sample's pores, beginning with those pores of largest diameter. Mercury porosimetry is based on the capillary law governing liquid penetration into small spaces. This law, in the case of a non-wetting liquid like mercury, is expressed by the Washburn equation:

$$D = \left(\frac{1}{\rho} \right) 4\gamma \cos \phi \quad (3.13)$$

where D is the pore diameter, P is the applied pressure, γ the surface tension of mercury and ϕ the contact angle between the mercury and the sample, all in consistent units. The volume of mercury V penetrating the pores is measured directly as a function of applied pressure. This P-V information serves as a unique characterisation of pore structure.

The Washburn equation assumes that all pores are cylindrical. Although pores are rarely cylindrical in reality, this equation provides a practical representation of pore distributions, yielding very useful results for most applications.

As pressure increases during an analysis, pore size is calculated for each pressure point and the corresponding volume of mercury required to fill these pores is measured. These measurements taken over a range of pressures give the pore volume versus pore size distribution for the sample material.

Mercury porosimetry can determine a broader pore size distribution more quickly and accurately than other methods. Comprehensive data provide extensive characterisation of sample porosity and density. Typical results include:

- Total pore volume
- Incremental volume
- Differential volume
- Log-differential volume
- % of total volume
- Total pore surface area
- Incremental area
- Median or mean pore diameter
- Pore size distributions
- Sample densities (bulk and skeletal)
- % porosity

5.1.6 *Surface Mapping*

By combining the SEM images and the compositional analysis obtained from EDXA spectra a compositional map of the surface of a deposit can be produced. Additionally software packages can be used to highlight specific features on a surface and can determine the area percentages. These can also be used to determine the degree of porosity, percentage ceramic, or percentage nickel.

5.1.7 *Microscopy*

Optical microscopy is a standard tool used in material characterisation. Combinations of both low and high power magnification in conjunction with digital imaging would be utilised in the course of the experimental examination of the electrodes produced.

5.1.8 *Dilatometry*

A dilatometer measures the expansion of a material when it is heated. A small sample of the material is placed into the instrument and then heated (or cooled) or in the case of a fuel cell material, cycled through heating and cooling to determine the long-term effects.

In pushrod Dilatometry a dimensional change caused by subjecting a sample to a change in temperature is measured. In principle, a simple arrangement is shown in Figures 17a and b. The sample pushes the two rods (A and B) as it is being heated, hence the name "pushrod". The sample will expand an amount shown by the shaded area, ΔL_s . However it is clear that this configuration will not produce the desired ΔL_s , since portions of both rods A and B are in the controlled environment, it is inevitable that they themselves will also expand (ΔL_A and ΔL_B respectively). Thus, the measured value of $(\Delta X_A + \Delta X_B)$ will contain $(\Delta L_A + \Delta L_B)$ in addition to ΔL_s . The sample's length change, ΔL_s , can therefore be written as:

$$\Delta L_s = (\Delta X_A - \Delta L_A) + (\Delta X_B - \Delta L_B) \quad (3.14)$$

Unless one can assign values to ΔL_A and ΔL_B , the true magnitude of ΔL_s cannot be determined from the measured values of ΔX_A and ΔX_B alone. Obviously, if ΔL_A and ΔL_B are

not present at all, the measurement becomes absolute, but as long as this is not the case, the measurement is, in principle, a relative one.

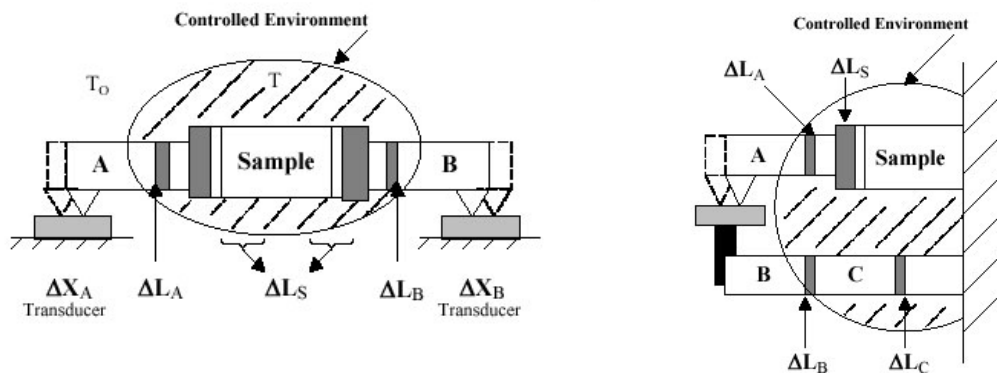


Figure 17 – An overview of Dilatometry.

(Image from Thermal Analysis Coursework, Netzsch Instruments, Daytona Beach 2009)

Commonly, very low expansion materials such as fused silica are used for rods A and B, and, for many applications, this is enough to reduce inaccuracies to a small fraction of the measured values when high expansion materials are examined. There are two basic types of dilatometer:

a. Standard Dilatometer

It is the basic device as previously described. To calibrate this kind of device, a standard or reference sample is tested repeatedly first and a calibration factor for the tube is then computed from these tests. The calibration factor is used when unknown materials are tested.

b. Differential Dilatometer

This device always measures the difference between two samples. The two samples are placed into the dilatometer tube, side-by-side, and two push-rods are used to track each sample independently. Since the measurement is one versus the other sample, the tube has no

other purpose than to support the samples. A differential dilatometer can be calibrated similarly to the standard dilatometer, but most frequently it is operated with the reference in place of one sample.

5.1.9 *UV-Vis spectrophotometry*

Many molecules absorb ultraviolet or visible light. Absorbance (A) is directly proportional to the path length, b , and the concentration, c , of the absorbing species. *Beer's Law* states that

$$A = \epsilon cb \quad (3.15)$$

where ϵ is a constant of proportionality, called the *absorbivity*.

Different molecules absorb radiation of different wavelengths. An absorption spectrum will show a number of absorption bands corresponding to structural groups within the molecule. The absorption of UV or visible radiation corresponds to the excitation of outer electrons. There are three types of electronic transition which can be considered;

1. Transitions involving π , σ , and n electrons
2. Transitions involving charge-transfer electrons
3. Transitions involving d and f electrons

When an atom or molecule absorbs energy, electrons are promoted from their ground state to an excited state. In a molecule, the atoms can rotate and vibrate with respect to each other. These vibrations and rotations also have discrete energy levels, which can be considered as being packed on top of each electronic level.

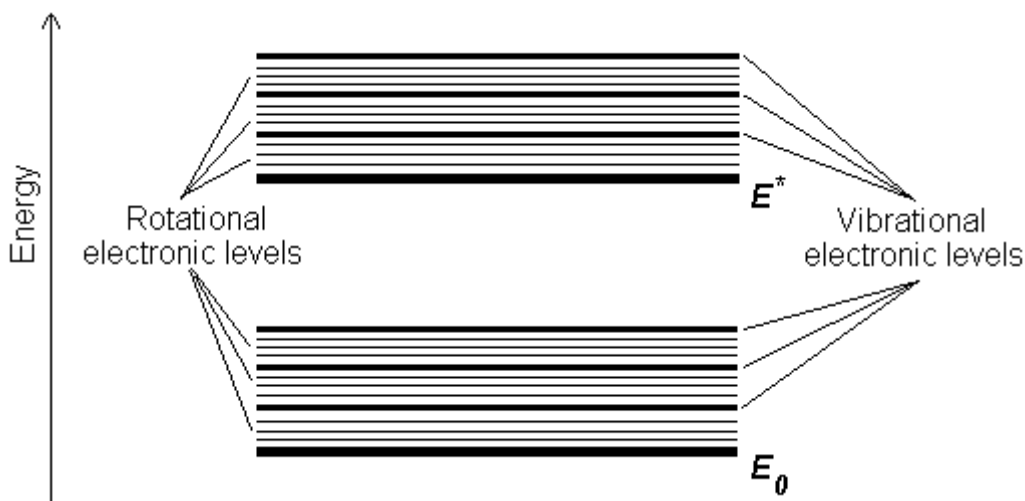


Figure 18 – Energy levels states.

(Image from Perkin Elmer UV-Vis spectrophotometry instruction manual)

Absorption of ultraviolet and visible radiation in organic molecules is restricted to certain functional groups that contain valence electrons of low excitation energy.

5.1.10 Scanning Electron Microscopy

Surface characteristics and compositional analysis of the samples were examined using a Cambridge Stereoscan 90 Scanning Electron Microscope (SEM) and an i-Scan Micro imaging system (EDX) using standard techniques.

A scanning electron microscope has many advantages over traditional microscopes.

1. The SEM has a large depth of field, which allows more of a specimen to be in focus at one time.
2. It also has a much higher resolution, so closely spaced specimens can be magnified at much higher levels.
3. As a SEM uses electromagnets rather than lenses, there is increased control in the degree of magnification.

A SEM produces a largely magnified image by using electrons instead of light to form an image. A beam of electrons is produced at the top of the microscope by an electron gun.

This beam follows a vertical path through the microscope, which is held within a vacuum. The beam travels through electromagnetic fields and lenses, which focus it down toward the sample. Upon the beam hitting the sample, electrons and X-rays are ejected. Detectors collect these X-rays, backscattered electrons, and secondary electrons and convert them into a signal that is sent to a display screen, which produces the final image. This is illustrated in Figure 19.

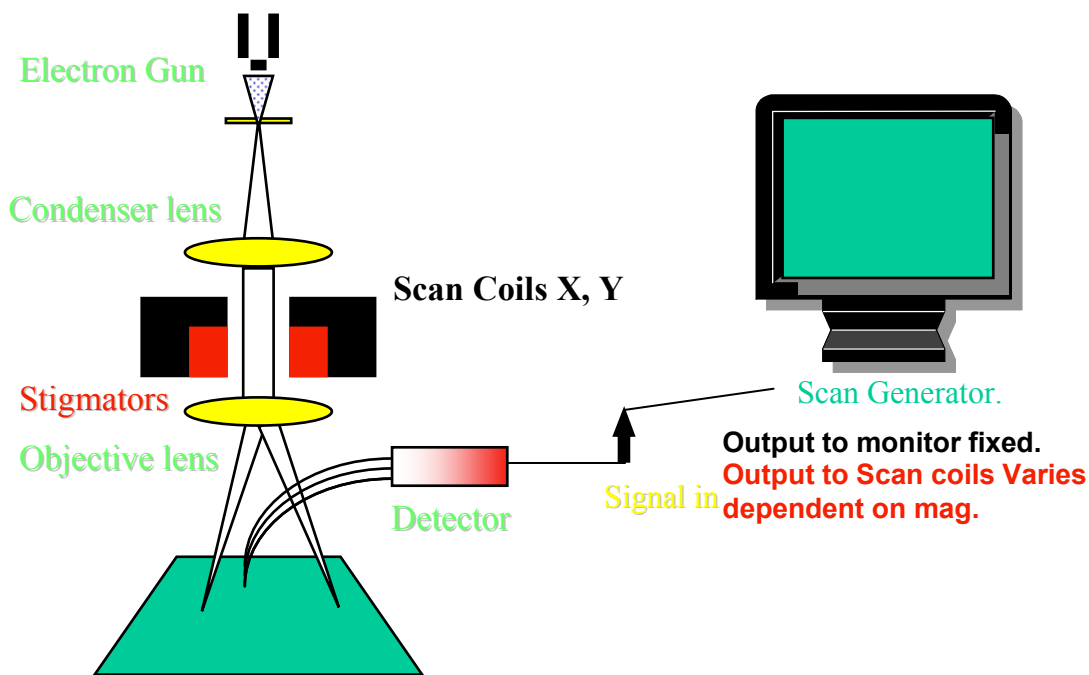


Figure 19 – Diagram of basic layout of a SEM.
(Image from Hitachi S4800 training presentation)

A typical SEM has the ability to analyze a particular sample utilizing several methods. Unfortunately, each type of analysis considered is an additional peripheral accessory for the SEM. The most common accessory equipped with a SEM is the energy dispersive x-ray detector or EDX. This type of detector allows a user to analyze the molecular composition of a sample.

5.2 Fuel Cell Testing

When performing fuel cell testing the following parameters must be considered and reported to ensure consistency between tests and test facilities.

5.2.1 *Wetting and drying gases.*

The standard level of water in a 'wet gas' is 3% by volume, which can be made by bubbling the test gas through a container of water at 25°C, but if the temperature of the surrounding apparatus is below the dew point then condensation can be a problem.

Drying gases is straightforward and normally involves passing the gas through a tube or column packed with a drying agent such as molecular sieve or phosphorous pentoxide.

Wherever possible gas flow rates should be stated in units of dm^3s^{-1} , which is the standard convention in fuel cell research.

5.2.2 *Standard hydrogen mixture.*

The use of dry hydrogen is not recommended since it imposes low oxygen partial pressures in the system. The 'wet' gas mixtures emulate more realistically the gases likely to be encountered in the fuel supply in commercial SOFC systems and stacks.

In the testing of half cells, a hydrogen/water mixture diluted in an inert carrier gas should be used, since this constitutes less of an explosion risk. Two recommended mixtures which will be initially considered are,

- i. Hydrogen saturated with water vapour (3%) at 25°C
- ii. Hydrogen saturated with water vapour (3%) at 25°C, balance inert gas.

5.2.3 *Standard cathode gas compositions*

For most applications dry air is recommended (21% oxygen + 79% nitrogen), but some studies may require water vapour, while others may require oxygen. The three compositions are listed below,

- i. Dry air
- ii. Wet air (3% water)

- iii. Dry oxygen

5.2.4 *Standard mixtures for conductivity measurements*

- i. Oxygen and inert gas
- ii. Hydrogen + water + inert gas

Accurate and repeatable control of the gas mixture can be achieved by using mass flow controllers which, due to their low drift, allow measurements to be made over an indefinite period. The use of rotameters (without pressure control) is not recommended since there is no provision for maintaining the flow rates accurately over long periods of time, which will certainly be required for service life testing.

5.2.5 *Temperature and duration*

Before measurements start, the sample should be stabilised at or above the highest temperature for a stated period of time. Measurements should then be made at decreasing temperatures.

5.2.6 *Conductivity measurements*

The relative density or porosity of the sample material must be specified, as well as the average grain size. The conductivity must be accompanied by the oxygen activity and temperature measurement. The recommended practice for measuring the conductivity of conductors involves the use of four-point contacts, two for current and two for voltage. This eliminates the impedance of the electrodes as well as the connecting leads. Both AC and DC measurements are possible by this technique.

Measured values of resistance less than 1Ω should be calibrated by measurements on a known standard with a resistance in the same order of magnitude as the sample under investigation.

Independent of the conductivity, the accuracy of this method is limited by the accuracies in the,

- a. Measurement of the distance between the voltage probes and the sample cross section in the region of the test area.
- b. Current uniformity between the voltage probes.

The distance between the neighbouring points must be an order of magnitude larger than the thickness of the film.

Four-point DC measurements were performed to determine the conductivity of the deposited anodes at different temperatures. An electric current was passed through while the temperature was stepwise reduced from 900°C to room temperature. Platinum wires were used as the lead connectors from the test apparatus to the measurement devices.

5.2.7 Cell Testing

High frequency AC or impedance spectroscopy measurements should be used to eliminate electrode impedances. The ohmic resistance of the electrodes cannot usually be eliminated by AC techniques and must thus be known or negligible. The lead resistance may be eliminated by still using four leads for the two electrodes. In more conductive materials, grain boundaries may be relatively resistive. They can contribute to the materials resistance, which may be seen in impedance spectroscopy at temperatures up to 700°C. Determination of grain boundary resistance is particularly important in zirconia electrolyte materials. Values for grain boundary resistance (or alternatively conductivity) can be expressed in various ways.

- a. Simply using the sample geometry, this gives a relative value with units of $\Omega\cdot\text{cm}$. This value is practical so as to compare with the bulk resistivity for the user of the actual material, but says nothing of the volume resistivity of the grain boundary phase.
- b. Using the known microstructure of the material to estimate the product of the grain boundary resistivity and the grain boundary thickness, in units of $\Omega\cdot\text{cm}^2$.
- c. Using the estimated grain boundary thickness to calculate the true resistivity of the grain boundary phase, in $\Omega\cdot\text{cm}$.

5.2.7.1 Half Cell Measurements

Half cell measurements are the primary investigative method in developing new electrodes. For the sake of clarity in reporting it is recommended that standard terms are adopted in describing cell geometry and gas control. However to date no internationally adopted standard has been published, but currently a number of working committees are working on this issue.

5.2.7.2 Divided and undivided cells.

A cell sandwiched between two different gas atmospheres is referred to as a divided cell, whereas a cell surrounded by a single gas environment is referred to as an undivided cell.

5.2.7.3 Symmetric and Asymmetric cells.

A symmetric cell has identical electrodes on both sides of the electrolyte membrane, whereas an asymmetric cell has different electrode materials. The most common type of asymmetrical cell has three electrodes comprising working, counter and reference electrodes. The terminology is taken in the electrochemical sense, hence the working electrode corresponds to the electrode which is under study. The counter electrode corresponds to the opposite current carrying electrode positioned on the opposite side of the electrolyte membrane to the working electrode. The reference electrode is used as a common point for controlling and measuring the potential of the working electrode, and does not carry any appreciable current. Where a potentiostat or galvanostat is used then the reference electrode lead is a very high impedance, and should therefore be protected by screening.

5.2.7.4 Thermal Cycling.

The ability of the half cell to withstand thermal cycling should be noted and it is customary to perform at the minimum three, but normally ten cycles from room temperature to the operating temperature. The reported figures should include heating and cooling rates, maximum and minimum temperatures and dwell times. A typical heating rate adopted for this study was $100^{\circ}\text{C hour}^{-1}$. It should be noted that divided cells do not withstand thermal cycling particularly well, due to sealing issues.

5.2.7.5 Ageing

This is related to the thermal cycling and refers to the decay in performance over long periods of time, normally in 1000 hour intervals. Ageing studies should only be performed post thermal cycling.

5.2.8 Electrochemical Impedance Spectroscopy

Electrochemical techniques are extremely useful in evaluating batteries and cells in service and also in comparing existing and new designs for performance. Electrochemical Impedance Spectroscopy (EIS) can provide detailed kinetic information, as well as monitoring in-cell properties under different operating conditions. EIS is a very sensitive technique, and can be used in a variety of applications such as,

- Testing and characterisation of fuel cells, batteries and superconductors.
- Corrosion studies and evaluation of coatings
- Evaluation of nanotechnology and microelectrodes

The EIS technique is now widely applied to the study of batteries and fuel cells^[83]. During EIS experiments, a small amplitude AC signal is applied to the system being studied. Therefore EIS is a non-destructive method for the evaluation of a wide range of materials, including coatings, anodised films, corrosion inhibitors, and can provide detailed information of the systems under examination. Parameters such as corrosion rate, electrochemical mechanisms, reaction kinetics, detection of localised corrosion, battery life and fuel cell performance can all be determined from this data.

Electrical impedance measurements can either be taken directly with an impedance analyser or with the combination of a Frequency Response Analyser (FRA) and an Electrochemical Interface (EI), as illustrated in Figure 20. A new integrated system is now available from Solatron called Modulab and one of these units has been purchased to further evaluate SOFC's manufactured under the Proof of Concept program sponsored by Scottish Enterprise. The technical brochure for this instrument is attached in Appendix C, Section 2.

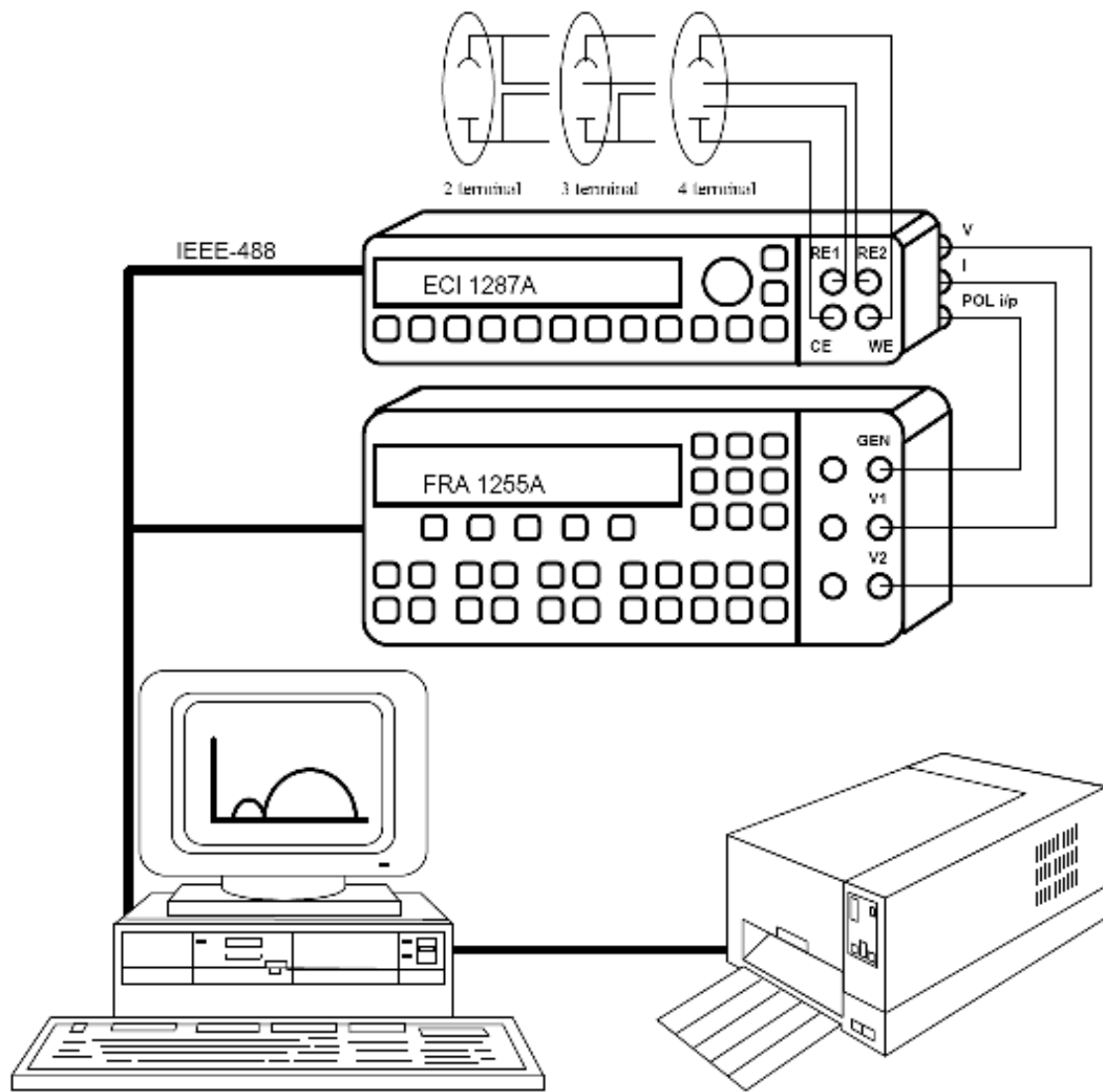


Figure 20 – Impedance Analyser set-up
(Image from Solartron Analytical application notes)

Impedance measurements have been widely used in the study of fuel cells and especially for the in-situ characterisation of experimental fuel cells.

EIS was initially used to determine the ionic conductivity of SOFC's and it is still used extensively for this application. The particular equivalent circuit is shown as follows for this application.

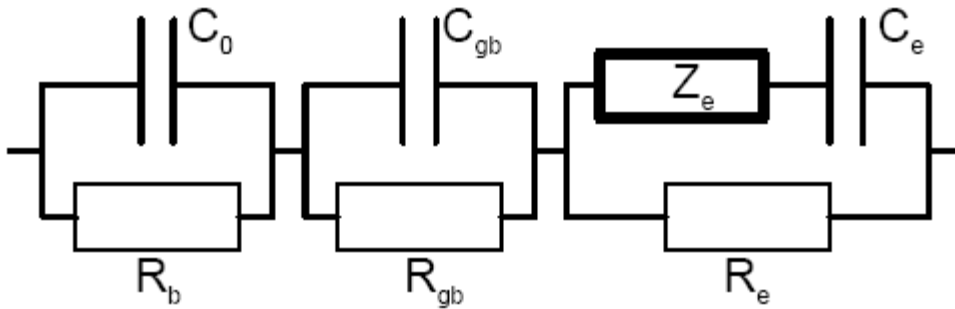


Figure 21 – Equivalence circuit for ionic conductivity of SOFC's
(Image from Solartron Analytical application notes)

- Where
- R_b is the bulk resistance
 - C₀ is the corresponding capacitance
 - R_{gb} is the grain boundary resistance
 - C_{gb} is the grain boundary capacitance
 - R_e is the kinetic resistance
 - C_e is the capacitance of the electrode
 - Z_e is the mass transfer contribution

EIS analysis should incorporate the development of a model through continual interpretation of the raw data^[75,82]. It was therefore proposed to use the flow diagram originally Orazem and Tribollet^[72], which is depicted in Figure 22.

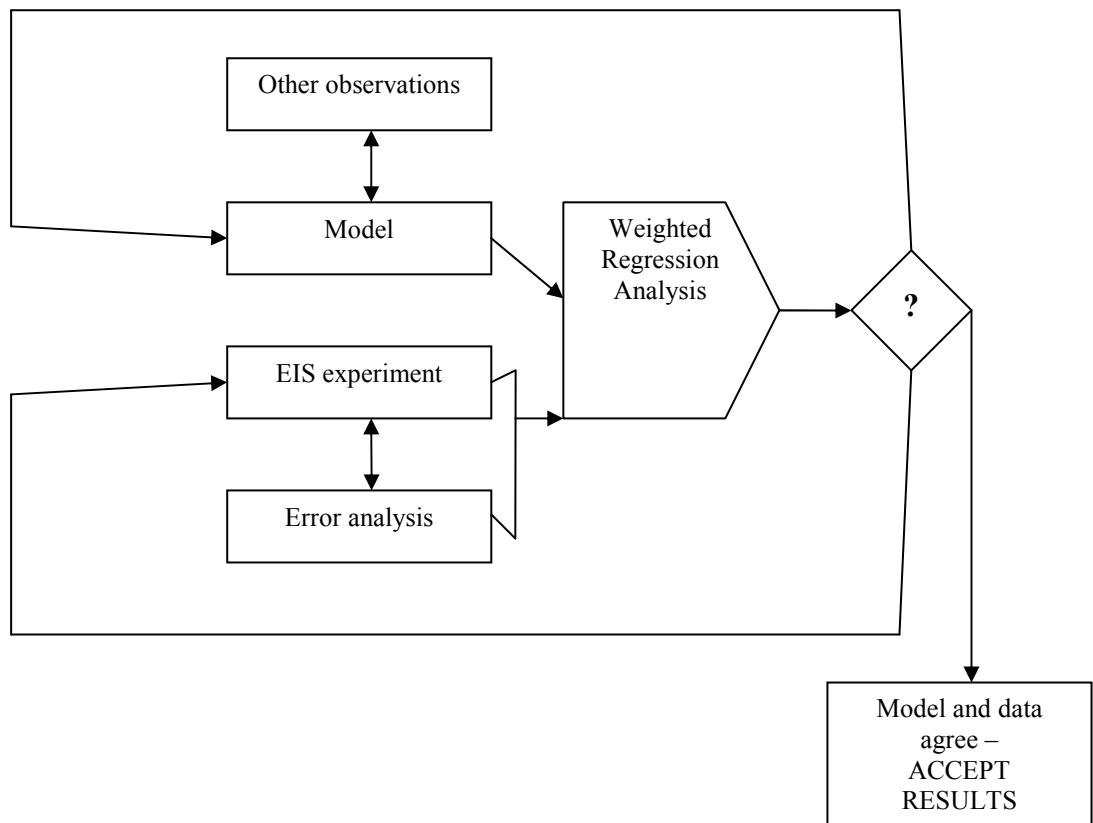


Figure 22 – Model for interpretation of EIS results^[72]

This model enables the analyst to correlate the experimental data, with the observations, and integrate this into the model which can constantly be updated to reflect any new experimental data.

The standard characterisation procedure for electrochemical systems is carried out in four steps,

1. Apply an electrical stimulus to the system under investigation
2. Observe the response.
3. Generate a mathematical impedance model or equivalent circuit
4. Identify the model parameters.

Generally the methods of characterising impedances are subdivided into frequency methods and time domain methods. EIS is an established frequency domain method, with Current Interrupt (CI) as the most common time domain method.

The approach of EIS is to measure impedance by applying successively single-frequency currents to the system and measuring the real and imaginary parts of the resulting voltage at that single frequency. Measuring the frequency response yields an impedance spectrum by nonlinear complex parameter identification. The prerequisites for good impedance spectra, known as the Kramer-Kronig conditions, are

- Linearity
- Causality
- Stability
- And finiteness of the system under investigation.

Consequently, an impedance spectrum of a nonlinear system, such as a fuel cell, is only valid in the neighbourhood of the operating point.

The main disadvantages of EIS are the relatively long measurement times involved and the expensive capital costs of the equipment.

5.2.8.1 Cathode testing by EIS

The complex, multi-step oxygen reduction continues to be an active field for investigation,^[38] since the determination of the rate-limiting step is extremely important for the optimisation of the cathode performance.

The two step reaction equivalent circuit and complex plane impedance diagram is depicted as illustrated in Figure 23, which shows the following information

- Initial Circuit resistance, R_1 , of $\sim 25\text{k}\Omega$
- Time constant A, first semicircle, indicates RC circuit (R_2C_1 , where R_2 is $\sim 85\text{ k}\Omega$)
- Time constant B, second semicircle, indicates RC circuit (R_3C_2 , where R_3 is $\sim 200\text{ k}\Omega$)

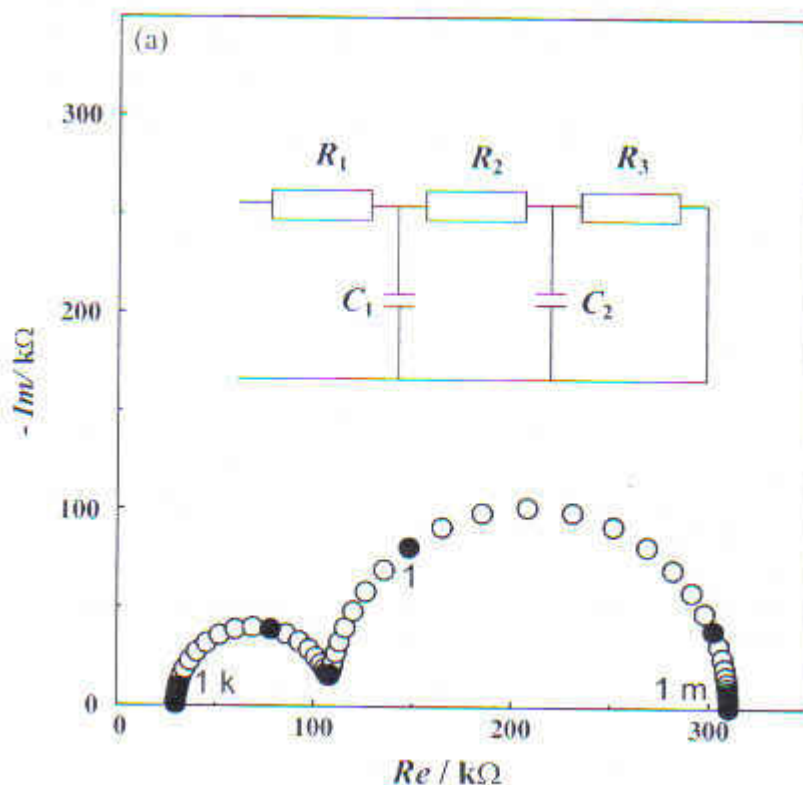


Figure 23 – Example of multi-step oxygen reduction at cathode.

(Image from *Electrochemical Impedance Spectroscopy Course, University of Bath, 2009*)

For LSM-based cathodes^[73] ion transport in the bulk is recognised as the rate-limiting step.

5.2.8.2 Anode testing by EIS

The anode reaction in SOFC's^[74] actually occurs in a limited active region inside the anode in an approximate 10 μ m layer adjacent to the anode / electrolyte interface. The anode reaction in the active region is limited by the spatial limitations of hydrogen supplied by gaseous diffusion through the anode pores, oxygen supplied by a solid – state vacancy transport mechanism through the YSZ phase of the anode, and electrons supplied through Ni phases of the anode.

Within the anode active zone, the reaction actually occurs at the triple phase boundaries among the gaseous fuel, the Ni phases, and the YSZ oxygen ion conductor. Therefore, the electrochemical cell performance^[74] of SOFC's in which the active layer in the anode is optimised can be maximised.

It is therefore extremely important to determine the porosity and the pore distributions of the anode, consisting of the anode support and the active layer, as well as the electrolyte. A series of further experiments using a mercury porosimeter are proposed for a future date.

It was previously reported^[74] that the porosities of the anodes decreased when the thicknesses of the anode active layer increased. It was therefore even more apparent that optimising the porosity of the anodes was vitally important to the successful development of an optimised anode.

5.3 *Experimental Materials*

The YSZ powder used in this study was manufactured and supplied by Unitec Ceramics Ltd, which had a nominal particle size of 2µm and was stabilised with 8% by weight of yttria.

YSZ substrates were supplied by Edinburgh Napier University and Fuel Cells Scotland for evaluation purposes as detailed in Table 1. Additional samples of brass substrates which were used in the initial experiments were supplied by Aerospace Machining Ltd (AMT Ltd).

AMT Ltd also provided the plating chemistries and the facilities for carrying out the plating operations. All non-proprietary solutions were prepared using Analytical Reagent (AR) grade chemicals and high purity deionised water. The electroless nickel chemistry was manufactured by Schloetter Company Ltd under the Tradename of Slotonip 2010. It produced a bright mid-phosphorous (6 – 9%) nickel deposit. The sensitising and activator solutions were manufactured by AlfaChimici under the tradename of Uniphase PHP.

Sample	Type	Description
1	Metallic	Polished brass sheet, 1mm thick (AMT Ltd)
2	Non-metallic	YSZ coated polymer film (Napier Uni)
3	Non-metallic	YSZ fuel cell substrate, tile (Fuel Cell Scotland)
4	Metallic	Aluminium alloy 6082 (AMT Ltd)
5	Non-metallic	Alumina tiles (purchased from Coors Tech)

Table 5 – Details on substrates used in experiments.

5.4 Initial Pre-treatment and plating.

Initially polished brass panels, 25mm × 20mm × 1mm were coated with the composite coating to establish if the process was feasible. The samples were degreased, electrocleaned and rinsed in deionised water prior to deposition of the coating. The coating that was deposited adhered to the substrate and it was uniform over its entire surface. The initial success with these metallic substrates prompted further experiments with non conducting ceramic substrates which are currently used in fuel cells.

To perform electroless deposition on insulating materials it is necessary to sensitise and activate^[1] the substrate surface. Therefore samples of a typical YSZ substrate were coated with the Nickel /YSZ after pre-treatment following the process sequence detailed in table 6. One batch of the substrates was treated in the as supplied condition using the aforementioned pre-treatment.

Process sequence	Make Up	Temperature, °C	Time, Minutes
Slotoclean FSA	As per manufacturer's instructions	60	15
Rinse	Deionised water	room	
Uniphase PHP Pre-catalyst	200g.l ⁻¹ part A + 20ml.l ⁻¹ HCl	20	15
Uniphase PHP Catalyst	200g.l ⁻¹ part A + 20ml.l ⁻¹ HCl + 20ml.l ⁻¹ part B	35	15
Rinse	Deionised water	room	
Electroless Nickel	As per manufacturer's instructions	89	30
Rinse	Deionised water	Room	
Rinse	Propan-2-ol	Room	
Air dry		Room	

Table 6 - Process procedure for pre-treatment of YSZ samples.

50g.l⁻¹ of the YSZ powder was added to the electroless nickel solution and kept in suspension through mechanical stirring. The solution was heated and the temperature maintained at 89°C using a Jenway hotplate /stirrer.

All plating operations were carried out within 3 hours of the pre-treatment chemistries being prepared to minimize any possible effects of degradation of the chemicals.

Initial SEM images were taken of the untreated YSZ powder which provided a baseline for subsequent testing of the treated samples. The results are attached as figure 24.

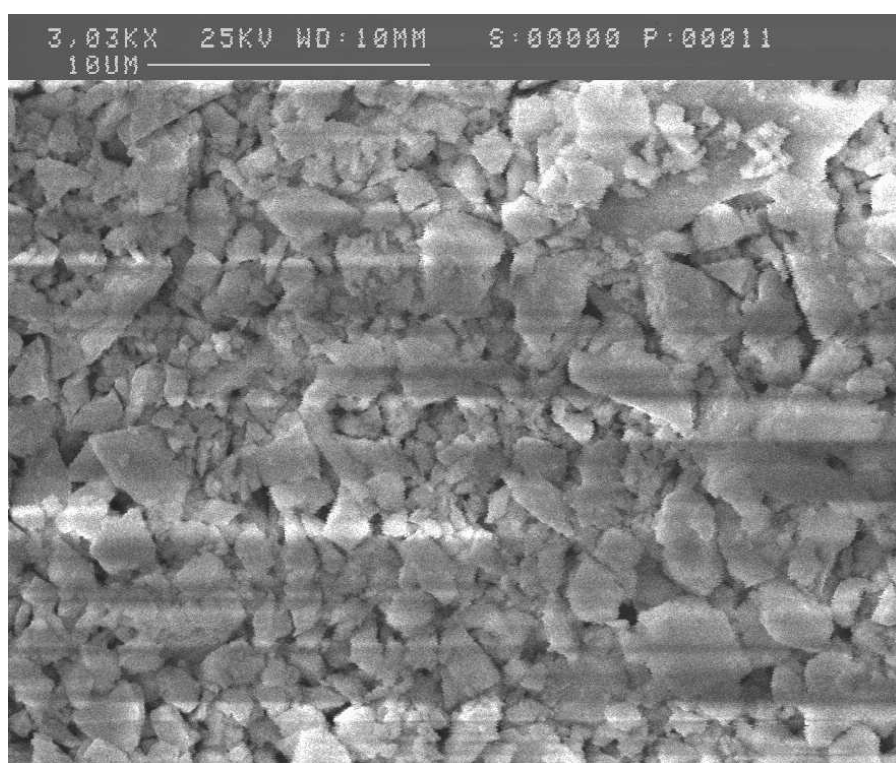


Figure 24 - SEM image of uncoated YSZ powder.

The nickel / YSZ co-deposited samples were examined to ensure that both the nickel and the YSZ had coated the substrates completely. This was achieved through examination under the SEM and confirmed by EDX analysis of the coating. The EDX spectra obtained was

compared against one previously acquired for electroless nickel. The results obtained are shown in figures 25 through 28.

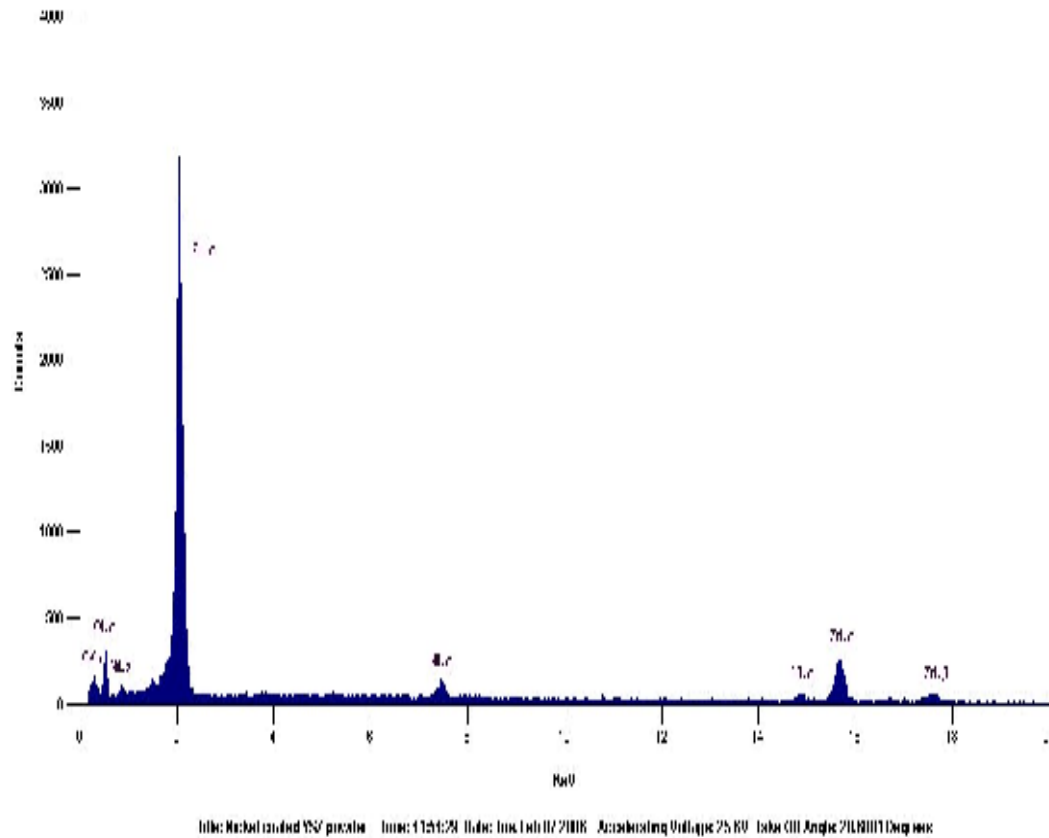


Figure 25 – Nickel coated YSZ substrate

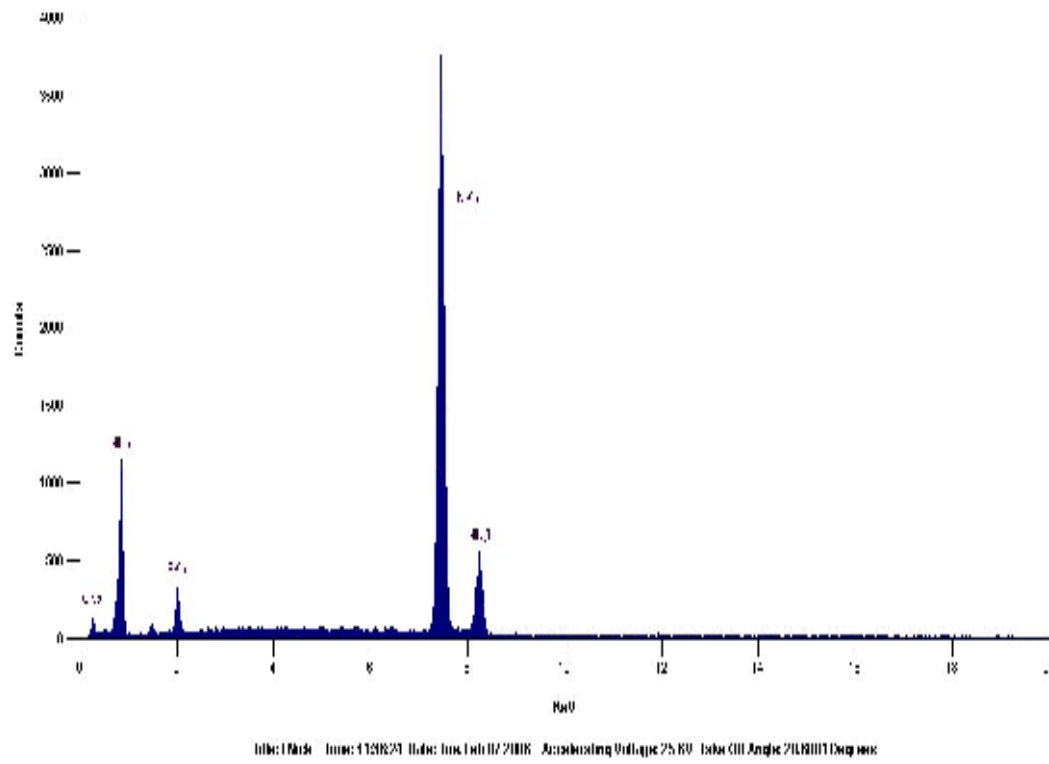


Figure 26 – EDX spectra for typical electroless nickel coating.

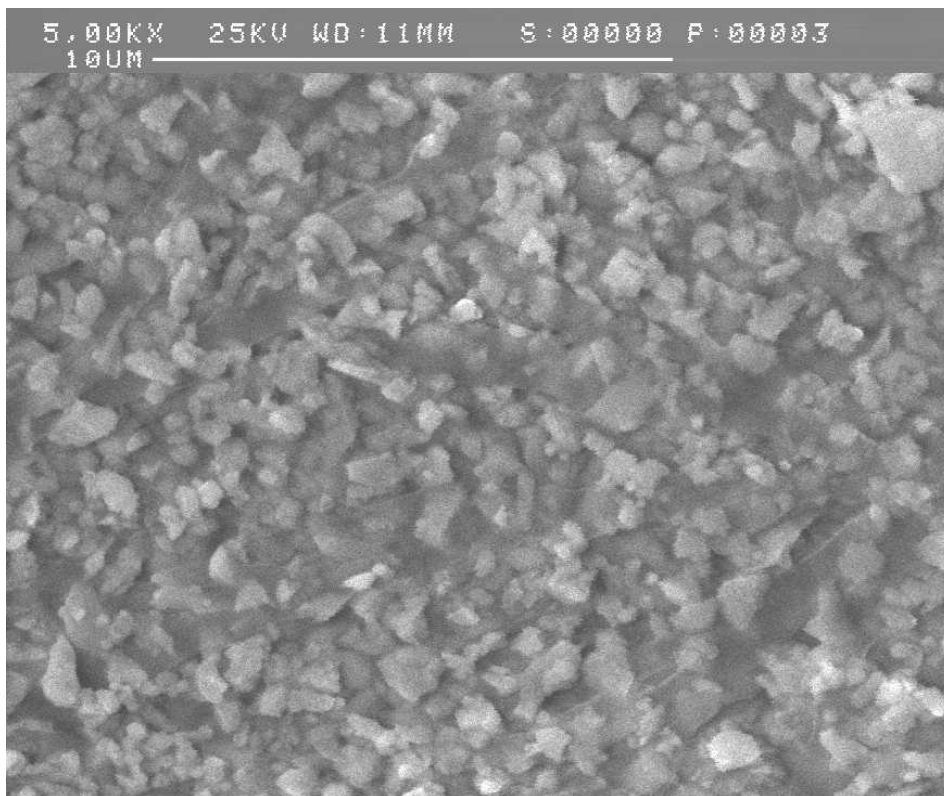


Figure 27 - SEM image of Ni/YSZ coating on Napier YSZ substrate

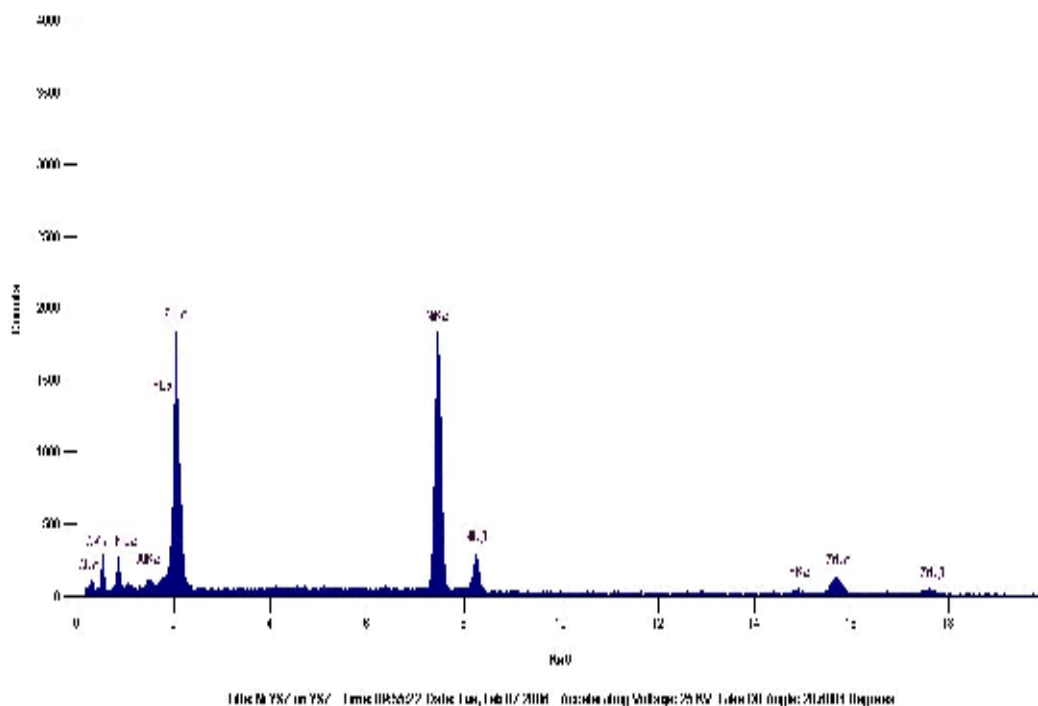


Figure 28 - EDX spectra for Ni/YSZ coating on Napier YSZ substrate.

The examination of the substrates showed that a uniform deposit of a Ni / YSZ composite had been achieved over the complete surface of the sample. Indeed, the pre-treatment had even been successful beyond the scope of this experiment in that the polymer film that the YSZ thin film had been supplied on had also been plated with the composite deposit. The adhesion properties of the Ni / YSZ deposit were relatively good in some areas, but overall could be improved through further pre-treatment operations. Analysis of the substrate using a Fisherscope XDL-Z X-Ray Fluorescence instrument showed that a coating thickness of approximately 9 to 11 μm had been achieved, which was consistent with standard deposition rates normally associated with the plating chemistry used. It was therefore decided to proceed with further experiments to determine if manipulation of the substrate roughness^[46] would improve the coating adhesion and improve the deposit for fuel cell applications.

5.5 Surface Roughness Experiments

To determine the effects of surface roughness on the substrates an initial experiment was constructed where a series of YSZ samples were etched in an acid solution comprising of 100ml.l⁻¹ of hydrofluoric acid and 100ml.l⁻¹ of sulphuric acid. The specimens were immersed

for 5 minutes at room temperature. They had been inspected before etching using a Taylor-Hobson 5-60 Talysurf instrument and further inspection was performed post-etching. Subsequently the samples were processed using the established plating procedure to evaluate the effect of the etching process on the final Ni / YSZ deposit. The results from the etching experiments are detailed in Table 7.

sample ID	PRE ETCHING				POST ETCHING				ROUGHNESS CHANGE
	<u>reading</u> 1	<u>reading</u> 2	<u>reading</u> 3	<u>Average</u>	<u>reading</u> 1	<u>reading</u> 2	<u>reading</u> 3	<u>average</u>	
1A	0.51	0.52	0.48	0.50	0.69	0.72	0.72	0.71	0.21
1B	0.67	0.56	0.56	0.60	0.71	0.73	0.68	0.71	0.11
2A	0.54	0.5	0.45	0.50	0.74	0.77	0.7	0.74	0.24
2B	0.53	0.54	0.54	0.54	0.67	0.78	0.76	0.74	0.20
3A	0.48	0.48	0.49	0.48	0.77	0.75	0.72	0.75	0.26
3B	0.46	0.83	0.83	0.71	0.84	0.83	0.87	0.85	0.14

Table 7 – Results of etching experiments (all results in μin , see Appendix C for conversion factor)

The etched and plated specimens were then characterised using the SEM and EDX techniques. The results are shown in Figures 29 and 30. It is apparent from the Talysurf data that there is an inconsistency in the etching process which needs further investigation. However, what is apparent from the SEM analysis is that the modification of the substrates surface has had a significant effect on the Ni / YSZ deposit. The surface roughness has increased and there would appear to be an increased porosity in the plated deposit. Both these factors would certainly improve the fuel cells performance from the view that there is an increase in surface area of the anode. Further experiments would certainly have to be performed to determine the repeatability of the process and optimise it to increase the fuel cells performance.

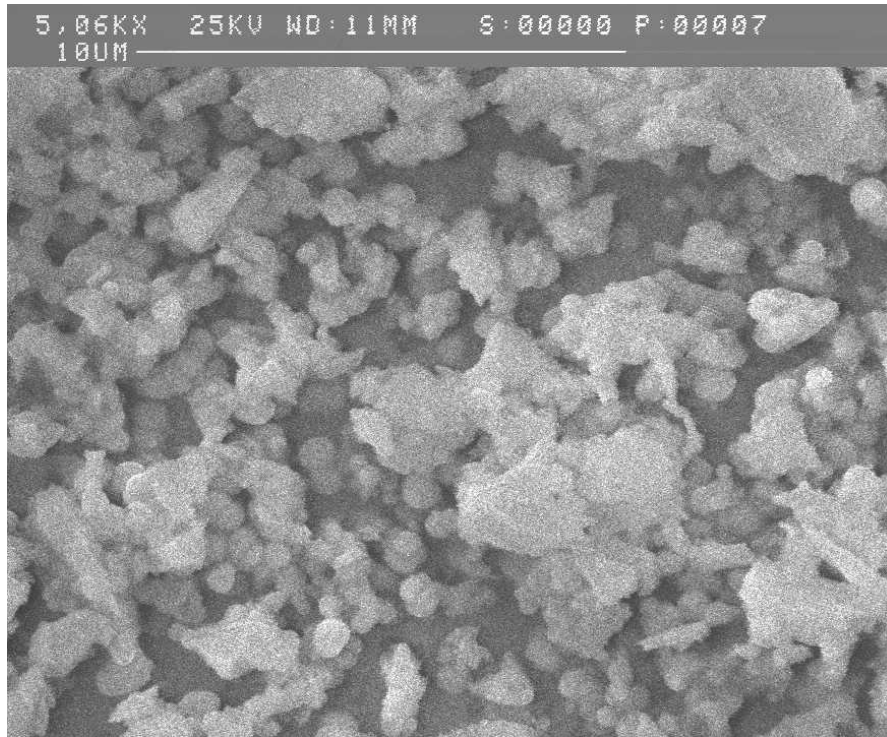


Figure 29 - SEM image of Ni/YSZ coating on etched YSZ substrate.

The EDX spectra of the Ni / YSZ composite coating on the etched substrate, in Figure 30, clearly shows that the composite deposit had been achieved and confirmed in conjunction with the SEM analysis that the surface of the specimens were uniformly coated.

XRF analysis of the deposit confirmed that the standard operating conditions that had previously been established had produced a coating thickness of 10 – 13 μ m, which is consistent with the standard variation between batches of plated components.

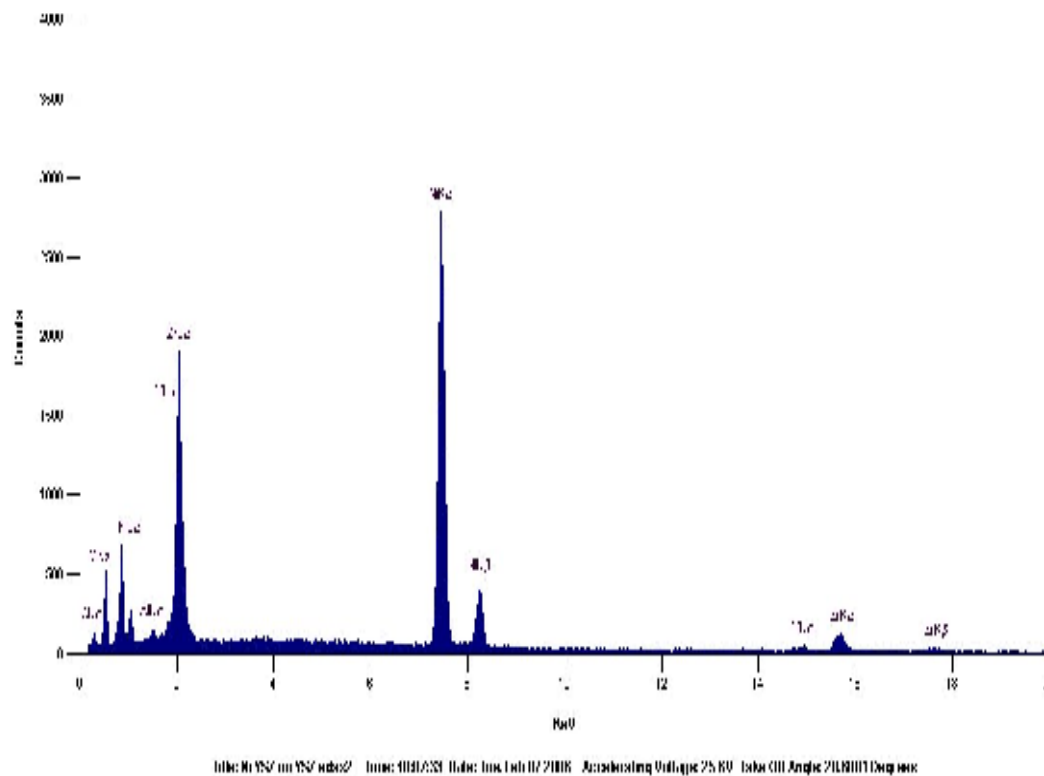


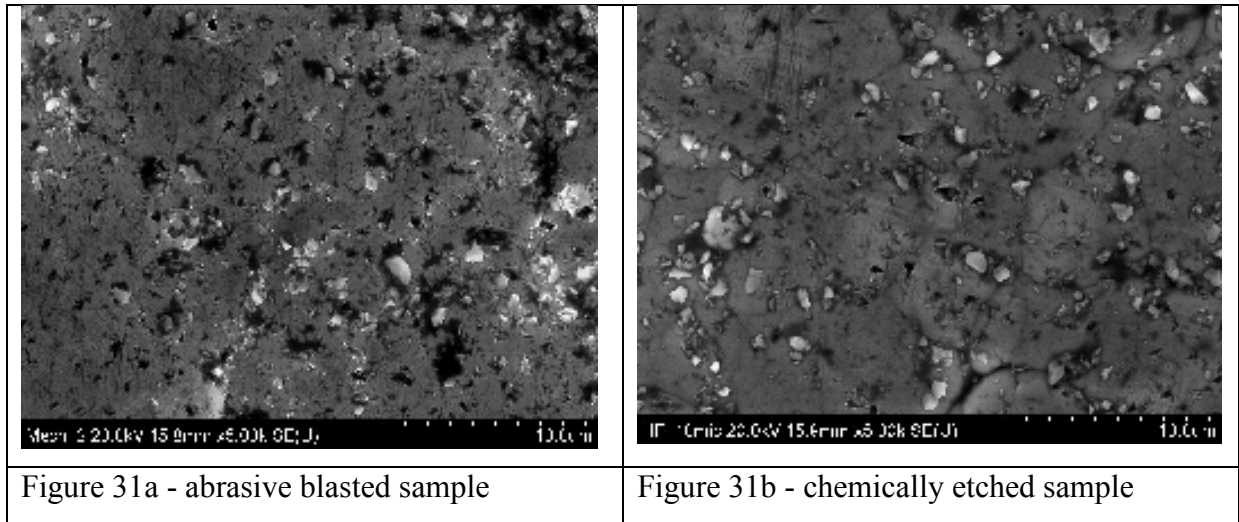
Figure 30 - EDX spectra for Ni/YSZ coating on etched YSZ substrate.

A comparison of samples which had been chemically etched with solution B (see appendix) and others which had been abrasive blasted using brown fused alumina was compared. A reference specimen of an untreated alumina tile was analysed using the Talysurf technique. The results of these experiments are detailed in Table 8. It is apparent that this new etching solution has had more of a polishing effect on the alumina tile when the results are compared with the non-treated substrate. The samples which were abrasive blasted were significantly rougher and this could be improved upon by utilising a rougher grade of blast media.

The samples were also examined using an SEM instrument and it was found that the abrasive blasted sample was indeed rougher, which confirmed the roughness results tabulated in Table 8. It also exhibited greater porosity than the chemically etched sample, as shown in figures 31a and 31b respectively.

Specimen	Ra / μin
Alumina untreated	27.81
Alumina abrasive blast 1	40.95
Alumina abrasive blast 2	40.20
Alumina HF etch 1	25.03
Alumina HF etch 2	22.21

Table 8 Surface roughness results of samples prepared by abrasive blasting and chemical etching.



5.6 Bath Loading Experiments.

One of the initial experiments which had to be performed was the effects of different ceramic bath loadings on the co-deposition of the ceramic in the nickel matrix. Initially 6082 aluminium alloy substrates were used as they were readily available and could be easily pre-treated using either the palladium chloride / stannous chloride technique or a commercially available double zincate process which is used in industrial applications. A number of aluminium samples of 100mm×25mm×2mm were etched and pre-treated using the double zincate process detailed below. They were immersed in a series Slotonip 1850 solutions at the operating temperature of 89°C which had been loaded with 13% mol YSZ ceramic particles as detailed in Table 9.

Aluminium pre-treatment procedure

- i. Alkaline hot clean, Slotoclean AK340, at 60°C for 2 minutes
- ii. Rinse in deionised water
- iii. Aluminium etch in 40% sodium hydroxide at 70°C for 2 minutes.
- iv. Rinse in deionised water
- v. Etch in aluminium desmut at room temperature for 2 minutes. Slotoclean DS10 solution.
- vi. Rinse in deionised water.
- vii. Zincate CNF10 solution for 1 minute at room temperature
- viii. Rinse in deionised water
- ix. Zinc strip Slotostrip ZN10 for 1 minute at room temperature
- x. Rinse in deionised water
- xi. Zincate CNF10 solution for 30 seconds at room temperature
- xii. Rinse in deionised water
- xiii. Immerse in electroless nickel solution at 89°C

Sample number	YSZ concentration, g.l ⁻¹	Sample orientation	Sample side
1	1	Horizontal	A
2	1	Horizontal	B
3	1	Horizontal	A
4	1	Horizontal	B
5	2	Horizontal	A
6	2	Horizontal	B
7	2	Horizontal	A
8	2	Horizontal	B
9	5	Horizontal	A
10	5	Horizontal	B
11	5	Horizontal	A
12	5	Horizontal	B
13	10	Horizontal	A
14	10	Horizontal	B
15	10	Horizontal	A
16	10	Horizontal	B

Table 9 – YSZ bath loading sample data

Once plated the samples were evaluated by SEM and EDXA to determine their morphology, composition and degree of porosity. The results are depicted in Figures 32 – 43 and are identified by their sample numbers from Table 9.

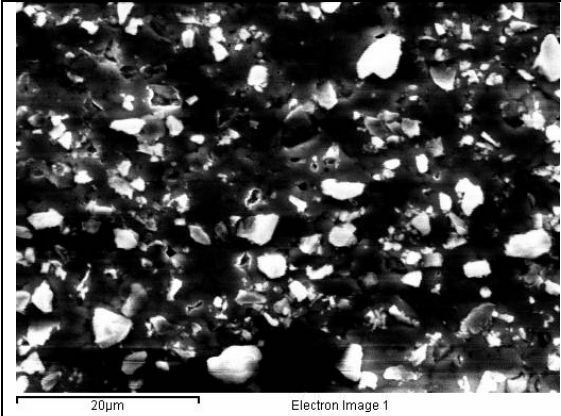


Figure 32a – sample 1 SEM image

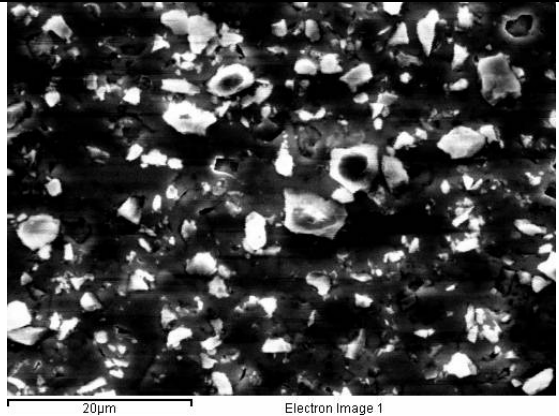


Figure 32b – sample 2 SEM image

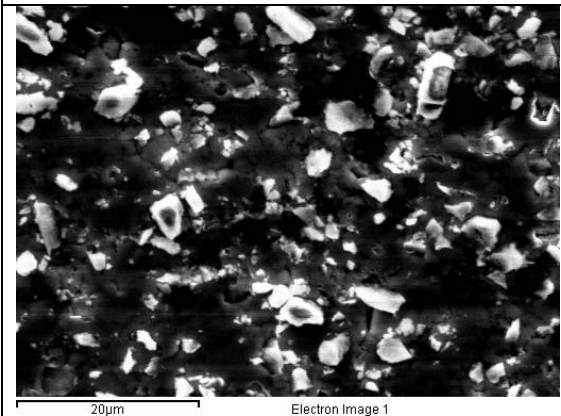


Figure 32c – sample 3 SEM image

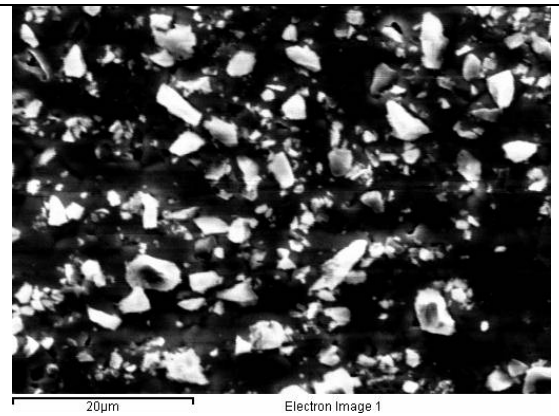


Figure 32d – sample 4 SEM image

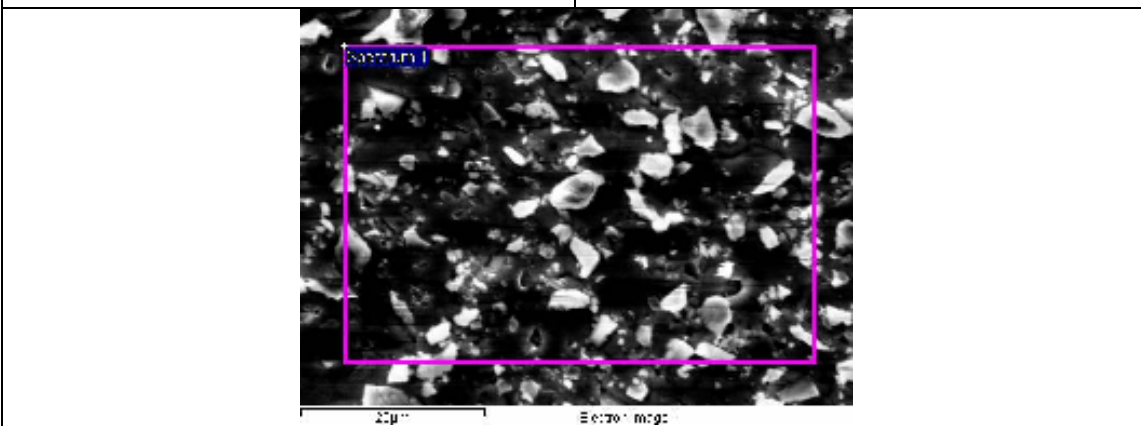


Figure 32e - Example of area where typical compositional data taken

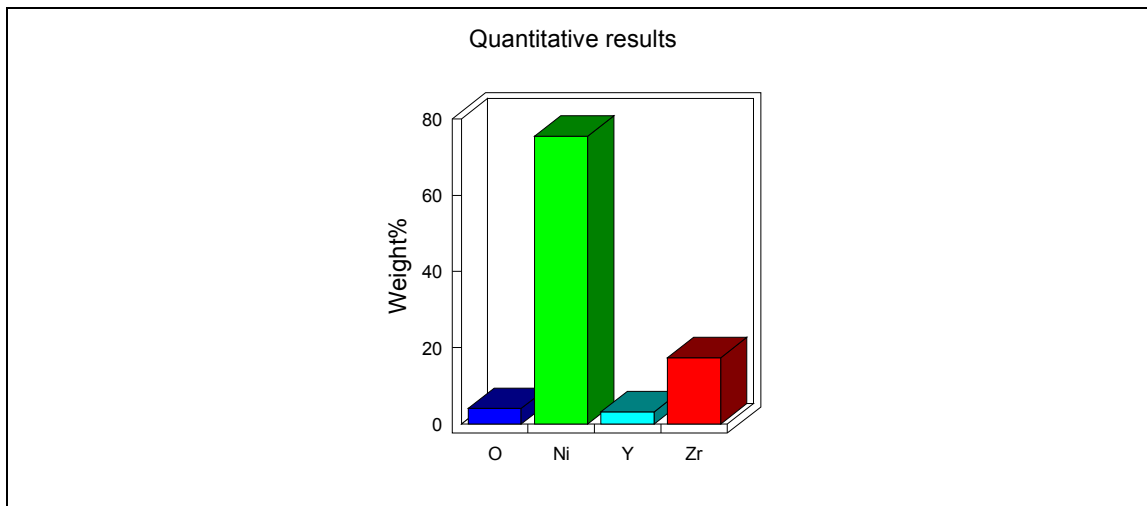


Figure 33 - Typical composition of deposits produced from 1g.l⁻¹ YSZ solution

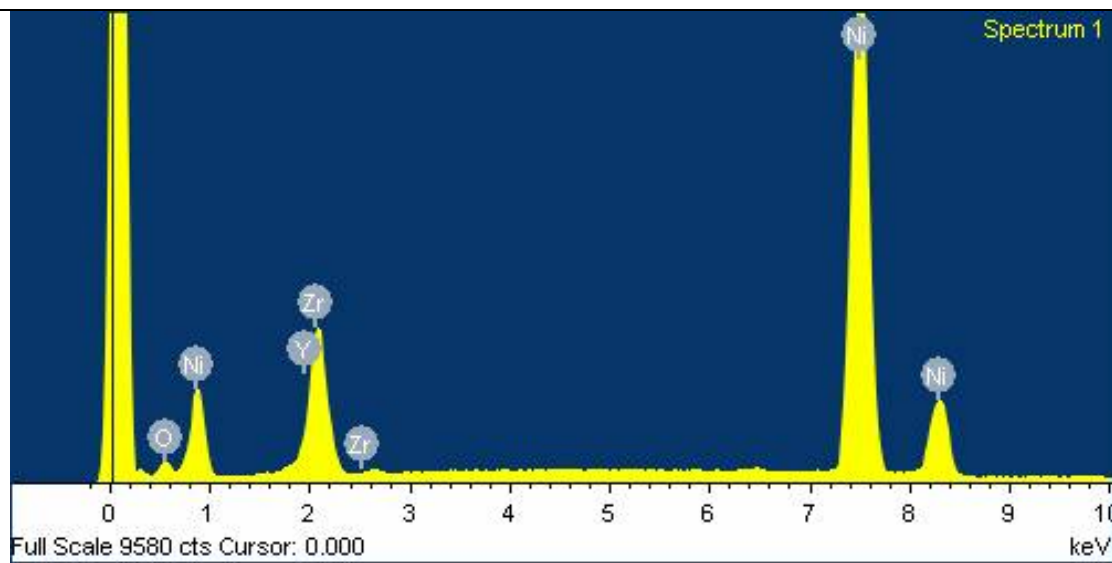
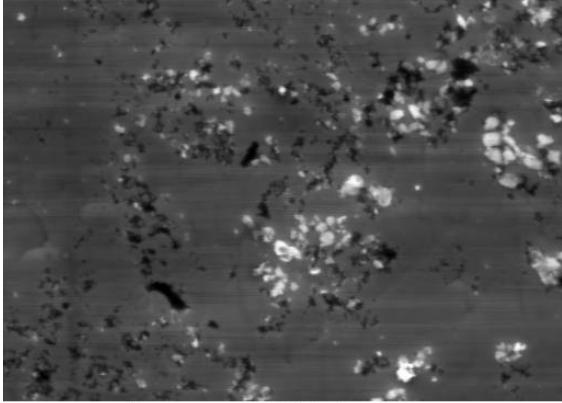
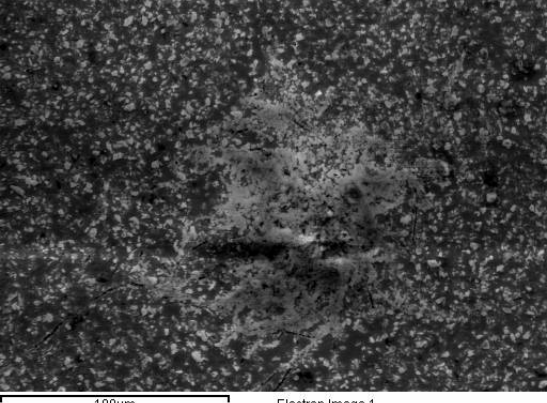
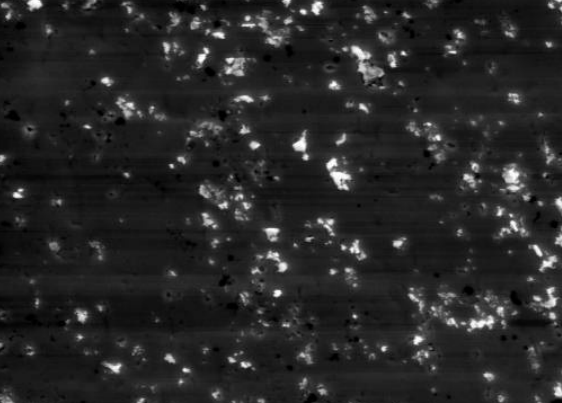
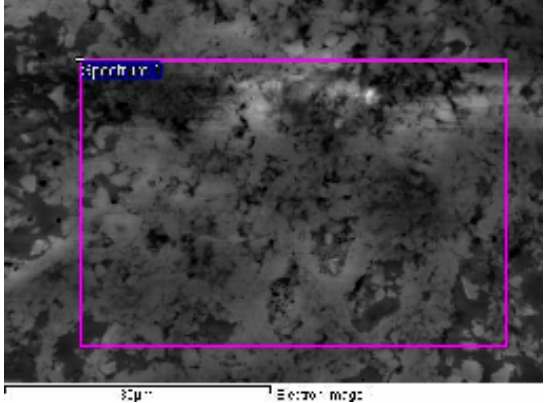
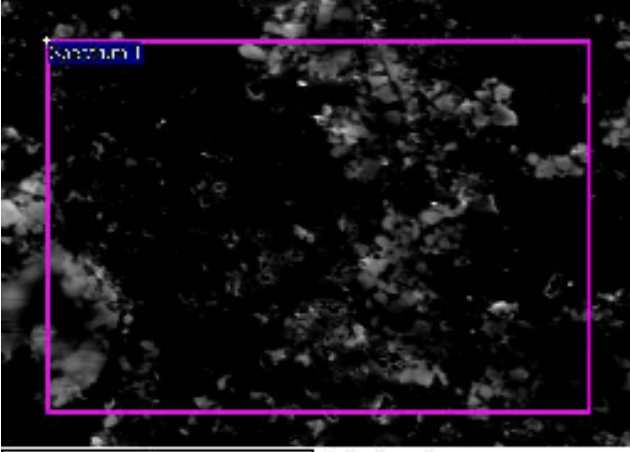


Figure 34 - Typical EDX analysis of deposits produced from 1g.l⁻¹ YSZ solution

	
<p>Figure 35a – sample 5 SEM image</p>	<p>Figure 35b – sample 6 SEM image</p>
	
<p>Figure 35c – sample 7 SEM image</p>	<p>Figure 35d – sample 8 SEM image</p>
	
<p>Figure 35e - Example of area where typical compositional data obtained for 2g.l⁻¹ solution</p>	

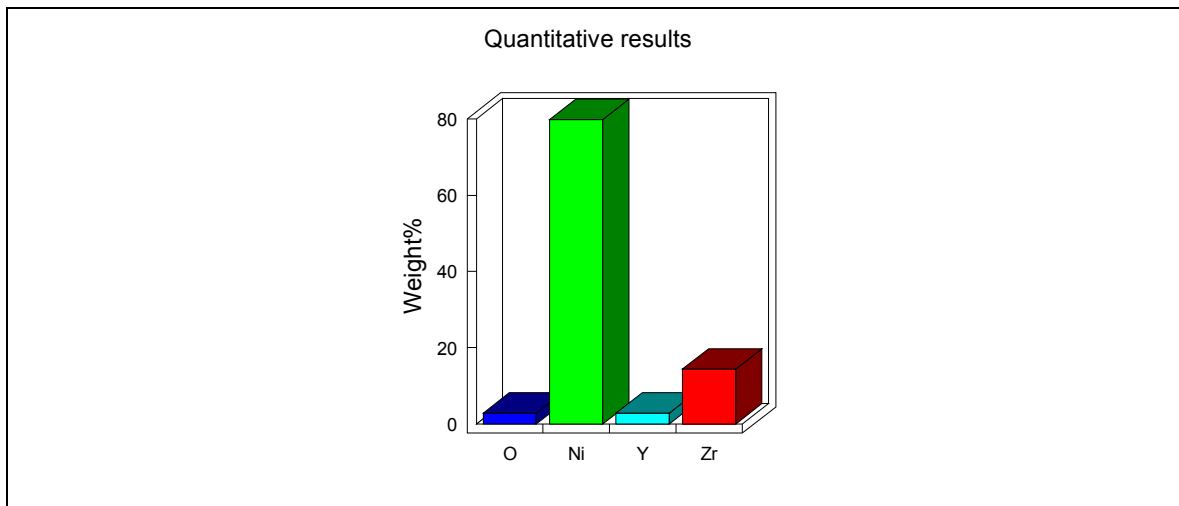


Figure 36 - Typical composition of deposits produced from 2g.l^{-1} YSZ solution

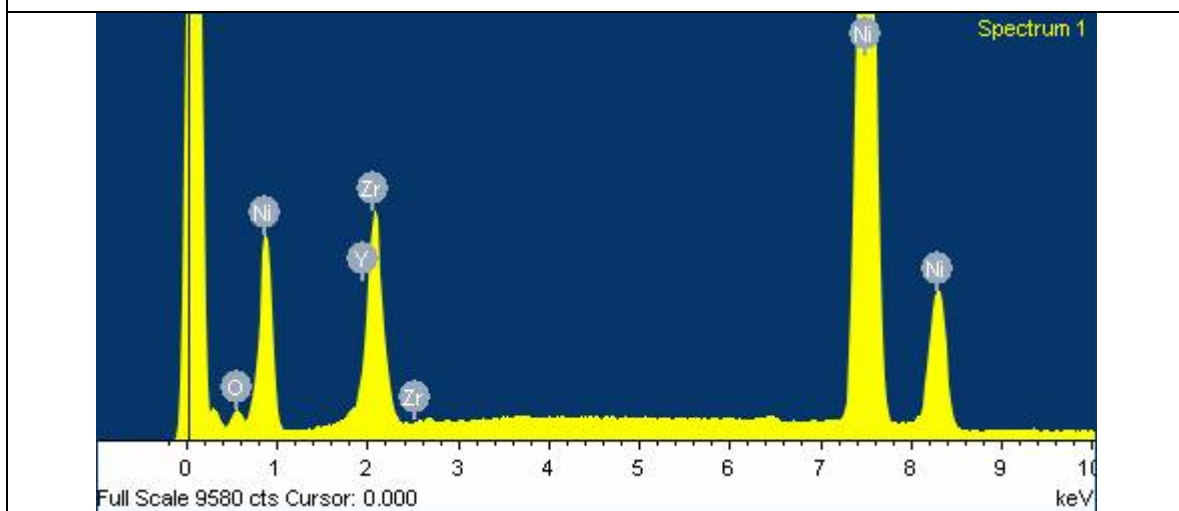


Figure 37 - Typical EDX analysis of deposits produced from 2g.l^{-1} YSZ solution

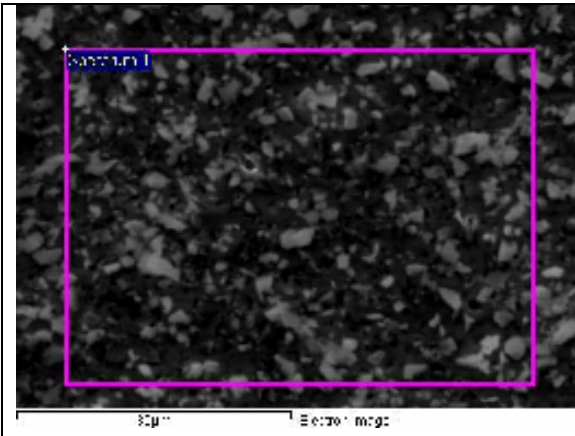


Figure 38a – sample 9 SEM image

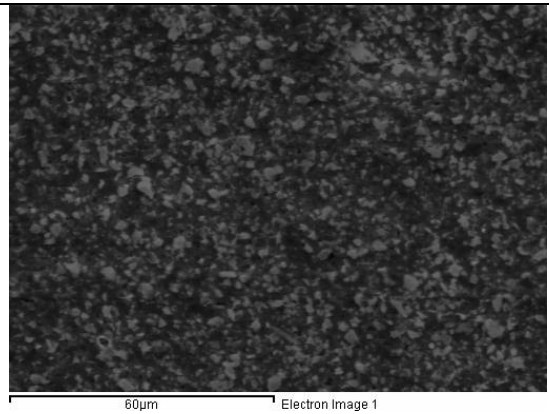


Figure 38b – sample 10 SEM image

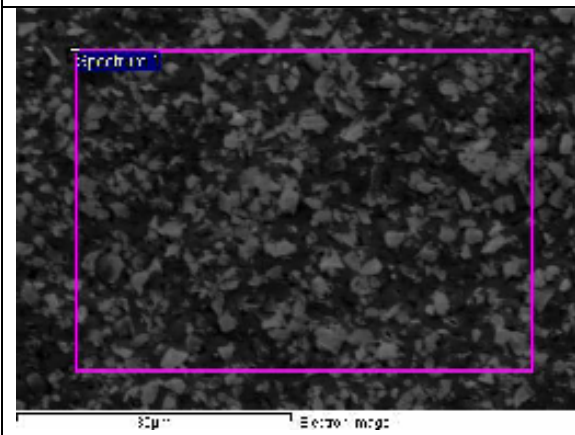


Figure 38c – sample 11 SEM image

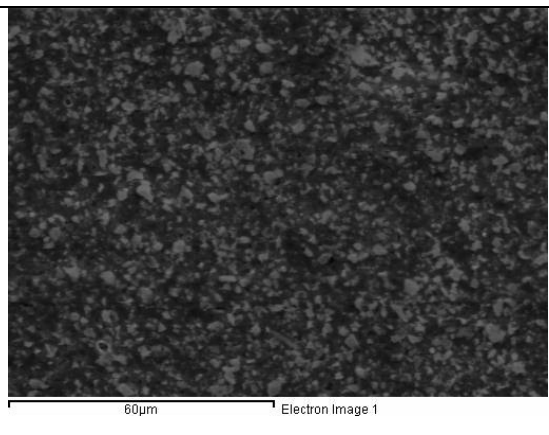


Figure 38d – sample 12 SEM image

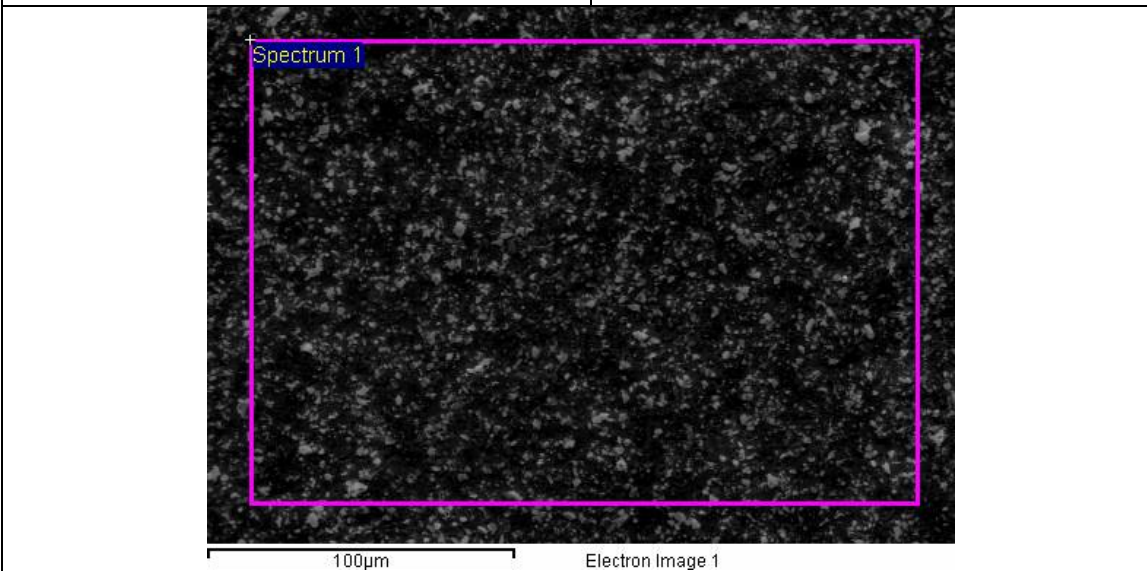


Figure 38e - Example of area where typical compositional data obtained for 5g.l^{-1} solution

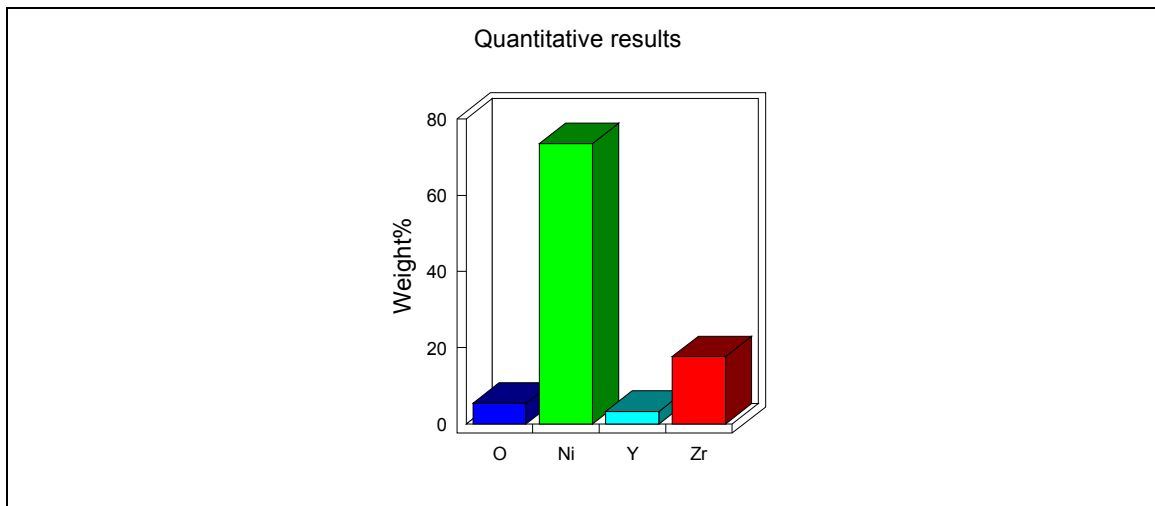


Figure 39 - Typical composition of deposits produced from 5g.l⁻¹ YSZ solution

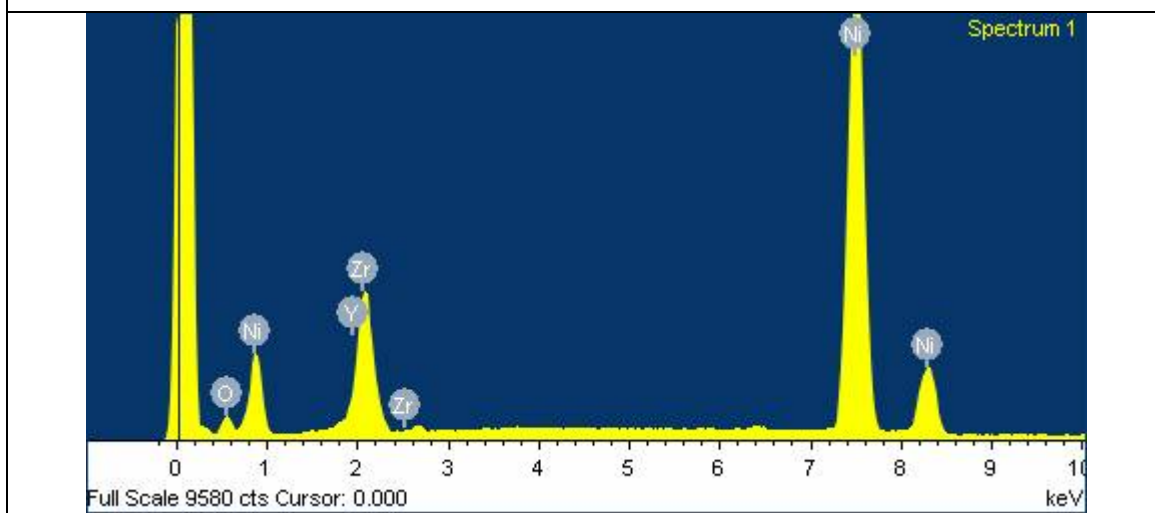
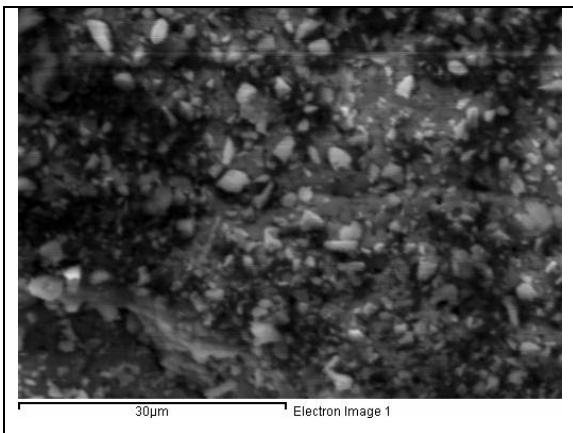
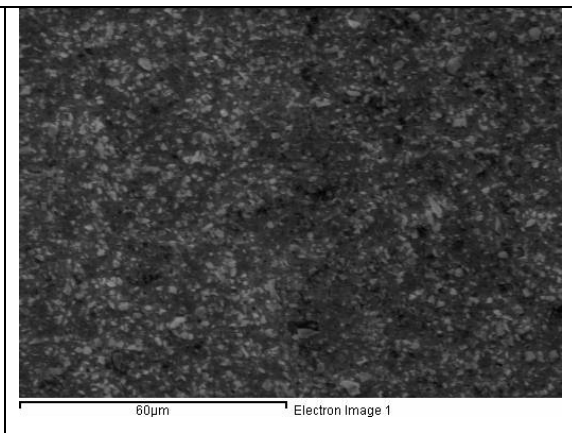
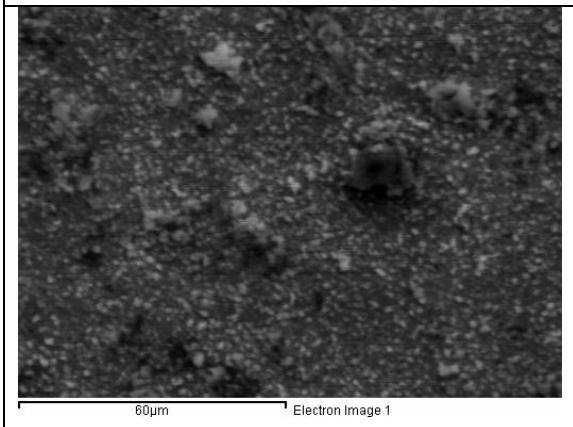
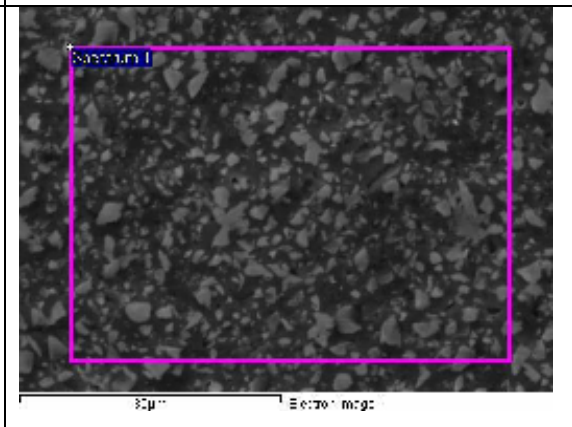
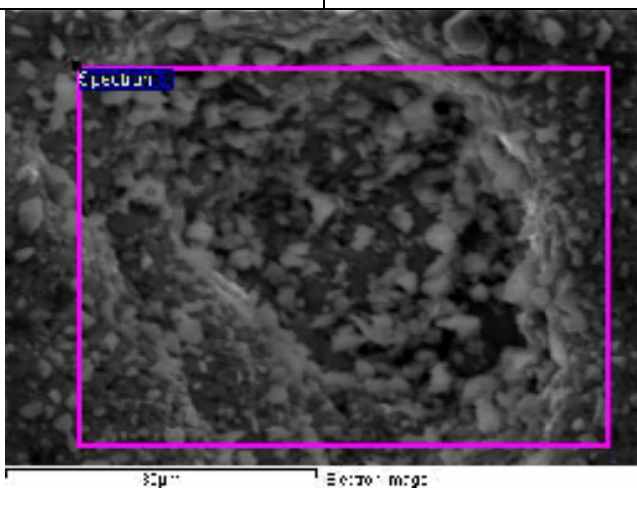


Figure 40 - Typical EDX analysis of deposits produced from 5g.l⁻¹ YSZ solution

	
<p>Figure 41a – sample 13 SEM image</p>	<p>Figure 41b – sample 14 SEM image</p>
	
<p>Figure 41c – sample 15 SEM image</p>	<p>Figure 41d – sample 16 SEM image</p>
	
<p>Figure 41e - Example of area where typical compositional data taken for 10g.l⁻¹ deposit</p>	

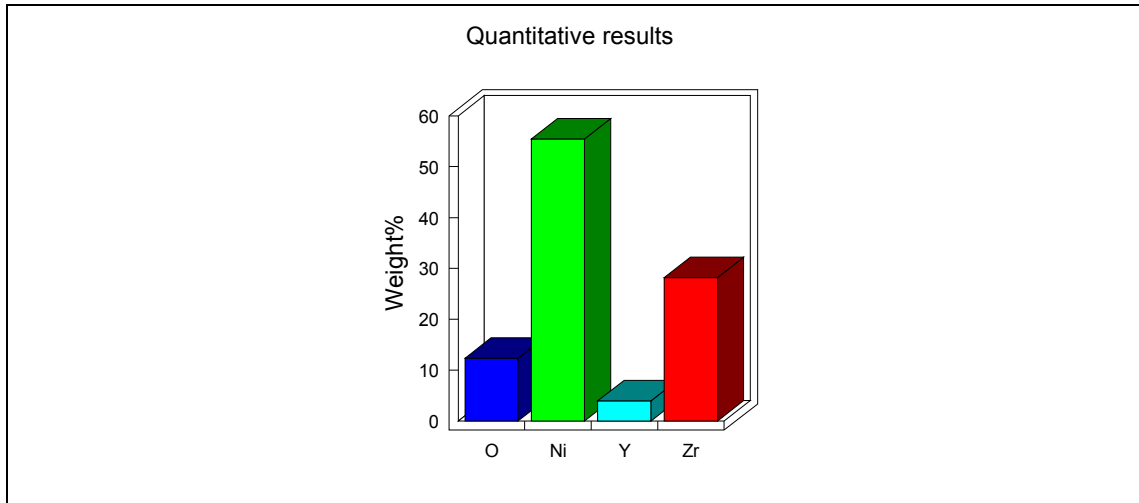


Figure 42 - Typical composition of deposits produced from 10g.l⁻¹ YSZ solution

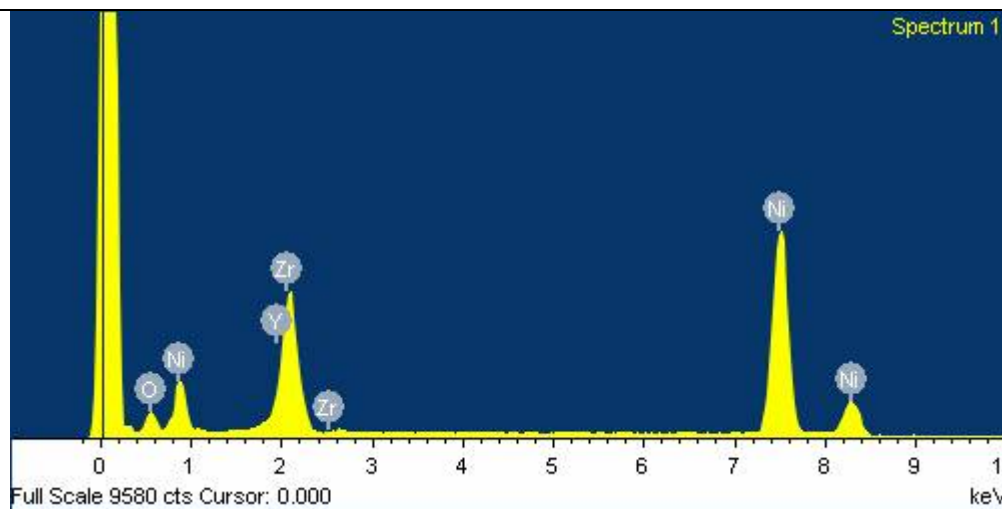


Figure 43 - Typical EDX analysis of deposits produced from 10g.l⁻¹ YSZ solution

From these experiments it is apparent that consistent and uniform results can be achieved with any of the bath loadings. What was disappointing was the relatively high nickel content of the composite deposit for the 1, 2 and 5g.l⁻¹ samples. The 10g.l⁻¹ bath loading exhibited some improvement at approximately 65% nickel but still well short of the required target of 50% Ni : 50% YSZ. Further experiments were performed with an intermediate concentration of 7.5g.l⁻¹ YSZ based on research performed on other reinforcement particles^[22,13,45], where intermediate concentrations produced increased percentages of reinforcement in the deposit. The pH of the bath solution was also controlled to slow the deposition rate and the agitation was achieved through mechanical action based on the research carried out in conjunction with other researchers within the university and which has been published^[94].

As the pH of the solution increases from 4 to 6 the phosphorus content of the deposit decreases, which is directly related to the reduction capacity of the sodium hypophosphite at those specific pH's. It was also found that the pH of the solution affected significantly the amount of ceramic particles which were co-deposited. It was found that the highest concentration of ceramic was deposited when the pH was at 3.4 (see figure 44). This is due to the charge accumulated on the surface of the ceramic powder which dictates the adsorption of ions or polarised particles on its surface. This in effect means that the zeta potential is critical to achieve the required co-deposition of the ceramic and that different ceramics or mixtures of ceramics will require to be individually tested to ensure the optimum pH. Alternatively the zeta potential is altered by the addition of a suitable surfactant to the solution. The surfactant, by electrostatic interactions between the different charged ions, is absorbed on the surface of the ceramic.

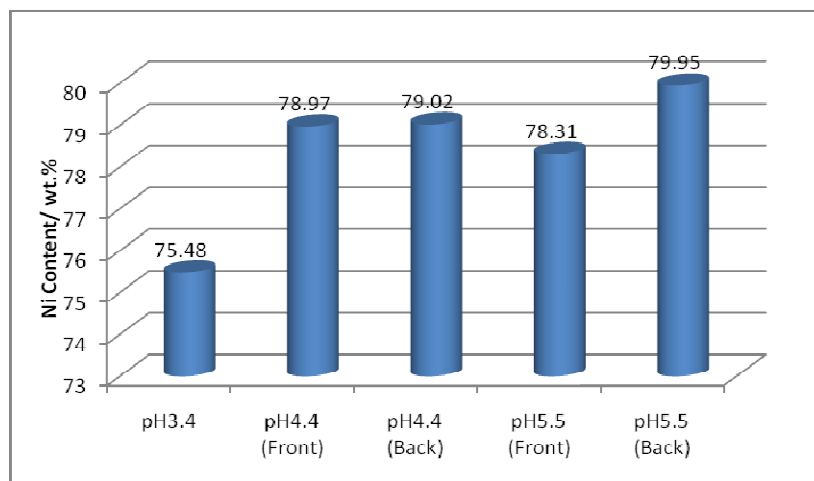


Figure 44 - Effect of solution pH on the ceramic reinforcement content of the deposit

Smaller particles in a narrow size distribution^[61] were firmly held by the matrix. However, a mixture of both large and small particles have in recent experiments, shown to improve the packing density and increased the incorporation into the matrix. Particle shape has also been found to be important. Samples which were produced from intermediately ball-milled YSZ had a higher level of incorporation, probably due to the more angular shaped particles anchoring themselves better into the matrix during the initial period of co-deposition.

Bath loadings greater than 10g.l⁻¹ have a higher risk of bath decomposition due to the high surface area of the particles. There is an optimum value for the bath loading which changes

according to the solution, operating parameters, and type/size of the ceramic particles. When this optimum value is exceeded the particles agglomerate and precipitate, resulting in a slight decrease in their incorporation into the deposit.

It was also found that the stirring action was also vitally important to ensure a steady rate of co-deposition. A series of experiments showed that the orientation of the sample in the solution and the type of agitation used affected the percentage of YSZ co-deposited and also the degree of porosity. This is illustrated in figure 45.

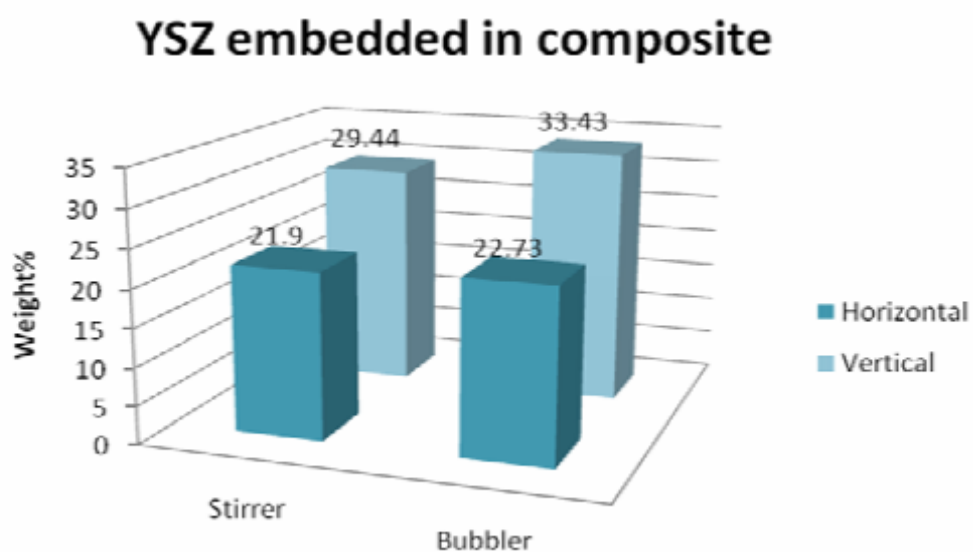


Figure 45 - Effect of agitation method on the co-deposition of ceramic particles.

Another important conclusion of this piece of research was that the ceramic content could be altered throughout the duration of the deposition process, through the manipulation of these key parameters. This therefore allows concentration gradients of the ceramic to be achieved which is certainly important in controlling the coefficient of thermal expansion whilst at the same time increasing the electrical conductivity at key areas in the anode.

During the series of multifactor experiments which were performed for this thesis the required ratio of nickel to YSZ was achieved using a 7.5g.l^{-1} YSZ concentration, controlling the pH of the solution at 4.2 and using air agitation in conjunction with minimal mechanical agitation. The results, which were consistently repeated, are shown in figures 46 and 47.

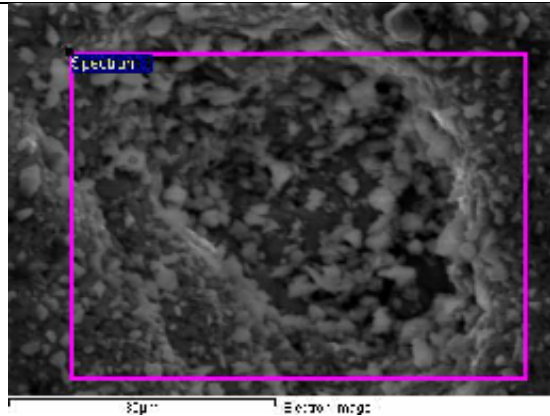


Figure 46 - Typical area of 7.5g.l⁻¹ deposit examined under SEM and EDXA

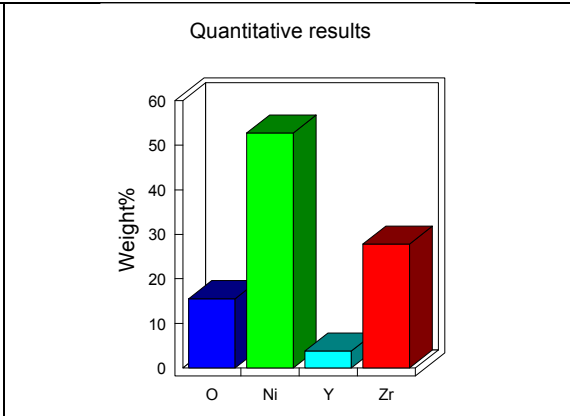


Figure 47 – Compositional analysis of area shown in figure 46.

The samples produced from the 7.5g.l⁻¹ YSZ solution met the required composition required by most commercial companies. This was one of the initial milestones required as part of the Proof of Concept program.

Another milestone was to increase the degree of porosity in the deposit. The aim was to achieve a porosity level of 20%. It was found that the samples produced with the 50% nickel content also exhibited this level of porosity as shown in Figures 48 and 49. The degree of porosity was established by mapping the areas of porosity in comparison to the areas of deposits and it was found that the ratio of deposit to porosity was 80:20

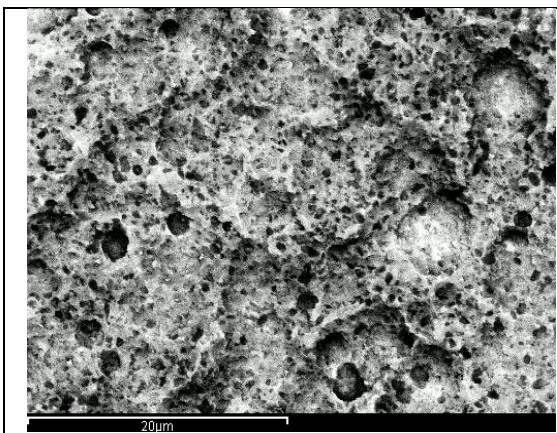


Figure 48 – area of porosity

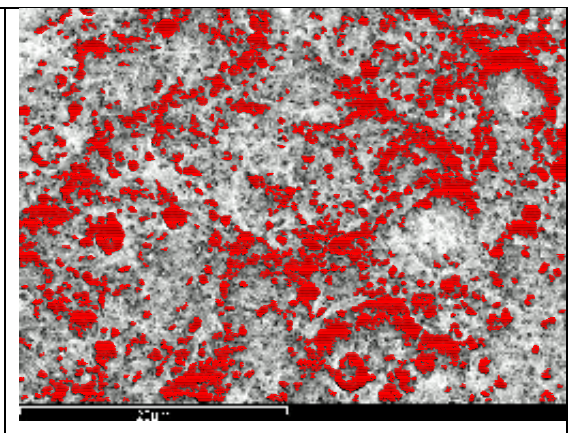


Figure 49 – mapped area of porosity (porosity indicated in red)

5.7 Spectrophotometer experiments

As has been previously discussed the zeta potential is a key parameter for the successful suspension of particles in the plating solution. Without access to an instrument for measuring the zeta potential directly, a series of basic experiments were developed to determine the relationship between particles and surfactants. Thus the optimum conditions for retaining the particles suspended in the plating solution could be determined. The longer the particles can be kept in suspension, then the greater the likelihood that these particles can be co-deposited.

Samples were prepared of a standard Slotonip1850 electroless nickel plating solution. Aliquots of this were then taken and to each of three samples, ceramic samples of LSM, YSZ and a mixture of LSM and YSZ were added as per the concentration detailed in Table 10.

Sample number	Solvent	Solute
Control	Deionised water	None
1	Slotonip 1850	None
2	Slotonip 1850	50g.l ⁻¹ YSZ
3	Slotonip 1850	50g.l ⁻¹ LSM
4	Slotonip 1850	15g.l ⁻¹ LSM + 35g.l ⁻¹ YSZ

Table 10 - Spectrophotometer samples.

Initially a sample of Slotonip 1850 was compared to a reference sample of deionised water and scanned over the wavelength range of 190-900nm. From the spectra obtained a standard absorbance peak at 410nm was selected. This was used to establish the effects of the precipitation of the ceramic particles over time from the electroless nickel plating solution. Altering the bath chemistry by the addition of a suitable surfactant it was hoped that the ceramic could remain in suspension for a longer period of time and thus increase the probability of co-deposition. Baseline results of absorbance were recorded for each of the samples detailed in Table 10 and the precipitation effects over time are depicted in figures 50 to 52.

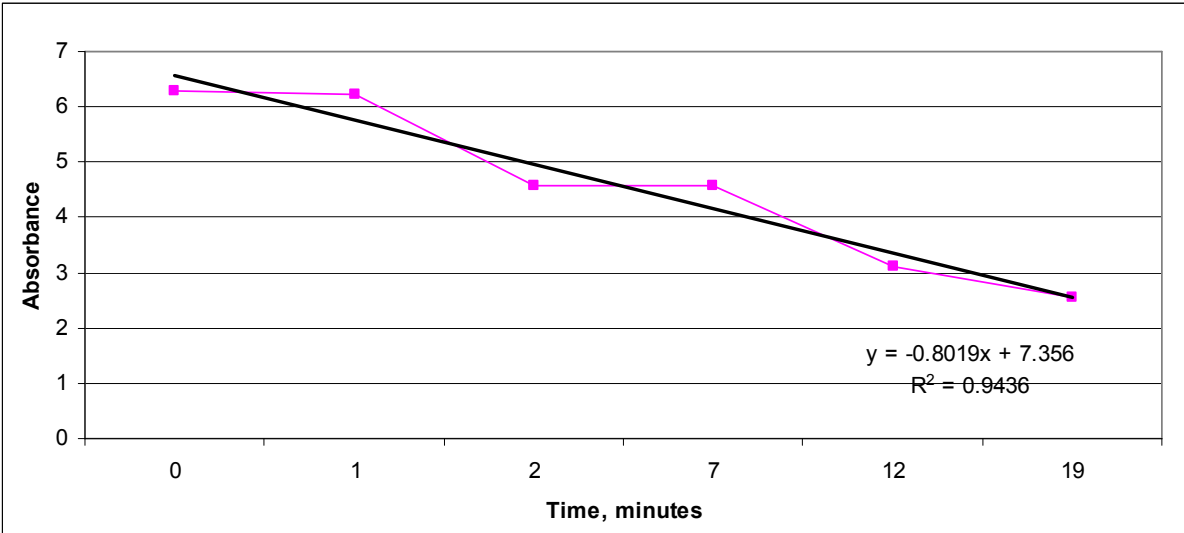


Figure 50 - Precipitation rate of YSZ from electroless nickel solution

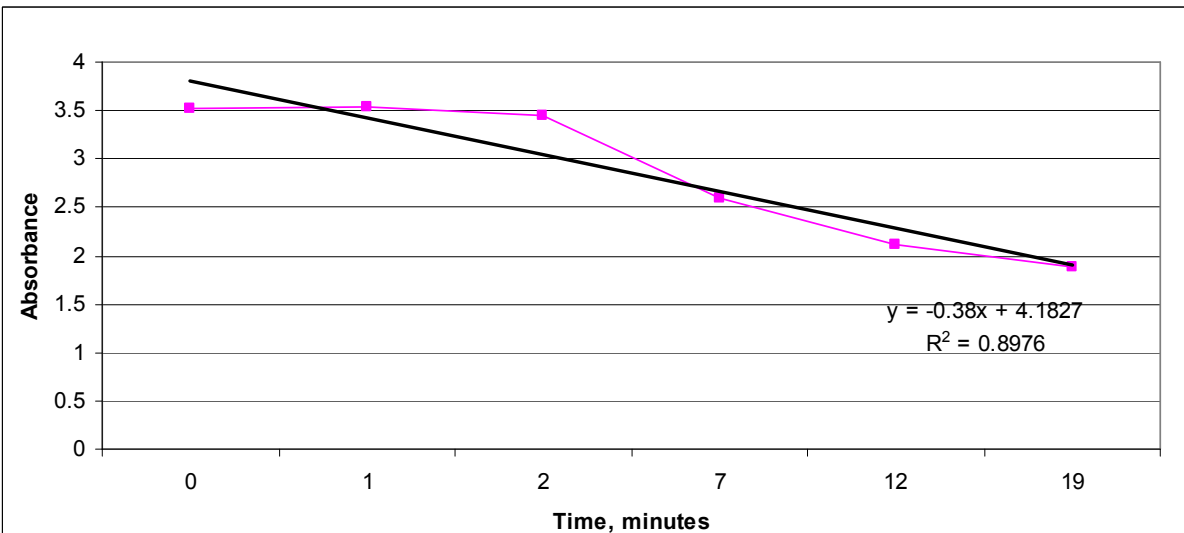
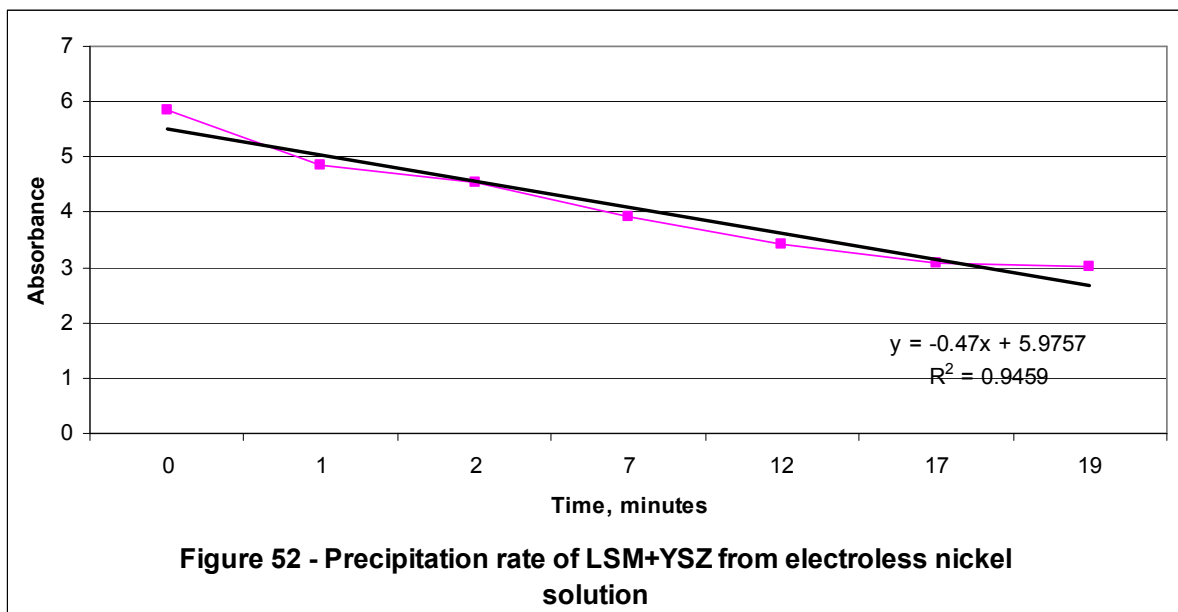


Figure 51 - Precipitation rate of LSM from electroless nickel solution



It is apparent from these simple experiments that the YSZ precipitates from the solution faster than the LSM. The higher absorbance exhibited with the YSZ would also indicate that initially it is capable of a greater degree of suspension within the nickel solution. If this could be maintained throughout the deposition period then theoretically the co-deposition would be the same throughout. The LSM and YSZ mixture also exhibited the higher initial absorbance but still had a higher absorbance at the end of the time period than either the LSM or YSZ. This indicates that there is some degree of interaction between the YSZ and LSM which is improving the suspension effect.

Further trials are planned once a selection of suitable surfactants are obtained and these will be evaluated at pH values ranging from 3.8 to 5.2. When using a surfactant the particles will be blended into the solution by mixing for at least 30 minutes to ensure complete wetting and homogenous distribution in the solution.

5.8 Experiments with polystyrene.

It was theorised that the porosity in the samples could be enhanced through the addition of a pore-forming material^[66]. Of the polymers which were considered, only polystyrene had a suitable range of particle sizes available commercially. Suspensions of 0.1 μ m, 0.5 μ m and 1.0 μ m particle sizes were purchased from Sigma-Aldrich and experiments were performed

using fixed volume additions in 150mls of Slotonip 1850 solution loaded with 7.5g.l⁻¹ YSZ under standard operating conditions as per Table 11.

Polystyrene, μm	3 drops	10 drops	20 drops
0.1	Solution 1	Solution 2	Solution 3
0.5	Solution 4	Solution 5	Solution 6
1.0	Solution 7	Solution 8	Solution 9

Table 11 - Polystyrene additions in electroless nickel plating solutions.

Using the experimental matrix detailed in Table 11 any correlation between polystyrene particle size and their distribution versus deposit porosity could be ascertained. Samples were heat-treated at 850°C for one hour to simulate cell ramp-up conditions and to evaluate the effects of that temperature cycle on the overall porosity of the deposit.

From the SEM and EDXA spectra shown in Figures 53 and 54, the 0.1 μm particles appear to be widely dispersed through the deposit and excellent microporosity has formed post burn out. The compositional analysis, Figure 59, showed that the YSZ was co-deposited with the nickel but that the ceramic content needs to be increased in further trials.

The 0.5 μm polystyrene also exhibited good microporosity with what appeared to be nickel nodules formed on the surface. This is shown in Figure 55. This may increase the triple phase boundary and therefore the catalytic rate. Similarly the YSZ was successfully co-deposited, but needs to be further increased in concentration within the deposit (figure 56).

The 1 μm polystyrene showed extensive and well dispersed microporosity and some degree of macroporosity. The ceramic content was detected by EDXA, as shown in Figure 61, but was on a similar level to that reported for the 0.1 and 0.5 μm particle sizes.

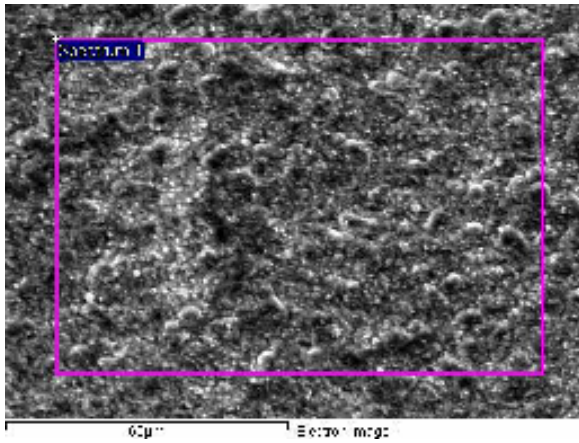


Figure 53 – SEM image of deposit plated with 0.1µm polystyrene particles.

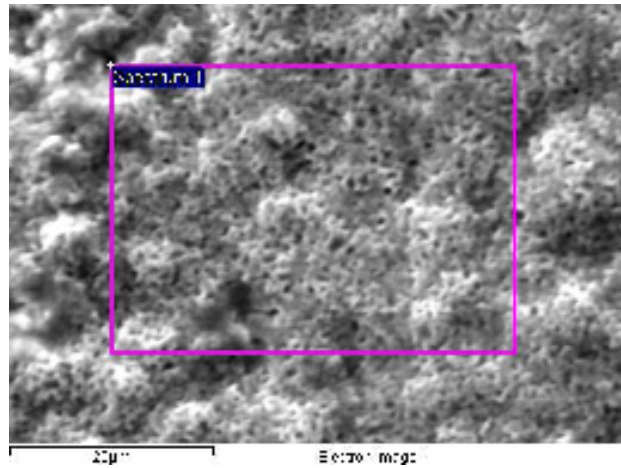


Figure 54 – SEM image of deposit plated with 0.1µm polystyrene particles post heat treat.

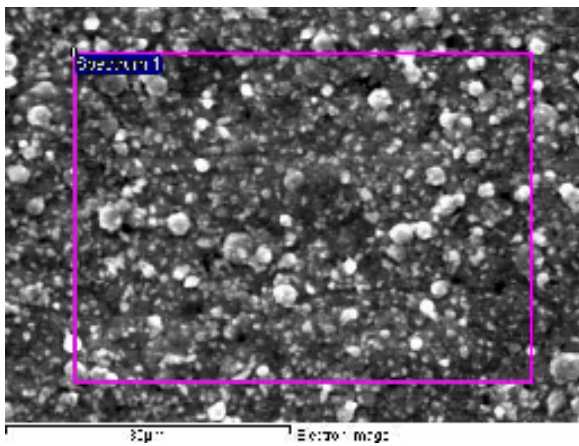


Figure 55 – SEM image of deposit plated with 0.5µm polystyrene particles.

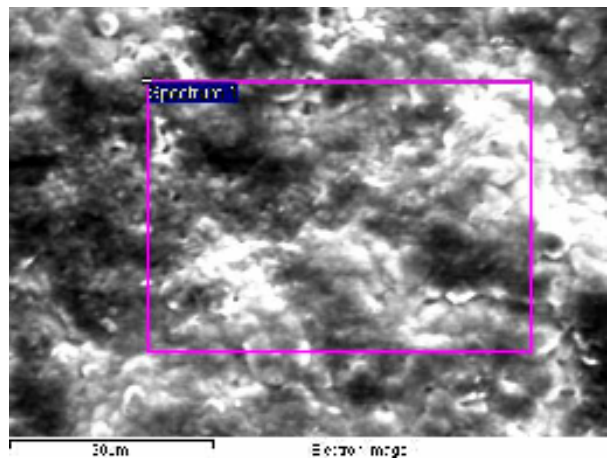


Figure 56 – SEM image of deposit plated with 0.5µm polystyrene particles post heat treat.

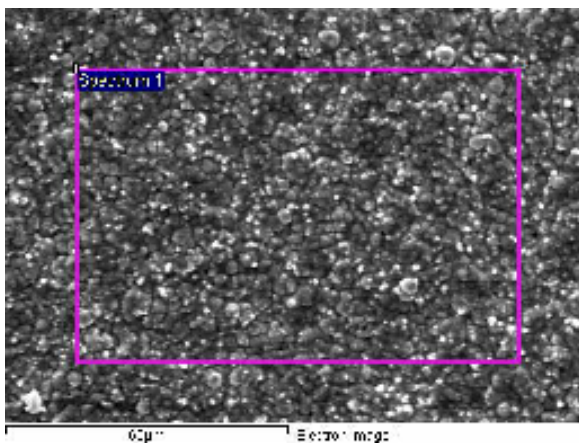


Figure 57 – SEM image of deposit plated with 1.0µm polystyrene particles.

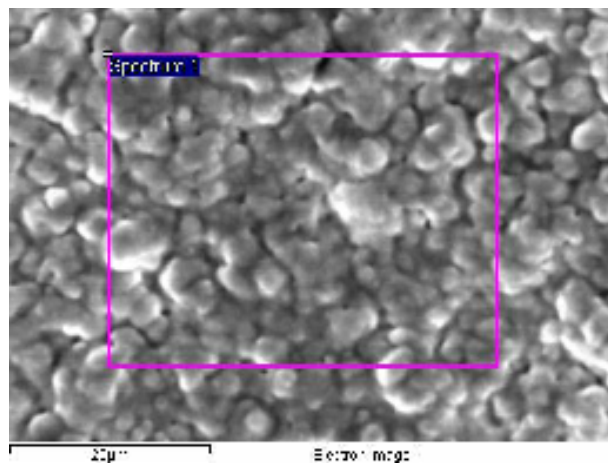


Figure 58 – SEM image of deposit plated with 1.0µm polystyrene particles post heat treat.

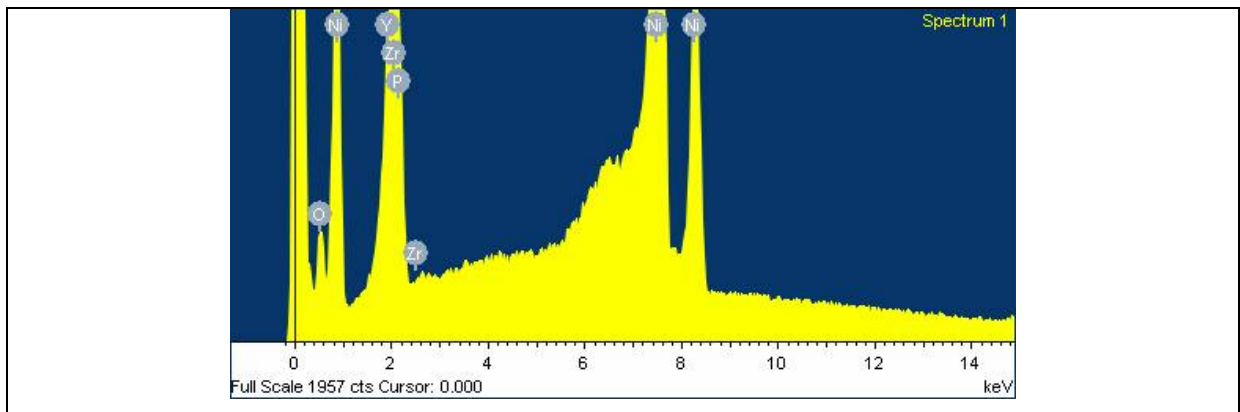


Figure 59 – EDXA spectra of deposit plated with 0.1µm polystyrene particles.

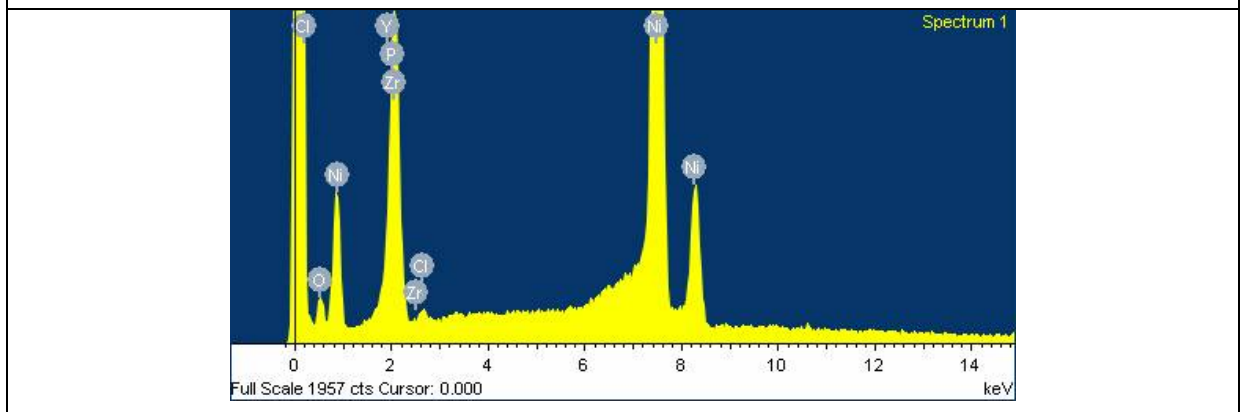


Figure 60 – EDXA spectra of deposit plated with 0.5µm polystyrene particles.

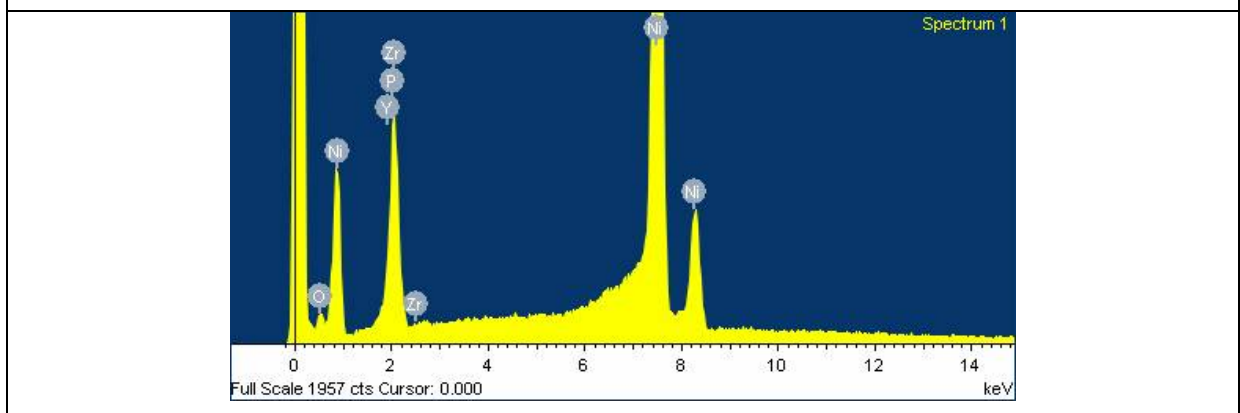


Figure 61 – EDXA spectra of deposit plated with 1.0µm polystyrene particles.

Further experiments are planned to evaluate the effects of combining various particle sizes of polystyrene in an attempt to maximise both the micro and macro porosity. Additionally it is hoped that one or more of the combinations could result in porosity gradients, especially if different particle sizes were added at different times during the deposition process.

One drawback to using the polystyrene is the high costs in purchasing the relatively small samples used in these experiments. Whilst not being totally cost prohibitive it would certainly not be economically viable in large scale production. It was therefore decided to attempt to manufacture polystyrene in the laboratory using traditional techniques for producing this polymer. Initial attempts at co-depositing this ‘in-house’ polymer have been successful, but further experiments will be required to fully evaluate its performance in comparison to the commercial variant already tested.

5.9 Flocculant experiments.

One batch of experiments examined the effects of adding a commercial flocculant on the dispersion of the YSZ in the plating solution. Most commercial flocculants are used in the effluent treatment industry and tend to be based on long chain polymers. A sample of flocculant was supplied by AMT Ltd.

Two drops of Floquat was added to 150mls of Slotonip 1850 solution which had been pre-loaded with 7.5g of 13% YSZ and which was at the operating temperature of 89°C. The effects were evaluated on several samples and it was found that the composition of the deposits was consistent. Table 12 confirms that all the required constituents were deposited, as shown in Figure 62. Examination of the deposits revealed a cauliflower-like structure which was consistent over all the samples, see Figures 63a – 63d.

		Elemental composition, %wt						
Sample	Position	O	P	Ni	Y	Zr	Na	K
A	1	2.87	4.02	83.62	0.80	8.70	-	-
B	1	3.26	3.97	82.19	1.24	9.34	-	-
C	1	2.74	5.06	80.77	0.94	6.42	5.06	4.08
D	1	2.97	3.86	83.70	0.90	8.57	-	-
D	2	1.00	0.83	96.15	-	2.08	-	-

Table 12 – EDXA compositional analysis of Floquat samples.

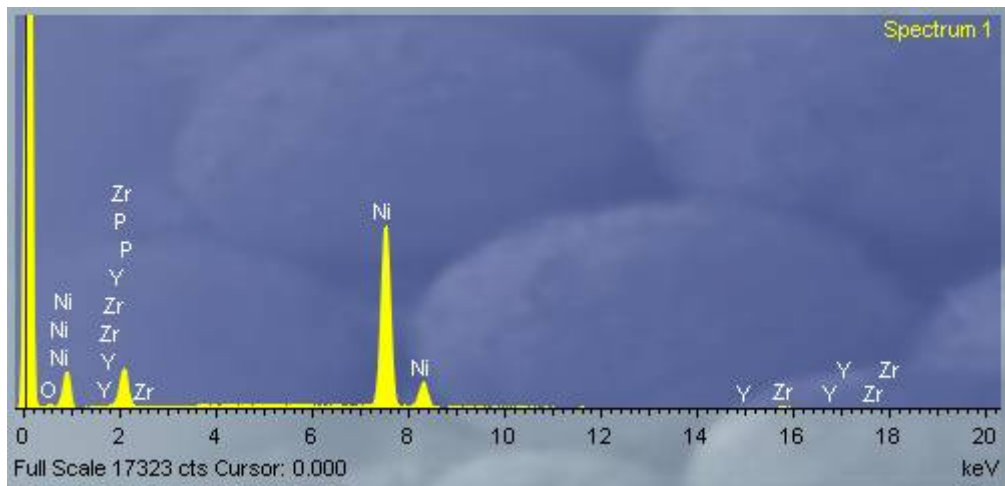


Figure 62 – Typical EDXA spectra of deposit with flocculant.

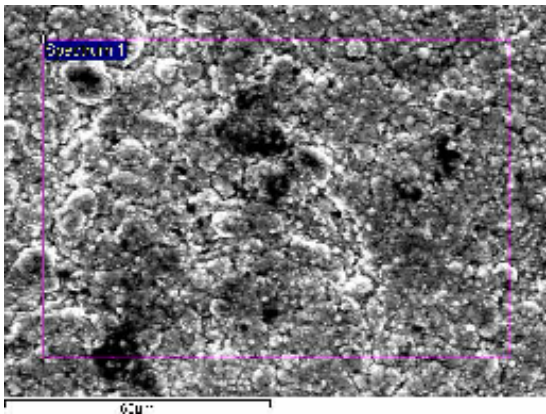


Figure 63a – Batch 1 with 2 drops of Floquat

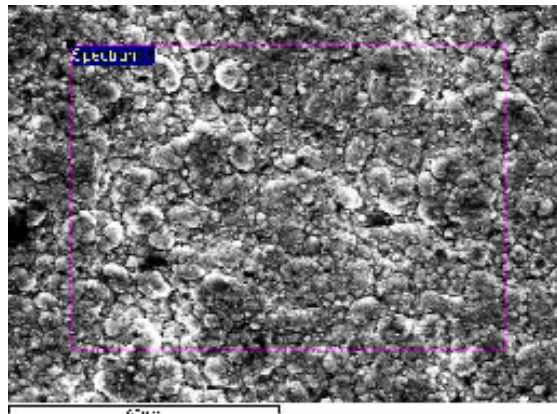


Figure 63b – Batch 2 with 2 drops of Floquat

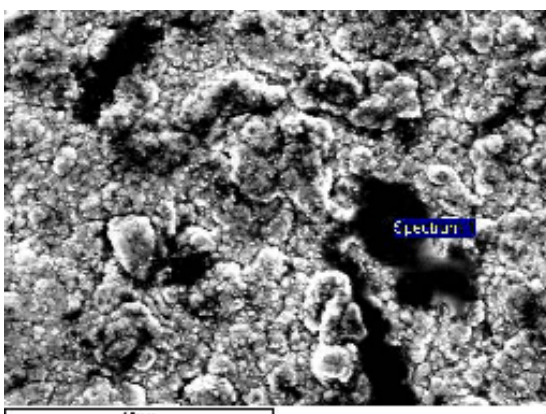


Figure 63c – Batch 3 with 2 drops of Floquat

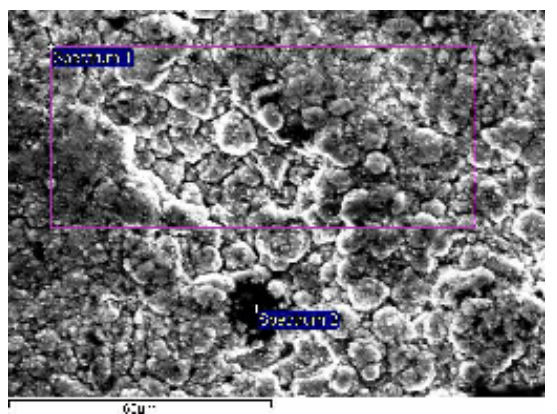


Figure 63d – Batch 4 with 2 drops of Floquat

Compared to previous samples produced without the flocculant additive, the YSZ in these experiments seemed smoother and more evenly dispersed, that is with less agglomeration. This was surprising as commercial flocculants are used to agglomerate species and assist in their precipitation. The porosity in the samples also appeared to be greater than obtained previously. The flocculants used commercially tend to be based on long chain polymers which when heated to the high temperatures in the furnace environment would burn out producing greater levels of porosity.

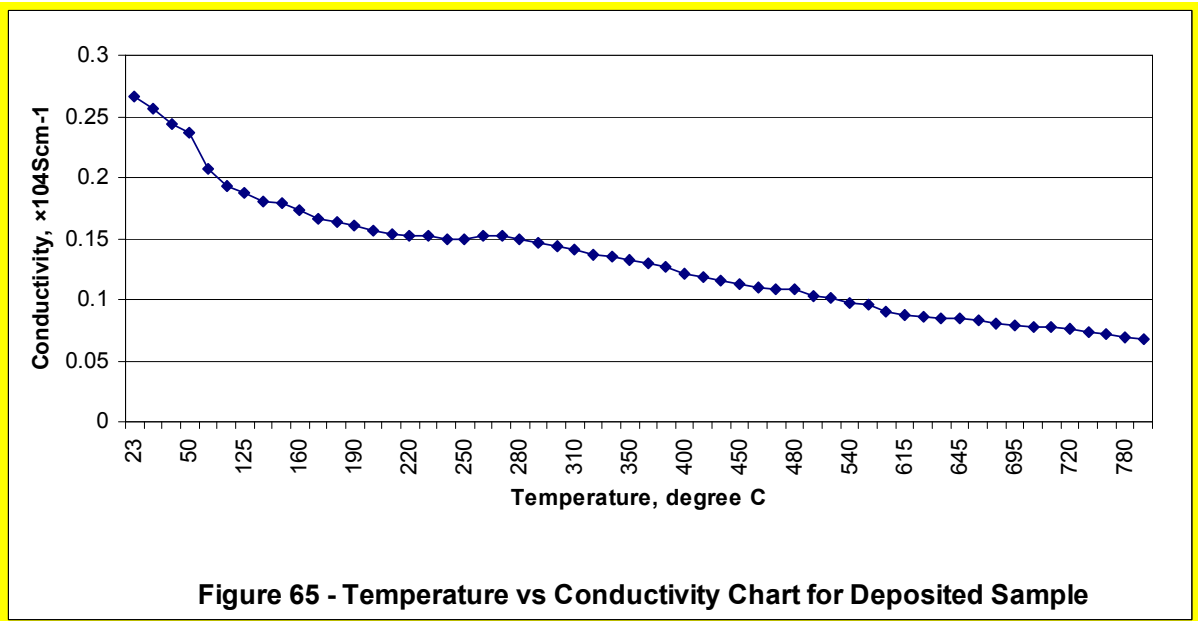
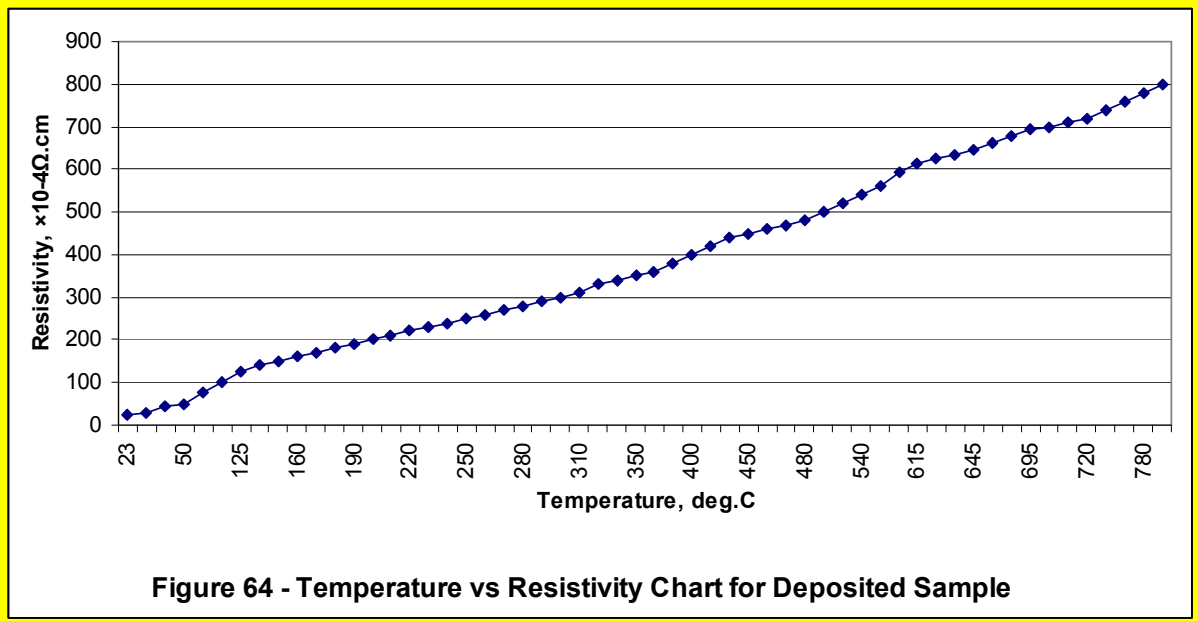
Further experimentation on samples produced by this technique will have to be evaluated in half cells to determine if it improves the cell performance. However these initial experiments have been encouraging and certainly warrant further investigation.

5.10 Electrical experiments

The electrical conductivity and resistivity of the anodes produced were determined using the four-point probe technique. Initially room temperature experiments were performed on the sample as a baseline. The samples were then heated to 850°C and cooled back to room temperature under vacuum to simulate the temperature that a cell would experience during service and the tests repeated. A simple test device was constructed and the test results at 20°C are detailed in Table 13 and the results charted in figures 64 and 65 for the resistivity and conductivity of the sample anode at temperatures up to 850°C in Table 14.

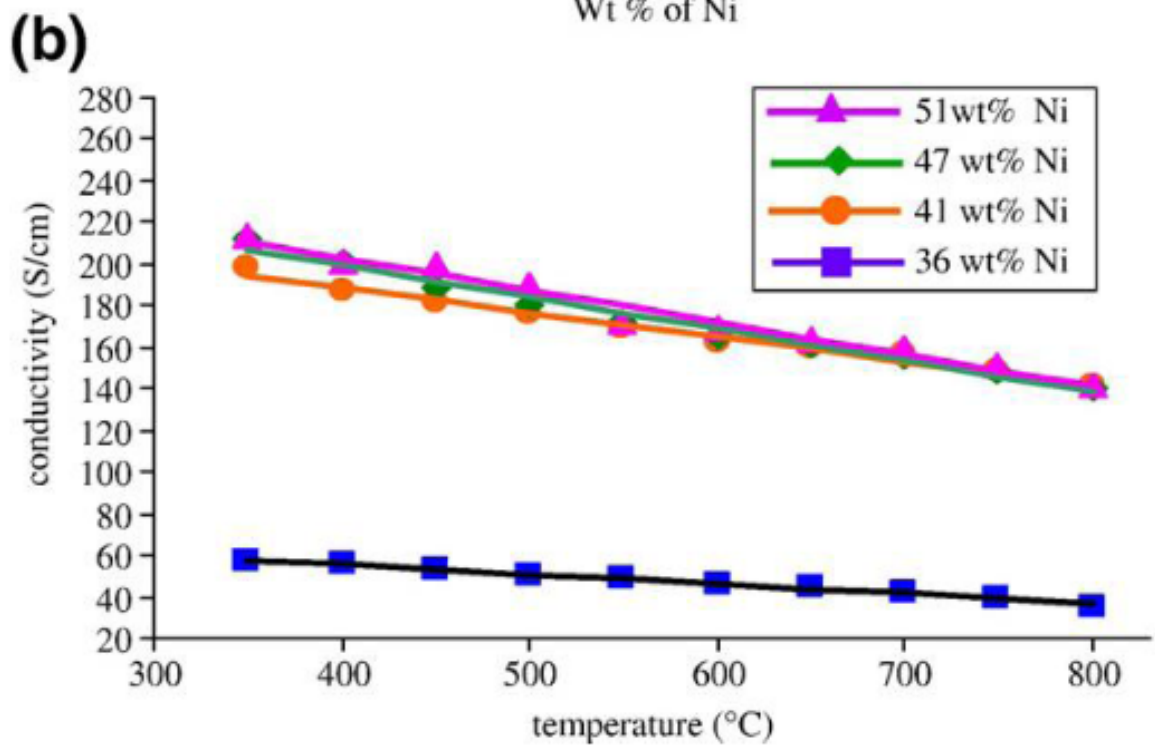
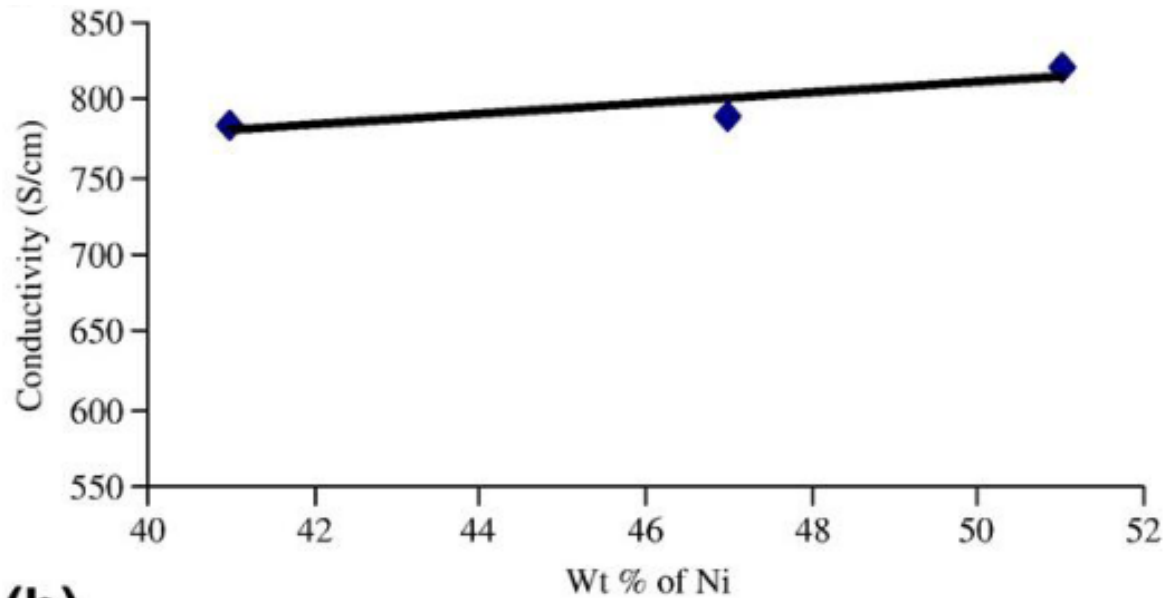
Sheet Resistance, R, Ω	0.117	0.210	0.353	0.425	0.317	0.261
Resistivity, ρ , $\Omega.cm$	1.52×10^{-4}	2.73×10^{-4}	4.59×10^{-4}	5.52×10^{-4}	4.12×10^{-4}	3.4×10^{-4}
Conductivity, σ , $S.cm^{-1}$	0.66×10^4	0.36×10^4	0.22×10^4	0.18×10^4	0.24×10^4	0.29×10^4
Current, I, mA	1	1	50	50	90	90

Table 13 – Initial electrical property results at 20°C



When compared to published data ^[62,69,84] for 50:50% nickel/YSZ anodes, we can see that the conductivity of the deposited anode is at least double that of the published data. This indicates that the likely performance of the anodes developed by this technique would be superior to the conventionally produced anodes. This can only be fully evaluated through live testing under fuel cell conditions using the Electrochemical Impedance Spectroscopy. Equipment has been purchased (Modulab system supplied by Solartron) and a training course in this technique with the equipment was completed at the University of Bath in July 2009

(certification and course syllabus attached in Appendix D section 6). These experiments will be performed over the next 8 months.



Electrical conductivity of Ni coated 8YSZ sintered body at (a) room temperature depending on Ni content and (b) depending on temperature.

Figure 66 a & b - Example of Published ^[69] Electrical Conductivity Data.

5.11 Cathode manufacturing experiments

To fully develop the potential of the process and enhance the manufacturing of the complete cell, experiments were performed to determine the feasibility of depositing the cathode using the same technique. The YSZ powder was substituted for LSM powder which is commonly used in cathode manufacture.

The initial experiments involved bath loadings of 10g.l^{-1} LSM in the Slotonip 1850 solution. Alumina tile substrates were pre-treated with the palladium chloride / stannous chloride procedure and plated for 30 minutes at the optimum plating conditions. The sample cathodes produced were evaluated using both the SEM and EDXA instruments. A conventional cathode was examined at high magnification and compared to the cathode produced in the experiments. The results are illustrated in figures 67 and 68 respectively.

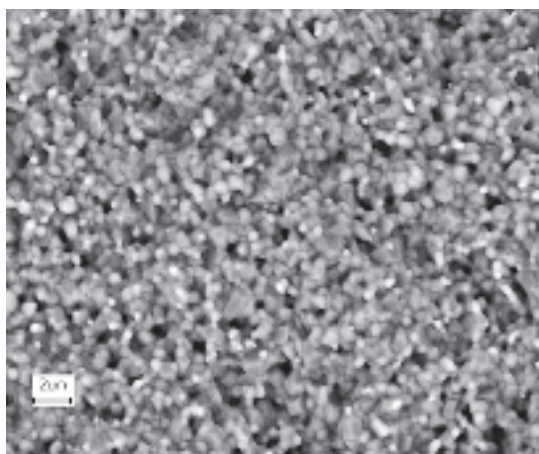


Figure 67 – Conventionally produced cathode, (*Kerafol GmbH sample*)

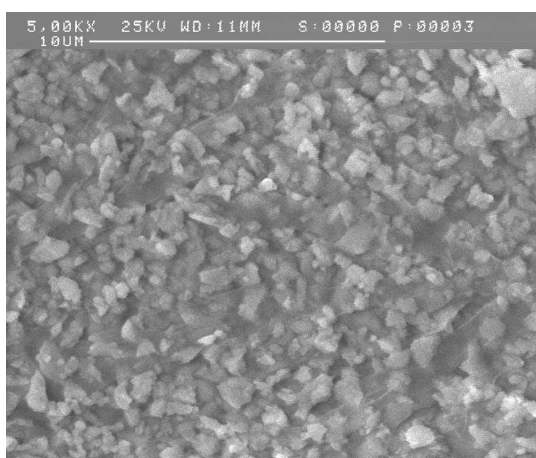


Figure 68 – Cathode produced by electroless deposition

To confirm that the LSM had been successfully co-deposited the sample was analysed to determine its composition and the EDXA spectra is shown below in figure 69.

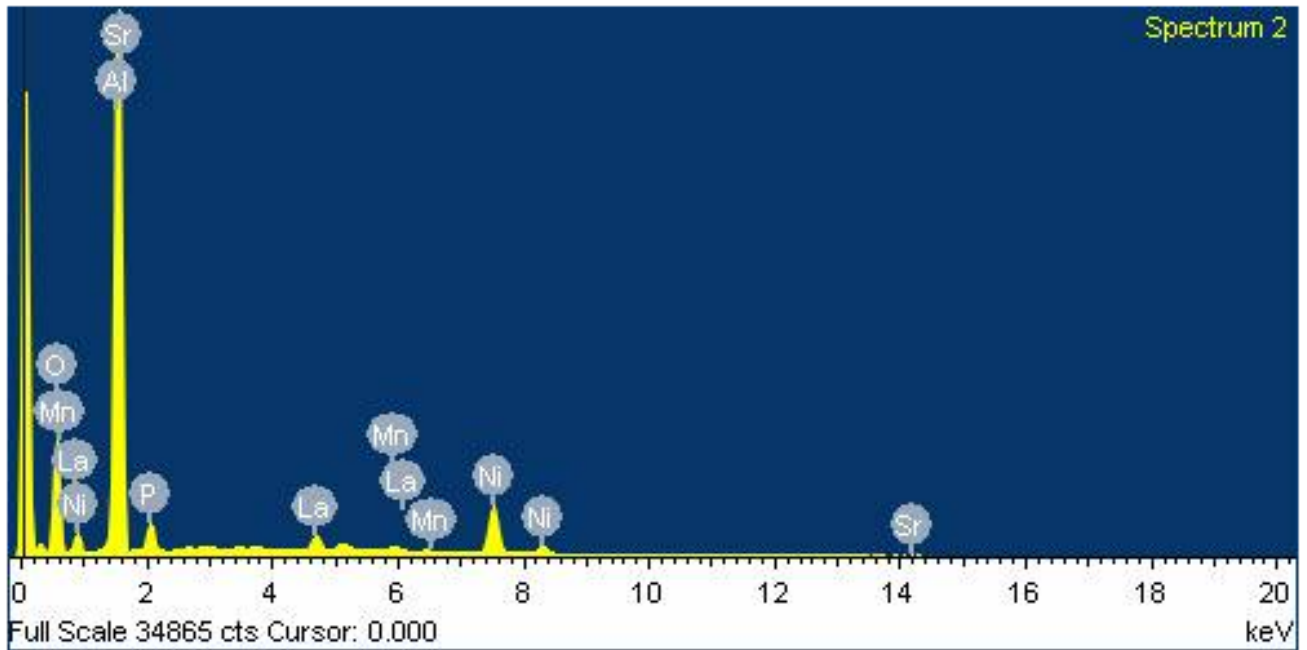


Figure 69 – Composition of cathode produced by electroless deposition.

From the spectra it is apparent that the LSM has been co-deposited as lanthanum, strontium and manganese peaks were detected. Optimisation of the deposit to meet the specifications of conventional cathodes will be the focus of future research.

CHAPTER 6. - *Discussion*

It is clear that solid oxide fuel cells have been extensively investigated over the years, but they are still not commercially viable. The main obstacle to their successful commercialisation is their high material and fabrication costs. If a viable manufacturing process could be established then the market could be staggering, as potentially a combined heat and power (CHP) stack could be fitted in every household as a replacement for the traditional gas boiler. On a larger scale commercial and industrial CHP systems could be used to power hospitals, industrial sites and office blocks. The technology could even be used for major grid power generation due to its scale-ability. Solid oxide fuel cells are therefore extremely attractive because of their simplicity, efficiency and low environmental impact.

Another obstacle to their development has been the lack of co-operation between academic institutes, industrial bodies and government, to drive the technology and industry forward. Whilst some collaborative initiatives have been successful, for example Supergen, there is still a need for further work to be done, especially at government level. One potential avenue that could be pursued would be for the government to establish and fund a technology research centre focusing on renewable energy projects. This would help to bring environmentally friendly technologies into the market faster, which would help the economy and also enable the government to meet its renewable energy targets.

It was apparent from the market and literature reviews that the vast majority of research in solid oxide fuel cell is currently focused in materials development. Additionally, both researchers and their industry counterparts would appear to be using almost exclusively the traditional manufacturing techniques. The drive to lower manufacturing costs and therefore the final stack prices is paramount to allow solid oxide fuel cells to successfully break into the market.

Electroless plating is a versatile technique can be used to deposit numerous metals and alloys. As it is a relatively low temperature chemical process it can be extremely cost effective, depending on the type of deposit. It is currently used in many diverse industries including the aerospace, oil and gas, marine and medical sectors. Coatings can be uniformly deposited

onto various substrates and these deposits can be accurately controlled even to stringent tolerances. Although the basic coatings are well understood, the complex parameters that are required for composite deposition make the technique extremely interesting for new research projects.

The electroless co-deposition technology which has been developed has advantages over some of the issues associated with the more traditional manufacturing methods, such as;

1. Substantially lower capital equipment costs.
2. Simplified, more cost effective process.
3. Wider range of nickel / ceramic ratios for the anode possible. Therefore able to cater to specific customer specifications.
4. Technique is capable of different metal to ceramic ratios throughout the thickness of the deposit (concentration gradients).
5. Overcomes the grain growth issues normally associated with high temperature sintering operations.

Various analytical techniques were employed in the experiments. It is especially important when investigating fuel cells to review the data from as many techniques as possible, so as to understand the complex mechanisms and reactions that are occurring and how the cell construction materials affect them. In this field of research, electrochemical impedance spectroscopy is an essential tool, but it is an extremely difficult technique to interpret without further information from additional techniques. As well as in research of new materials, it can also be used as a diagnostic tool in stack design and evaluating service life performance.

From the initial experimental work performed it was apparent that Ni/YSZ anodes could be successfully prepared using this technique. Adhesive nickel/YSZ coatings were deposited onto various metallic and ceramic substrates. It was also shown that the porosity and surface roughness of the deposit can be influenced using etching and abrasive blasting techniques,

which in turn may have a beneficial influence on the cells performance by increasing the anode surface area and allowing greater diffusion of the fuel gas, through the pore network.

A number of key milestones were identified at the beginning of this project these being:

1. Manufacture of planar anodes with a range of Nickel : YSZ ratios up to 50% YSZ.
2. Manufacture of planar anodes with at least 20% porosity.
3. Breakdown of the cost benefits of the new production process versus currently available methods.
4. Demonstrate the viability of cathode production by the co-deposition process.
5. Completion of initial market assessment with commercial interest from at least two end users who would consider adoption of the process as it would provide commercial benefits for their manufacture of SOFC's.

It was clearly understood that only if these initial five milestones were completed would the project be commercially viable. With that in mind the experiments detailed in this thesis were developed to manufacture and evaluate the performance of the anodes and cathodes against those milestones.

However as well as meeting those criteria a successful pre-treatment procedure for deposition onto non-metallic substrates has also been established, which may allow the deposition process to be adopted into other fuel cell systems, eg Proton Exchange Membrane (PEM's)^[26].

The coating thickness can be accurately controlled and deposits ranging from 5 - 100 μ m can be achieved. This will encompass the vast majority of specifications required by any potential customers.

Deposition of the composite coating on aluminium alloys has also been successfully performed. Although this is not relevant for solid oxide fuel cell applications, it may be a very efficient wear and/or chemical resistant surface treatment. Further work will have to be performed to fully evaluate the deposit for other potential applications.

During the course of the experiments it was found that the ratio of ceramic to metal could be consistently altered by manipulation of the ceramic bath loading and the deposition parameters. This would allow for compositional gradients to be deposited within a deposit to maximise the anodes performance and properties at specific areas through its thickness.

It was vital that the 50:50 ratio of nickel to YSZ was achieved to meet the same composition of commercial anodes. Only with this ratio could the process be equivalent to existing alternative techniques. Only through careful control of the bath loading at 7.5g.l^{-1} in conjunction with controlling the pH and agitation of the solution was this achieved. It is apparent that control of the zeta potential is critical to achieve co-deposition of the nickel and ceramic. Surfactants are necessary to improve the performance and efficiency of the co-deposition and it is anticipated that these will be vitally important in the pilot plant where the agitation will be more difficult to control.

Ranges of bath loading, effective surfactants, solution pH and agitation rates will have to be determined for each new process involving either a new plating solution (another matrix metal) or new reinforcement (ceramic type or size), based upon the experimental techniques already established in this project. Whilst a porosity level of 20% was achieved and this is an acceptable level compared to commercial anodes the level could be increased by further co-deposition of a third polymeric phase. During the project both polystyrene particles and commercial flocculant was successfully co-deposited along with the YSZ. These polymers were then 'burnt-out' to increase the porosity of the anode. This could lead to further gradients in porosity and composition in the anode if the polymer was added at different periods during the deposition process.

The four point electrical testing results have been extremely encouraging and they have generated interest from the commercial contacts. The results to date for the anodes have been significantly superior to the commercial cells which have been made available for testing.

To fully determine the efficiency of these new anodes Electrical Impedance Spectroscopy (EIS) experiments will have to be performed under fuel cell operating conditions, but in order for this to proceed, test apparatus had to be designed and components purchased. This has delayed these essential tests but it has allowed time for training to be undertaken and to become proficient in the use of the equipment. Six button cell test stations are currently being assembled which will be used for the rapid prototyping of the anodes, cathodes and the complete cells, as well as development of new fuels, for example biofuels currently being developed at Edinburgh Napier University.

The process has also been adapted to produce cathodes, which clearly enhances its potential to manufacture complete cells on a suitable electrolyte substrate, but these cathodes will have to be evaluated using EIS experiments, in conjunction with the anodes to determine the full potential of any cell system which may be developed.

CHAPTER 7. - *Conclusions*

The main conclusions from the research are presented below;

1. The traditional manufacturing techniques are well established, and have been adopted by both academic and industrial institutes for fabricating cells for solid oxide fuel cells. The deposition technique developed in this thesis is novel and offers distinct advantages which have been previously discussed. However, despite these advantages, manufacturing companies may be reluctant to adopt the technology, especially if they have already heavily invested in traditional fabrication plant. This technique may be more readily accepted by fledgling companies or more established companies who are developing next generation systems.
2. Suitable pre-treatment processes have been proposed for a range of metallic and non-metallic substrates, both of which have been successfully used to produce composite coatings of nickel and YSZ. By accurately controlling the process, uniform and adherent deposits have been produced to specified thicknesses.
3. Abrasive blasting has been shown to produce significantly rougher surfaces than the chemical etching solutions which have been evaluated to date. These rougher substrates have in turn resulted in composite deposits with increased porosity and surface area. Both increased porosity and surface area are key parameters in fuel cell performance.
4. The following parameters have been shown to be critical in increasing the ceramic ratio in the final deposit;
 - a. Bath loading – optimal concentration of 7.5g.l^{-1}
 - b. pH – Lower pH produces deposits with increased ceramic content by slowing the deposition rate.

c. Agitation method – Air agitation improved the suspension of the ceramic particles in the solution.

d. Component orientation – Horizontal positioning improves co-deposition of ceramic.

Manipulation of these factors allowed a target of 50% nickel : 50% YSZ to be consistently achieved.

5. Deposits with concentration gradients through the thickness of the coating can be produced. This could be advantageous by increasing the electrical conductivity nearer to the interconnect, to improve cell performance. It would also assist in matching the coefficient of thermal expansion in key areas of the cell.
6. A target of 20% porosity was identified as an industry standard. This was achieved experimentally by manipulation of both the bath chemistry combined with the abrasive blasting of the substrate, both of which have been discussed previously. Further experimentation with polystyrene particles and commercial flocculants has further increased the porosity. Altering the porosity by this method should produce a honeycomb effect in the deposit, which would greatly improve gas diffusion and improve cell performance.
7. The anodes and cathodes produced to date have had significantly greater electrical conductivity than their commercial counterparts. This indicates that the likely performance of the electrodes produced by this novel technique would be superior.

CHAPTER 8. - *Commercial Implications*

During the course of this research project there has been considerable support from the Edinburgh Napier University Commercial Development department who considered that the research should be patented. In light of this, numerous patent searches have been performed, the details of which are contained in Appendix II. These clearly show that no previous work on this topic has been performed with regard to Fuel Cell research and development. It was felt that the proposed technique offered particular advantages both technically and in potential manufacturing cost savings to any enterprise involved in manufacturing fuel cell anodes or complete systems.

Over the course of the initial two year work period of the thesis numerous meetings have been concluded and currently the situation exists that funds have been made available by Edinburgh Napier University to assist in furthering the research. This has comprised of purchasing a fuel cell stack system from Fuel Cells Scotland to perform testing of anode samples in an actual working cell to determine their performance against existing anode types. Additionally, funding has been made available to patent the research work which has now been filed under WO 2009/044144 and a copy is attached in appendix D.

In 2008 an application for research funding was also made to the Scottish Enterprise Network under the title of 'Low Cost Manufacture of Anodes for Solid Oxide Fuel Cells'. The application was approved and a two year funded project began in September 2008. To date, collaborative projects with other Scottish Universities in renewable energy, and in particular in SOFC research is being sought, in the hope that the experience gained to date can be further utilised.

The project team has also established contacts with local SME's and international companies who would be interested in assisting in the any future research work and currently both Fuel Cell Scotland and Ceres Power are interested in how the research develops. Finally the University also held discussions with a Venture Capitalist (ACM Catalyst Limited) who expressed an interest in the research. However this has been put on hold for the time being, whilst other potential investors are investigated.

Due to the commercial interest being shown it was decided in conjunction with Edinburgh Napier Commercial Department that no research would be published until the patent matter had been successfully filed and reached the PCT stage. Additionally an invitation to present a poster presentation at a conference titled ‘Scientific Advances in Fuel Cell Systems’ in Turin on the 13-14th September 2006 had to be declined as it was felt that the research should not be made public at that time. However since the patent filing date, a joint publication was published titled ‘Manufacture of Electroless Nickel / YSZ Composite Coatings’ in the Proceedings of World Academy of Science, Engineering and Technology Vol. 37, January 2009 (ISSN 2070-3740) ^[94].

Outwith the scope of this thesis a market assessment has been completed by an independent market research company which has confirmed that the process would enable any potential user to make dramatic savings in both labour time and production costs. Unfortunately this market data is confidential and for that reason the marketing information has been omitted from the thesis. However two companies have lodged letters of interest in the technology and it is hoped that business links can be established with one if not more companies in the next twelve months.

CHAPTER 9. - *Future Work*

Further research work is planned in continuation of that already completed. The existing method will be optimised further using multifactoral experimentation techniques. The specimens produced would then be tested in the button cell apparatus^[80] which is currently under manufacture and any efficient cells would undergo further testing in the fuel cell stack system that has been purchased.

Additionally other metals which can be deposited by the electroless plating technique will be evaluated in conjunction with different types and sizes of ceramic particles.

Other parameters which could also be considered at a later date would include,

- i. Evaluate ceramic composition gradient effects on the fuel cell performance
- ii. Deposit thickness for cell performance (porosity and conductivity)
- iii. Cell performance per metal deposited.

The research has also highlighted the need for additional investigation of the etching solutions as the results have been inconsistent, when compared to the abrasive blasting technique.

The incorporation of the polystyrene or flocculant appears to have a significant effect on the degree of porosity within the deposit. The work completed to date certainly suggests that the co-deposition of these polymer materials be further investigated.

The wear resistance and chemical resistance of the composite coating should be evaluated and its suitability for other applications determined.

Optimisation of the anodes and cathodes should continue in conjunction with further experiments to evaluate both new matrix and reinforcement materials. It is proposed that the following multifactorial experiments would be used to produce the new electrodes.

Parameters for consideration

- i. Matrix type : Ni, Co, Rh, Pd, Ru or Pt.
- ii. Reinforcement type : CeSZ or YSZ or LSM (or combinations of these materials)
- iii. Reinforcement particle size : 2µm or 10 µm
- iv. Surface roughness of substrate :

These would be evaluated in several phases as follows,

PHASE 1

Factors to be examined during phase 1,

Parameters

	Parameter	+	-
1)	Reinforcement	YSZ	CeSZ
2)	Substrate roughness	etched	Unetched
3)	Deposit thickness	2µm	10µm
4)	Fraction of reinforcement	10%	20%

Use four factors in sixteen runs : 2⁴

Random order	Standard order	A	B	C	D	Response
9	1	-	-	-	-	
6	2	+	-	-	-	
13	3	-	+	-	-	
11	4	+	+	-	-	
4	5	-	-	+	-	
15	6	+	-	+	-	
1	7	-	+	+	-	
7	8	+	+	+	-	
12	9	-	-	-	+	
3	10	+	-	-	+	
8	11	-	+	-	+	
10	12	+	+	-	+	
2	13	-	-	+	+	
14	14	+	-	+	+	
16	15	-	+	+	+	
5	16	+	+	+	+	

All effects are free from aliases.

PHASE 2

Repeat experiments using same parameters for Co, Rh, Pd, Ru, Pt as the matrix metals.

	Parameter	+	-
1)	Reinforcement	YSZ	CeSZ
2)	Substrate roughness	etched	Unetched
3)	Deposit thickness	2 μ m	10 μ m
4)	Fraction of reinforcement	10%	20%

Use four factors in sixteen runs : 2^4

Random order	Standard order	A	B	C	D	Response
9	1	-	-	-	-	
6	2	+	-	-	-	
13	3	-	+	-	-	
11	4	+	+	-	-	
4	5	-	-	+	-	
15	6	+	-	+	-	
1	7	-	+	+	-	
7	8	+	+	+	-	
12	9	-	-	-	+	
3	10	+	-	-	+	
8	11	-	+	-	+	
10	12	+	+	-	+	
2	13	-	-	+	+	
14	14	+	-	+	+	
16	15	-	+	+	+	
5	16	+	+	+	+	

All effects are free from aliases.

Then the following phases could commence,

PHASE 3

Determine optimum parameters for each matrix metal.

PHASE 4

Test each in stack to determine best cell performance.

PHASE 5

Establish costs per run / cell performance to determine the most Cost Effective Method.

It is proposed that these parameters would be concluded over the next two years of research and it is envisaged that all the samples produced would be on 25mm diameter electrolyte samples which would allow for them to be tested on the six button test rigs which are currently being manufactured. These test rigs will allow for the rapid prototype testing in conjunction with the Modulab EIS system.

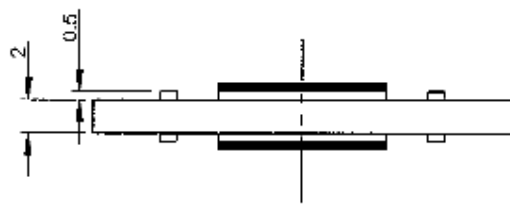
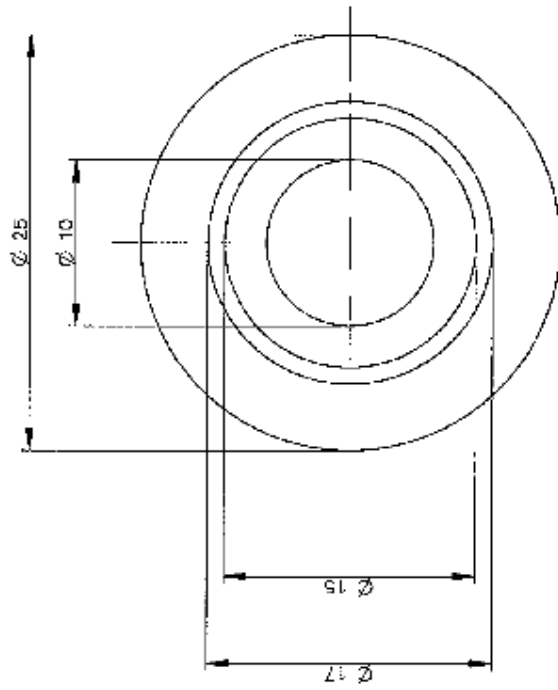
Whilst it is apparent that the current process can be performed successfully under small scale laboratory conditions, further development will be necessary to establish a pilot production plant and to manufacture batches of prototypes for customer evaluation.

APPENDIX A

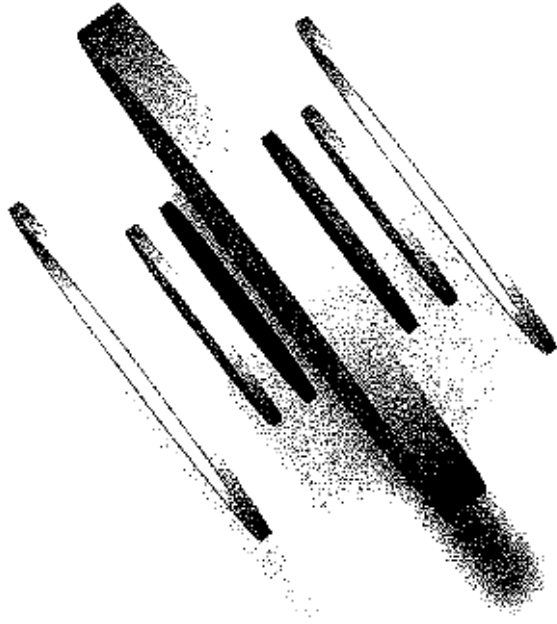
PLANS FOR EXPERIMENTAL TEST APPARATUS

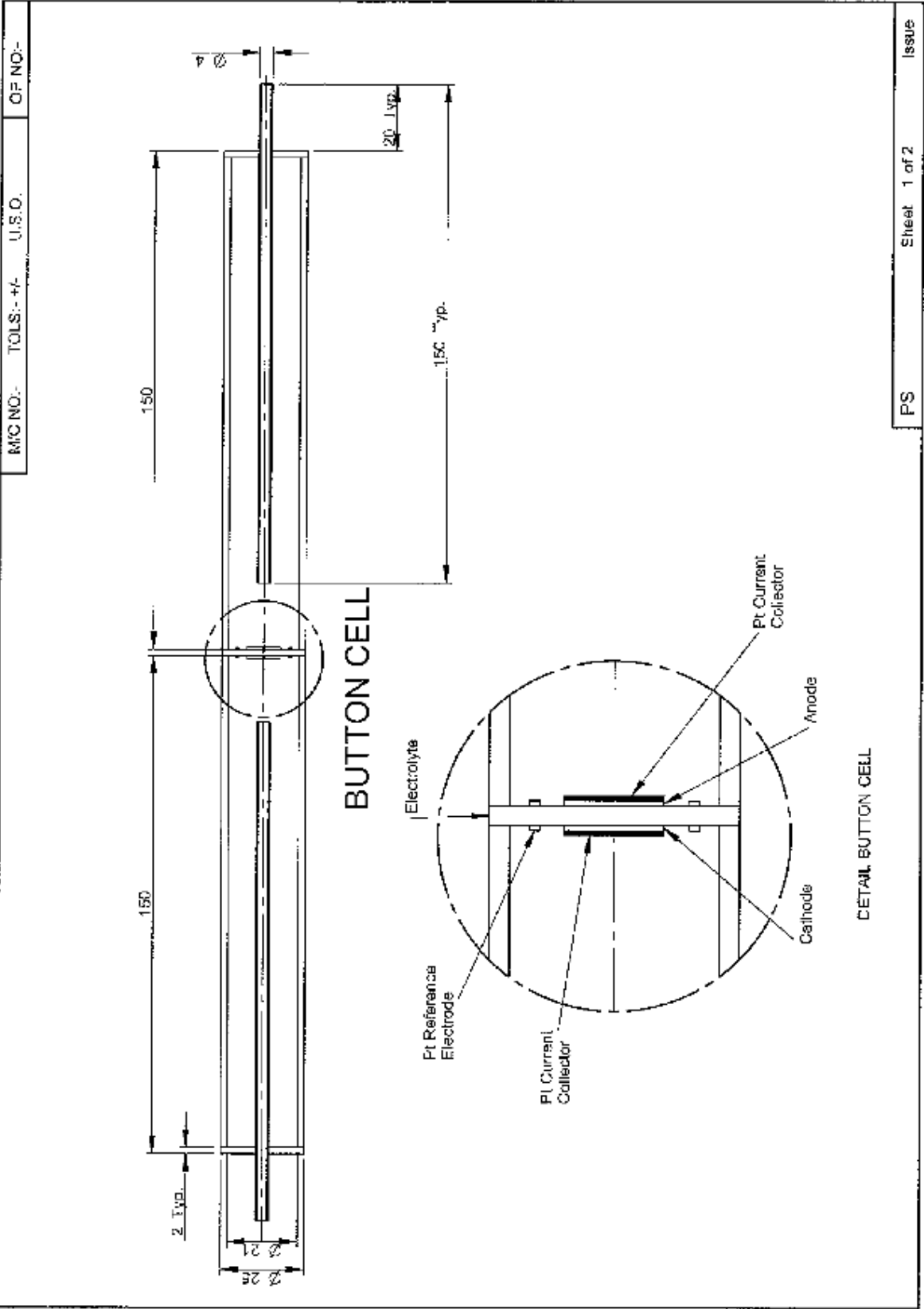
1. BUTTON CELL
2. BUTTON CELL TEST RIG
3. 4 POINT ELECTRICAL TEST APPARATUS

FULL DRAWINGS AND MODELS ON ATTACHED CD ALONG WITH FREE
PROGRAM FOR VIEWING FILES.



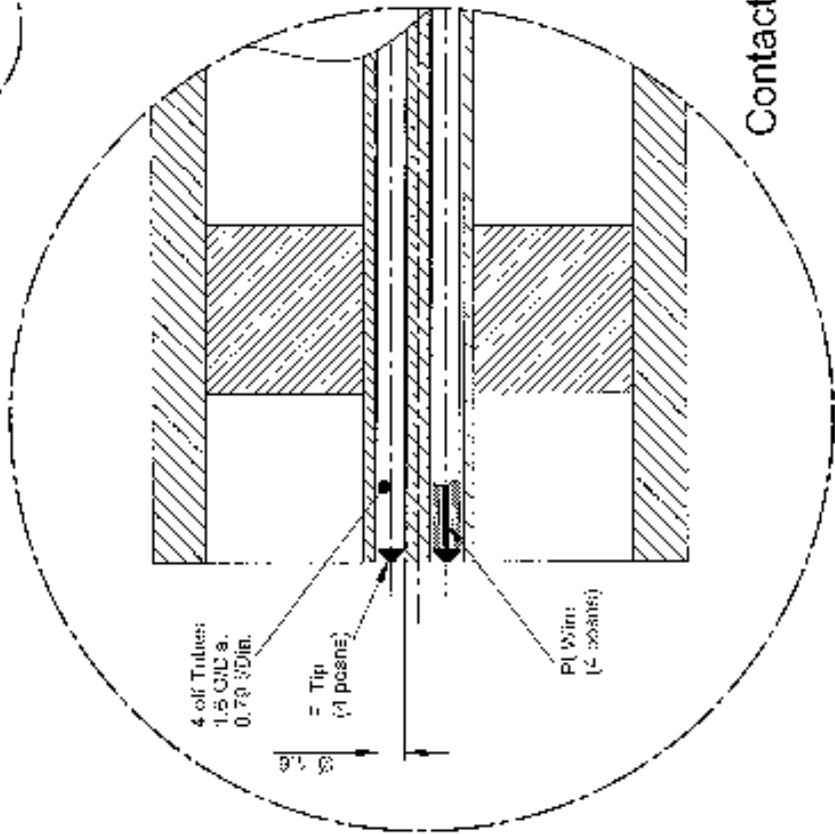
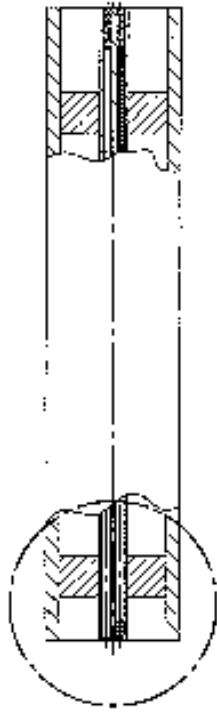






Four Point Electrical Test Apparatus

ALL DIMENSIONS IN INCH

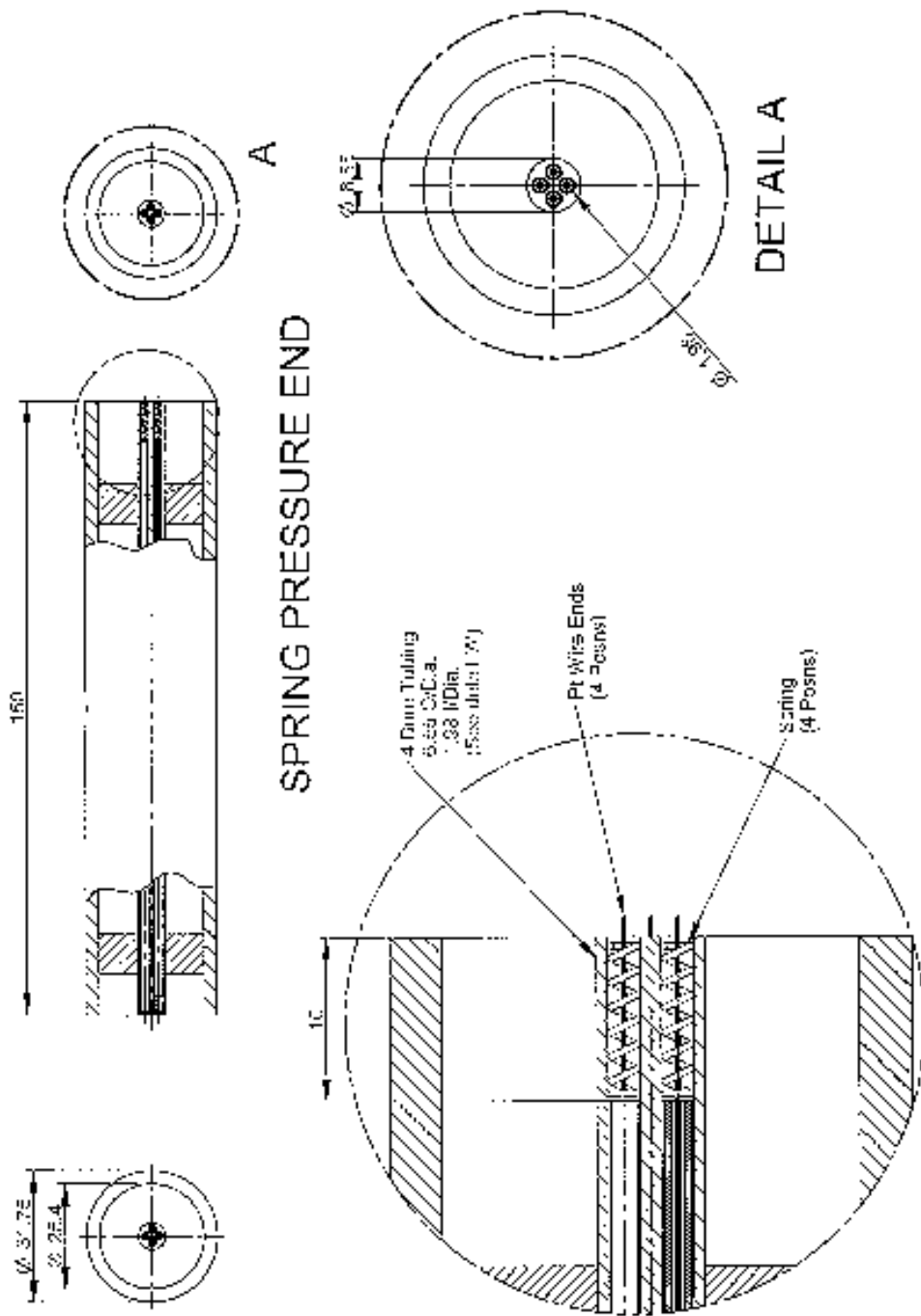


Contact End Detail

Four Point Electrical Test Apparatus

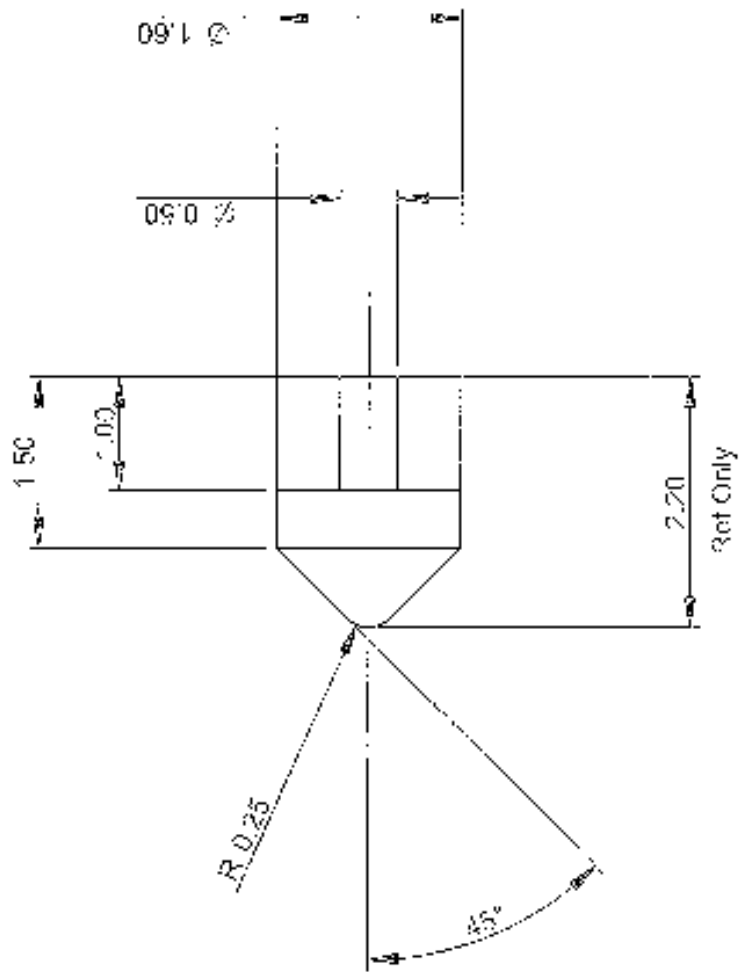
M/C NO:- TOLS:- +/- U.S.C. OP NO:-

A. I. DIMENSIONS IN .001"

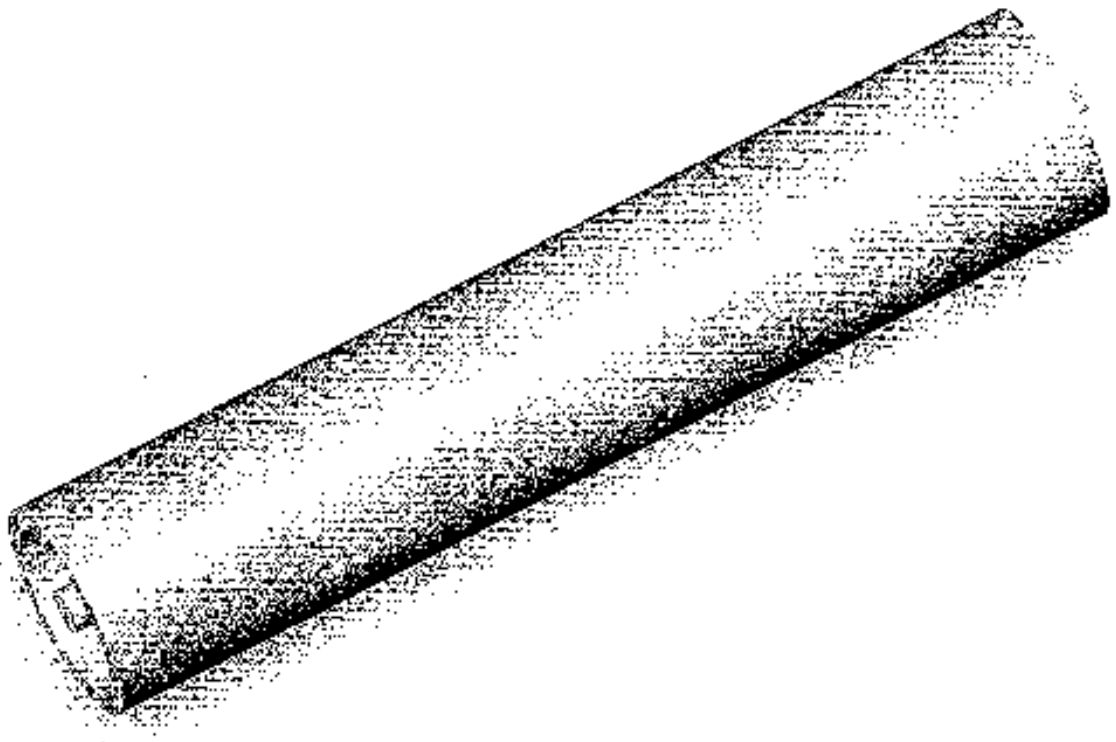


DETAIL SPRING PRESSURE END

PS Shear 1 of 2 Issue



Material: Titanium



APPENDIX B

SAFETY DATA

1. RISK ASSESSMENTS
2. COSHH ASSESSMENT
3. HYDROGEN SAFETY
4. INVENTORY OF MATERIAL SAFETY DATA SHEETS
5. ADDITIONAL LEGISLATION

ALL DATA INCLUDED ON ATTACHED CD

SECTION 1 – RISK ASSESSMENTS

General lab analysis

Abrasive blasting of components

Inspection of plated components

Maintenance and control of effluent plant

Risk Assessment
 Assessment 74 Version 1
 Date 07/08/2007 Review Date 07/08/2008
 Department Plating
 Description General lab analysis. Quality control of plating solutions using volumetric & gravimetric techniques for metal fasting. All analysis performed to manufacturers approved methods or per std methodologies
 Scope Areas are bunded to handle spillages and all wastes treated in effluent plant. Local exhaust ventilation used and PPE worn.
 Assessed By William Waugh
 Reason Initial version.

Attached Files
 RA74_1_08.doc

Hazard	Risk Group	Controls	Future Actions	S*	L	A	Responsibility
slips, trips, falls on the same level	Plating department personnel	Operators have been trained in correct manual handling techniques. Manual handling should be minimised as much as possible and lifting aids used.		S-2	L-1	Y	
chemicals / harmful substances	Plating department personnel	Care should be taken when handling hot chemical solutions and heaters	No further action required	S-2	L-1	Y	
electricity	operators	LEVs used on processing solutions. Operators wear specific PPE where required. Area is bunded and all spills and waste solutions are channelled through effluent treatment plant.	Not required	S-2	L-1	Y	
high noise levels	operators	PPE worn at all times when handling chemicals and powders. LEV should also be used when handling and decanting chemicals and powders	Operators trained in correct procedures for handling chemicals.	S-3	L-1	Y	
manual handling	operators						
hot surfaces	operators						
spills / leaks / vapours	operators						
particles / dusts / fumes	operators						

Footer

Viewed On 02 May 2009
 Viewed By William Waugh
 Copyright © AART Ltd

Risk Assessment

Assessment 40 **Version** 1
Date 01/08/2007 **Review Date** 01/08/2008
Department Plating
Description Abrasive blasting of components as per work instruction W107/6-42, including preparation of blasting medium and replenishment
Scope Work procedure can be used daily for up to 4 hours depending on workload. Area is bunded to handle spillages and all waste treated in effluent plant. Local exhaust ventilation used and PPE worn
Assessed By William Waugh
Reason Initial version.

Attached Files
 RA40_1_44.doc

Hazard	Risk Group	Controls	Future Actions	S*	L	A	Responsibility
slips, trips, falls on the same level	Plating department personnel	PPE should be used.	Noise assessment required	3-8	L-4	N	William Waugh
chemicals / harmful substances	Plating department personnel	Operators have been trained in correct manual handling techniques. Manual handling should be minimised as much as possible and lifting aids used.		3-3	L-1	Y	
electricity	operators	Care should be taken when handling hot chemical solutions and heaters	No further action required	3-2	L-1	Y	
high noise levels	operators	LEVs used on processing solutions. Operators wear specific PPE where required. Area is bunded and all spills and waste solutions are channelled through effluent treatment plant.	Not required	3-2	L-1	Y	
manual handling	operators	PPE worn at all times when handling chemicals and powders. LEV should also be used when handling and decanting chemicals and powders	Operators trained in correct procedures for handling chemicals.	3-3	L-1	Y	
hot surfaces	operators	Employees have received training and department is restricted to authorised personnel only.	Care should be taken due to the bunding, dustboards and liquids which may be present within the department.	3-2	L-1	Y	
spills / leaks / vapours	operators	Personnel trained in correct handling and use of chemicals. LEVs used in process. Department is restricted to authorised personnel only. COSHH assessment has been carried out. PPE used.	NOTE : Cyanides in use	3-5	L-1	Y	
particles / dusts / fumes	operators	PAT testing performed on portable appliances by maintenance dept and fixed equipment tested by sub-contractors.	Not applicable	3-5	L-1	Y	

Footer

Viewed On 02 May 2009
 Viewed By William Waugh
 Copyright © AMT Ltd

Risk Assessment

Assessment 56 Version 1
 Date 02/03/2007 Review Date 04/08/2008
 Department Planting
 Description inspection of plated products as per work instruction W10716-60.
 Scope
 Assessed By William Waugh
 Reason Initial version.

Attached Files
 RA5B_1_56.doc

Hazard	Risk Group	Controls	Future Actions	S*	L	A	Responsibility
slips, trips, falls on the same level	Planting department personnel	PPE should be used.	Noise assessment required	S-3	L-4	N	William Waugh
chemicals / harmful substances	Planting department personnel	Operators have been trained in correct manual handling techniques. Manual handling should be minimised as much as possible and lifting aids used.		S-3	L-1	Y	
electricity	operators	Care should be taken when handling hot chemical solutions and heaters	No further action required	S-2	L-1	Y	
high noise levels	operators	LEVs used on processing solutions. Operators wear specific PPE where required. Area is fenced and all spills and waste solutions are channelled through effluent treatment plant.	Not required	S-2	L-1	Y	
manual handling	operators	PPE worn at all times when handling chemicals and powders. LEV should also be used when handling and decanting chemicals and powders	Operators trained in correct procedures for handling chemicals	S-3	L-1	Y	
hot surfaces	operators	Employees have received training and department is restricted to authorised personnel only.	Care should be taken due to the bonding, ductboards and liquids which may be present within the department.	S-2	L-1	Y	
spills / leaks / vapours	operators	Personnel trained in correct handling and use of chemicals. LEVs used in process. Department is restricted to authorised personnel only. COSHH assessment has been carried out. PPE used.	NOTE : Cyanides in use	S-5	L-1	Y	
particles / dusts / fumes	operators	PAT testing performed on portable appliances by maintenance dept and fixed equipment tested by sub-contractors.	Not applicable	S-5	L-1	Y	

Footer

Viewed On 02 May 2008
 Viewed By William Waugh
 Copyright © AMT Ltd

Risk Assessment

Assessment 78 **Version** 1
Date 07/08/2007 **Review Date** 07/08/2008
Department Plating
Description Maintenance & control of effluent treatment plant to ensure that all waste streams from plating department properly treated prior to discharge. Calibration of the plant to ensure correct operation.
Scope Filling of reagent tanks & dosing of treatment tanks as reqd. All use of hazardous chemicals within plant using correct PPE & pumping equipment. Manual handling transport & storage of reagent chemicals.
Assessed By William Waugh
Reason Initial version.

Attached Files
 RA/78_1_70.doc

Hazard	Risk Group	Controls	Future Actions	S*	L	A	Responsibility
slips, trips, falls on the same level	Plating department personnel						
chemicals / harmful substances	Plating department personnel						
electricity	operators						
high noise levels	operators						
manual handling	operators	Employees have received training and department is restricted to authorised personnel only.	Care should be taken due to the handling, duckboards and liquids which may be present within the department.	5-2	L-1	Y	
wet surfaces	operators	Personnel trained in correct handling and use of chemicals. LEVs used in process. Department is restricted to authorised personnel only. CIBHH assessment has been carried out. PPE used.	NOTE : Cyanides in use	5-5	L-1	Y	
spills / leaks / vapours	operators	PAT testing performed on portable appliances by maintenance dept and fixed equipment tested by sub-contractors.	Not applicable	5-5	L-1	Y	
particles / dusts / fumes	operators	PPE should be used.	Noise assessment required	5-3	L-4	N	William Waugh

Footer

Viewed On 02 May 2009
Viewed By William Waugh
Copyright © AMT Ltd

SECTION 2 – COSHH ASSESSMENTS

Hydrazine, monohydrate

COBHH Assessment

Assessment Performed By	AV Dusy, Alan Leon	Version	2
Assessment Date	10/01/2000	Review Date	12/31/2005
Abbreviation		Substance	HYDRAZINE MONO-HYDRATE, REAGENT
CAS Number		GRADE	
Trade Name	207542	Emergency Contact Reason	1747 H.0100 etc.

Hazard Identification

Hazard



Toxic



Dangerous to the Environment

Risk Phrases

Phrases

- R34, Causes burns
- R10, Flammable
- R45, May cause cancer
- R43, May cause sensitization by skin contact
- R20/21/22, Toxic by inhalation, in contact with the skin and if swallowed
- R20/23, Very toxic to aquatic organisms, may cause long-term adverse effects in the aquatic environment

Safety Phrases

Phrases

- S45, In case of accident or if you feel unwell seek medical advice immediately (show the label where possible)
- S53, Avoid exposure - obtain special instructions before use
- S60, This material and its container must be disposed of as hazardous waste
- S61, Avoid release to the environment. Refer to special instructions/safety data sheet

Control Measures

Measures



Wear Face Protection



Wear Eye Protection



Wear Respiratory Protection



Wear Gloves

Other Control Measures

Measure

- Access is restricted to safety shower and eye bath. Use only in a chemical fume hood.
- Do not breathe vapor. Do not get in eyes, on skin or clothing. Avoid prolonged or repeated contact.
- Wash or decontaminate clothing before reuse. Remove contaminated shoes. Wash thoroughly after handling.
- Use respirators and components tested and approved under appropriate government standards such as NIOSH (EU).
- Use respirators with built up engineering controls.
- Wear compatible chemical-resistant gloves and chemical safety goggles.
- Wear face shield if splash is a concern.

Workplace Exposure Limits

Substance	CAS No.	& LTEL(ppm)	LTEL(mg/m ³)	CLTE	STEL(ppm)	STEL(mg/m ³)	OSHA
HYDRAZINE MONO-HYDRATE, APPROX 64% HYDRAZINE	7805-57-0	54					
HYDRAZINE ANHYDROUS	502-01-2	64					

Health Surveillance

Group Exposed

Amalgamators

First Aid Measures

Exposure Route

Inhalation

Symptom

Toxic if inhaled. Material is extremely corrosive to the tissues of the mucous membranes and upper respiratory tract. Readily absorbed through skin. Toxic if

Treatment

Remove to fresh air. If not breathing give artificial respiration. If breathing is difficult, give oxygen. Flush with copious amounts of water for at least

	absorbed through skin.	15 minutes. Remove contaminated clothing and shoes. Call a physician.
Eye contact	Causes burns.	Flush with copious amount of water for at least 15 minutes. Assume adequate flushing by separating the eyelids with fingers. Call a physician.
Ingestion	Toxic if swallowed.	wash Out mouth with water (provided person is conscious). Call a physician. Do not induce vomiting.
General signs of exposure	Fatigue, Dizziness, Irritation, Stimulation, Confusion, Hypoglycemia, Anorexia, Convulsions, Coma, Cyanosis, inflammation and edema of the larynx and bronchi, chemical pneumonitis, and pulmonary edema, burning sensation, coughing, wheezing, laryngitis,	

Fire Fighting Measures

Extinguishing Media

For small fires, use alcohol foam, dry chemical, or carbon dioxide, or gas fires use water mist.

Hazards

Emits toxic fumes under fire conditions. Combustible liquid.

Procedures

Hydrazine vapor in air is flammable at 4.7 to 100% hydrazine by volume. Handle under nitrogen.

Equipment

Wear self-contained breathing apparatus and protective clothing to prevent contact with skin and eyes.

Accidental Release Measures

Spill Prevention

Evacuate area, shut off all sources of ignition.

Environmental Protection

Do not allow to enter water course or sewer.

Clean Up

Flow with dry lime or soda ash, pick up, keep in a closed container, and hold for waste disposal. Ventilate area and wash spill site after material pickup is complete.

Disposal Arrangements

Contact a licensed professional waste disposal service to dispose of this material.

Handling & Storage

Handling Arrangements

Do not breathe vapor. Do not get in eyes, on skin or clothing. Avoid prolonged or repeated exposure.

Storage Arrangements

Keep tightly closed. Keep away from heat and open flame. Store in a cool dry place.

Attached Files

Footer

Revised On: 04 May 2009
 Revised By: William W. Culp
 Copyright © 4M Ltd.

SECTION 3 – HYDROGEN SAFETY

ALL DOCUMENTS IN ATTACHED CD

Fuel Cell Hydrogen Fuel Vehicle Safety

Hydrogen safety – NASA

Hydrogen and the law

H₂ fact sheet - safety

SECTION 4 – INVENTORY OF MATERIAL SAFETY DATA SHEETS

ALL DOCUMENTS IN ATTACHED CD

No	MATERIAL SAFETY DATA SHEETS (MSDS)
1	0.1 M EDTA
2	6 M Hydrochloric Acid
3	0.1 N Iodine
4	0.1 N Sodium Thiosulphate
5	Acetone
6	Ammonia 0.88 SG
7	Ammonium Chloride
8	Borane Dimethylamine Complex
9	Buffer Solution pH4
10	Buffer Solution pH7
11	Buffer Solution pH10
12	Cobalt (II) Acetate
13	Cobalt (II) Chloride
14	Cobalt (II) Nitrate
15	Cobalt (II) Sulphate
16	Cobalt Standard Metal Solution 1000ppm
17	Cuprolite X84
18	Enfinity 4 LF Part A
19	Enfinity 4 LF Part B
20	Enfinity 4 LF Part C
21	Enfinity 4 LF Part D
22	Gold Potassium Cyanide
23	Gold Standard Metal Solution 1000ppm
24	Hydrazine Monohydrate
25	Microshield Stop-off Lacquer
26	Murexide Indicator
27	Nickel (II) Acetate
28	Nickel (II) Bromide
29	Nickel (II) Chloride
30	Nickel (II) Nitrate
31	Nickel (II) Oxide
32	Nickel (II) Sulphate
33	Nickel Phosphide

- 34 Nickel Standard Metal Solution 1000ppm
- 35 Phosphorus ICP Standard Solution
- 36 Potassium Sodium Tartrate
- 37 Ruthenium (III) Chloride
- 38 Slotonip 2010 A
- 39 Slotonip 2010 B
- 40 Slotonip 2010 R
- 41 Slotonip RP 1850 Electroless Nickel RFU
- 42 Slotonip RP 1851 Starter
- 43 Slotonip RP 1852 Nickel Solution
- 44 Slotonip RP 1861 Starter
- 45 Slotonip RP 1862 Nickel Solution
- 46 Slotonip RP 1863 Replenisher
- 47 Uniphase PHP A
- 48 Uniphase PHP B

SECTION 5 – ADDITIONAL LEGISLATION

ALL DOCUMENTS IN ATTACHED CD

2. RoHS regulations guidance notes 2006
3. SOFC Safety legislation

APPENDIX C

-
1. REFERENCES
 2. IMPEDANCE APPLICATION NOTES
 3. STANDARDS
 4. ELECTROLESS PLATING SOLUTION FORMULATIONS
 5. ETCHING SOLUTION FORMULATIONS
 6. ELECTRICAL TEST RESULTS
 7. TECHNICAL DATA SHEETS
 8. CONVERSION FACTORS
 9. SI UNITS

1. REFERENCES (see attached CD for copies)

No.	TITLE	PUBLICATION	AUTHORS
1	Reaction Process of Two-Step Catalysation Pre-Treatment for Electroless Plating on Non-Conducting Substrates	Trans Inst Met Fin, 2004, 82 (3-4) p114 – 117	K. Yamagishi <i>et al</i>
2	Sensitivity of Nickel Cermet Anodes to Reduction Conditions	Journal of Power Sources 145 (2005) 154 - 160	Christian Mallon, Kevin Kendall
3	Preparation of Nickel Coated YSZ Powder for Application as an Anode for Solid Oxide Fuel Cells	Journal of Power Sources 129 (2004) 138 – 142	Swadesh K. Pratihari <i>et al</i>
4	Electrical Behaviour of Nickel Coated YSZ Cermet Prepared by Electroless Coating Technique	Materials Chemistry and Physics	Swadesh K. Pratihari <i>et al</i>
5	Microstructural Control of Ni-YSZ Cermet Anode for Planar Thin-Film Solid Oxide Fuel Cells	Thin Solid Films 496 (2006) 49-52	H. Abe <i>et al</i>
6	Deposition of Yttria-Stabilised Zirconia Films using Arc Ion Plating	Surface and Coatings Technology 200 (2005) 1401 – 1406	J.T. Chang <i>et al</i>
7	Performance and Electrode Behaviour of Nano-YSZ Impregnated Nickel Anodes used in Solid Oxide Fuel Cells	Journal of Power Sources 147 (2005) 1 – 7	S. P. Jiang, W. Wang, Y.D. Zhen
8	A New Low-Temperature Electroless Nickel Plating Process	Plating and Surface Finishing September 1997, p80 – 82	K. Chen & Y. Chen
9	Fabrication of a Dense La _{0.2} Sr _{0.8} Co O _{3.8} / CoO Composite Membrane by Utilising the Electroless Cobalt Plating Technique	Journal of Membrane Science 198 (2002) 95 – 108	Liang Hong & Weisheng Chua
10	The Formulation of Electroless Nickel – Phosphorus Plating Baths	Plating and Surface Finishing February 1987 p60 - 65	Konrad Parker
11	Permselectivity of a Nickel – Ceramic Composite Membrane at Elevated Temperature : A New Prospect in Hydrogen Separation ?	Journal of Membrane Science 288 (2007) 208 - 217	Barbara Ernst <i>et al</i>

No.	TITLE	PUBLICATION	AUTHORS
12	Low Phosphorus Electroless Nickel Coating Technology	Inst. Metal Finishing 1990, 68 (3), 75	Brian Jackson <i>et al</i>
13	Codeposition of Mixtures of Dispersed Particles with Nickel – Phosphorus Electrodeposits	Plating and Surface Finishing October 1994 p68 – 71	N. Periene <i>et al</i>
14	Characteristic Evaluation of Electroless Nickel – Phosphorus Deposits with different Phosphorus Contents	Microelectronic Engineering 84 (2007) 2552 – 2557	Jeong-Won Yoon <i>et al</i>
15	Counterion Effects During Electroless Nickel Plating	Metal Finishing March 2003 p41 – 47	Nicholas M. Martyak
16	Artificial Neural Network Modelling of Plating Rate and Phosphorus Content in the Coatings of Electroless Nickel Plating	Journal of Materials Processing Technology 205 (2008) 207 – 213	Wu Yating <i>et al</i>
17	Modelling the Stability of Electroless Plating Bath - Diffusion of Nickel Colloidal Particles from the Plating Frontier	Journal of Colloid and Interface Science 262 (2003) 89 – 96	X. Yin, L. Hong, B-H, Chen & T-M Ko
18	Electroless Ni – Co – P Ternary Alloy Deposits: Preparation and Characteristics	Surface and Coatings Technology 172 (2003) 298 – 307	T.S.N. Sankara Narayanan <i>et al</i>
19	Effect of Coating Time and Heat Treatment on Structures and Corrosion Characteristics of Electroless Ni – P Alloy Deposits	Surface and Coatings Technology 176 (2004) 318 – 326	H. Ashassi – Sorkhabi & S.H. Rafizadeh
20	The Corrosion Resistance of Electroless Deposited Nano – Crystalline Ni – P Alloys	Electrochimica Acta 53 (2008) 3364 – 3370	Maura Crobu <i>et al</i>
21	A Study on the Influence of Process Parameters on Efficiency and Crystallinity of Electroless Ni – P Deposits	Journal of Materials Processing Technology 169 (2005) 308 – 313	J.T. Winowlin Jappes <i>et al</i>
22	Co-Deposition Mechanism of Nanodiamond with Electrolessly Plated Nickel Films	Electrochimica Acta 52 (2007) 3047 – 3052	Hiroshi Matsubara <i>et al</i>

No.	TITLE	PUBLICATION	AUTHORS
23	Effect of Agitation on Electroless Nickel Deposition	Plating and Surfacing Finishing March 1993 p56 – 58	K. Sevugan <i>et al</i>
24	Properties of Electroless Nickel – Phosphorus Deposits after Crystallization	Metal Finishing November 1992 p13 – 18	P.R. Krishnamoorthy <i>et al</i>
25	Characterisation of Ni –P Electroless Deposits with Moderate Phosphorus Content	Surface Engineering 1997 Vol 13. No. 4 335 – 228	M.H. Staia
26	New Electroplated Aluminium Bipolar Plate for Pem Fuel Cell	Journal of Power Sources 177 (2008) 131 – 136	Sanaa A. Abo El-Enin <i>et al</i>
27	Fabrication of Composite SOFC Anodes	Materials Science and Engineering B 121 (2005) 120 – 125	M A Haldane & T H Etsell
28	The Impact of Wood-Derived Gasification Gases on Ni-CGO Anodes in Intermediate Temperature Solid Oxide Fuel Cells	Journal of Power Sources 126 (2004) 58 – 66	Sylvia Baron <i>et al</i>
29	The Environmental Impact of Solid Oxide Fuel Cell Manufacturing	Fuel Cells Bulletin No 15 P4 – 7	Nigel Hart <i>et al</i>
30	Observation of Initial Deposition Process of Electroless Nickel Plating by Quartz Crystal Microbalance Method and Microscopy	Electrochimica Acta 47 (2002) 4011 – 4018	Hiroshi Matsubara <i>et al</i>
31	Electroless Pure Nickel Plating Process with Continuous Electrolytic Regeneration System	Surface and Coatings Technology 169 - 170 (2003) 132 - 134	Seiichiro Nakao <i>et al</i>
32	Formation of Electroless Ni-B Coatings using Low Temperature Bath and Evaluation of Their Characteristic Properties	Surface and Coatings Technology 200 (2006) 6888 – 6894	I Baskaran <i>et al</i>
33	Parametric Optimization and Prediction of Electroless Ni-B Deposition	Materials and Design 28 (2007) 2138 – 2147	B Oraon <i>et al</i>

No.	TITLE	PUBLICATION	AUTHORS
34	Ultrasound Influence on the Activation Step Before Electroless Coating	Ultrasonics Sonochemistry 10 (2003) 363 – 368	F Touyeras <i>et al</i>
35	Electroless Deposition in Nanotechnology and ULSI	Microelectronic Engineering 69 (2003) 384 – 390	T N Kopperia
36	Evaluation of Haynes 242 Alloy as SOFC Interconnect Material	Solid State Ionics 177 (2006) 559 – 568	S J Geng, J H Zhu & Z G Lu
37	Formation and Characterization of Borohydride Reduced Electroless Nickel Deposits	Journal of Alloys and Compounds 365 (2004) 197 – 205	T S N Sankara Narayanan & S K Seshadri
38	Oxygen Transport in La _{0.6} Sr _{0.4} Co _{0.2} Fe _{0.8} O ₃₋₅ / Ce _{0.8} Ge _{0.2} O _{2-x} Composite Cathode for IT-SOFCs	Solid State Ionics 175 (2004) 63 – 67	Audrey Esquirol, John Kilner, Nigel Brandon
39	Hardness Evolution of Electroless Nickel-Phosphorus Deposits with Thermal Processing	Surface and Coatings Technology 168 (2003) 263 – 274	K G Keong, W Sha, S Malinov
40	Chemical and Electrochemical Depositions of Platinum Group Metals and Their Applications	Co-ordination Chemistry Reviews 249 (2005) 613 – 631	Chepuri R K Rao & D C Trivedi
41	Electroless Ni-P / Ni-B Duplex Coatings: Preparation and Evaluation of Microhardness, Wear and Corrosion Resistance	Materials Chemistry and Physics 82 (2003) 771 – 779	T S N Sankara, Narayanan <i>et al</i>
42	Properties of Ni / YSZ Cermet as Anode for SOFC	Solid State Ionics 132 (2000) 253 – 260	Hideto Koide <i>et al</i>
43	SOFC Anodes for the Direct Oxidation of Hydrocarbons	Powerpoint Presentation University of Pennsylvania	R J Gorte
44	Evaluation of Interconnect Alloys and Cathode Contact Coatings for SOFC Stacks	6 th European Solid Oxide Fuel Cell Forum 28 June – 2 July 2004 p319	Nico Dekker <i>et al</i>

No.	TITLE	PUBLICATION	AUTHORS
45	An Investigation into Microstructure and Particle Distribution of Ni-P / Diamond Composite Thin Films	Journal of Microscopy Vol 185, PT2, February 1997, pp2283 - 291	B Bozzini, G Gionannelli, P L Cavallotti
46	The Impact of Substrate Roughness on Porosity: A Comparison of Electroplated Palladium, Palladium – Nickel & Cobalt Hard Gold	Plating and Surface Finishing January 1997 p37 – 37	E J Kudrak, J A Abys, F Humiec
47	Electrodeposition Process Modeling Using Continuous and Discrete Scales	Computers and Chemical Engineering 31 (2007) 980 – 992	Philippe Mandin <i>et al</i>
48	Gd _{1-x} A _x Co _{1-y} Mn _y O ₃ (A= Sr, Ca) As a Cathode for the SOFC	Solid State Ionics 123 (1999) 131 – 138	M B Phillipps <i>et al</i>
49	Energy and Exergy Analysis of Simple Solid-Oxide Fuel-Cell Power Systems	Journal of Power Sources 103 (2002) 188 – 200	S H Chan, C F Low, O L Ding
50	A Solid Oxide Fuel Cell with a Gadolinia – Doped Ceramic Anode: Preparation and Performance	Solid State Ionics 123 (1999) 199 – 208	Olga A Marina <i>et al</i>
51	Sintering and Phase Evolution of Electroless-Nickel-Coated Alumina Powder	Journal American Ceramic Society 81 [9] 2481 – 84 (1998)	Jung-Jen Lin, Bor-Feng Jiang
52	Oxide Anode Materials for Solid Oxide Fuel Cells	Solid State Ionics 177 (2006) 1529 – 1541	Jeffrey W Fergus
53	Electrocatalysis in Solid Oxide Fuel Cell Electrode Domains	J Electrochem Soc 142, No2, February 1995	K Ravindranathan Thampi, <i>et al</i>
54	Anode-Supported Solid Oxide Fuel Cell with Ytria-Stabilised Zirconia / Gadolinia – Doped Ceria Bilayer Electrolyte Prepared by Wet Ceramic Co-sintering Process	Journal of Power Sources 162 (2006) 1036 – 1042	Q L Liu, K A Khor, S H Chan, X J Chen
55	Multilayer Tape-casting Method for Anode – Supported Planar SOFCs	Fuel Cells Bulletin August 2007 p12 – 15	Zhenrong Wang <i>et al</i>

No.	TITLE	PUBLICATION	AUTHORS
56	Performance and Stability of SOFC Anode Fabricated from NiO – YSZ Composite Particles	Journal of Power Sources 110 (2002) 91-95	Takehisa Fukui <i>et al</i>
57	Development of a Multilayer Anode for Solid Oxide Fuel Cells	Solid State Ionics 152 – 153 (2002) 537 – 542	Axel C Muller <i>et al</i>
58	Effect of Starting Powder on Screen-Printed YSZ Films Used as Electrolyte in SOFCs	Solid State Ionics 177 (2006) 281 – 287	Yaohui Zhang <i>et al</i>
59	Improved Production Methods for YSZ Electrolyte and Ni – YSZ Anode for SOFC	Riso National Laboratory Materials Dept	C Bagger
60	Effects of Heat Treatment on the Structure Corrosion Resistance and Stripping of Electroless Nickel Coatings	M & T Chemicals Lts Ruislip Technical Centre	M Sadeghi, P D Longfield, C F Beer
61	Agglomerate and Particle Size Effects on Sintering Ytria – Stabilised Zirconia	Journal of the Americal Ceramic Society Vol64, No1, p19 – 22 Jan 1981	W H Rhodes
62	Configuration and Electrical Behaviour of Ni-YSZ Cermet with Novel Microstructure for Solid Oxide Fuel Cell Anodes	J Electrochem SOC Vol 144, No2, February 1997 p641 – 646	Hibiki Itoh <i>et al</i>
63	Development of Standard Ni – YSZ Cermet Anode for Intermediate Temperatures	Federal Institute of Technology Lausanne Switzerland (Report)	Jan Van Herle
64	The Kinetics of Hydrogen Oxidation on a Ni-YSZ SOFC Electrode at 1000°C	Riso National Laboratory (Report)	M Mogensen & T Lindegaard
65	Electroless Deposition of Electrodes in Solid-Oxide Fuel Cells	J Electrochem Soc Vol 141, No8 August 1994 p94 - 96	M M Murphy <i>et al</i>
66	Influence of Porous Composite Microstructure on the Processing and Properties of Solid Oxide Fuel Cell Anodes	Solid State Ionics 166 (2004) 251 – 259	R M C Clemmer & S F Corbin
67	Electrodeposited Nickel – Alumina Composites	Plating January 1973, p55 – 59	P K Sinha <i>et al</i>

No.	TITLE	PUBLICATION	AUTHORS
68	Studies of Porosity in Electroless Nickel Deposits on Ferrous Substrates	Trans IMD 1996, 74 (6), p214 – 220	C Kerr, D Barker & F C Walsh
69	Microstructure Characterisation and Electrical Conductivity of Electroless Nano Ni Coated 8 YSZ Cermets	Surface & Coatings Technology (2007)	A H M Esfakur Rahman <i>et al</i>
70	Novel Anode Materials for Multi – Fuel Applicable Solid Oxide Fuel Cells	Journal of Alloys and Compounds 408 – 412 (2006) 622 – 627	Ryuji Kikuchi <i>et al</i>
71	Performance and Durability of Ni – Coated YSZ Anodes for Intermediate Temperature Solid Oxide Fuel Cells	Solid State Ionics 177 (2006) 931 – 938	Sun-Dong Kim <i>et al</i>
72	An Integrated Approach to Electrochemical Impedance Spectroscopy	Electrochimica Acta 53 (2008) 7360-7366	Mark E. Orazem, Bernard Tribollet
73	Impedance Studies of Cathode / Electrolyte Behaviour in SOFC	Electrochimica Acta 53 (2008) 7491 0 7499	D E Vladikova <i>et al</i>
74	Characteristics of SOFC Single Cells with Anode Active Layer via Tape Casting and Co-firing	International Journal of Hydrogen Energy 33 (2008) 2826 – 2833	Hwan Moon <i>et al</i>
75	Electrochemical Parameter Identification – An Efficient Method for Fuel Cell Impedance Characterisation	Journal of Power Sources 183 (2008) 55 – 61	Michael A Danzer, Eberhard P Hofer
76	Electrochemical and Microstructural Analysis of Nickel – Yttria – Stabilized Zirconia Electrode Operated in Phosphorus – Containing Syngas	Journal of Power Sources 183 (2008) 485 – 490	Mingjia Zhi <i>et al</i>
77	Degradation Measurement and Analysis for Cells and Stacks	Journal of Power Sources 184 (2008) 251 – 259	Randall S Gemmen, Mark C Williams and Kirk Gerdes

No.	TITLE	PUBLICATION	AUTHORS
78	Improvement of Anode – Supported Solid Oxide Fuel Cells	Solid State Ionics 179 (2008) 1593 – 1596	Z R Wang <i>et al</i>
79	Performance Analysis of Cobalt – Based Cathode Materials for Solid Oxide Fuel Cell	Solid State Ionics 179 (2008) 1490 – 1496	Jung Hyun Kim <i>et al</i>
80	Effect of Operating Conditions on the Electrochemical Behaviour of Hydrogen – Fed Solid Oxide Fuel Cells	International Journal of Hydrogen Energy 33 (2008) 5073 – 5082	Ta-Jen Huang, Meng-Chin Huang
81	Stability of Nano - Microsized Particles in Deionized Water and Electroless Nickel Solutions	Journal of Colloid and Interface Science 314 (2007) 514 – 522	B S Necula <i>et al</i>
82	Impedance Simulations of SOFC Pattern and Cermet Anodes from Detailed Electrochemical Models	Ninth International Symposium on Solid Oxide Fuel Cells (SOFC-IX) May 15 – 20, Quebec City, Canada (2005) Electrochemical Society Proceedings Volume 2005 – 07, P708 – 718	Wolfgang G Bessler <i>et al</i>
83	Electrical and Microstructural Investigations of Cermet Anode / YSZ Thin Film Systems	Journal of the European Ceramic Society 21 (2001) 1861 – 1865	Darja Kek, Peter Panjan, Elke Wanzenberg, Janez Jamnik
84	Nickel Coarsening in Annealed Ni/8YSZ Anode Substrates for Solid Oxide Fuel Cells	Solid State Ionics 132 (2000) 241 – 251	D Simwonis, F Tietz, D Stover
85	Kinetics of Electroplating Process of Nano-Sized Ceramic Particle / Ni Composite	Materials Chemistry and Physics 78 (2003) 574 – 580	Sheng-Chang Wang, Wen-Cheng J Wei
86	Synthesis and Properties of Ni-YSZ Cermet : Anode Material for Solid Oxide Fuel Cells	Solid State Ionics 111 (1998) 45 – 51	S T Aruna, M Muthuraman, K C Patil
87	Deposition of Electroless Ni-P Graded Coatings and Evaluation of Their Corrosion Resistance	Surface & Coatings Technology 200 (2006) 3438 – 3445	T S N Sankara Narayanan

No.	TITLE	PUBLICATION	AUTHORS
88	Quantitative Analysis of Microstructure and its Related Electrical Property of SOFC Anode, Ni – YSZ Cermet	Solid State Ionics 148 (2002) 15 – 26	J-H Lee <i>et al</i>
89	Optimisation of a Bath for Electroless Plating and its Use for the Production of Nickel – Phosphorus – Silicon Carbide Coatings	Trans. Inst. Metal Finishing 1993, 71 (2) 55	M R Kalantary <i>et al</i>
90	Thiophene Hydrodesulfurization Over Nickel Phosphide Catalyst : Effect of the Precursor Composition and Support	Journal of Catalysis 231 (2005) 300 – 313	Stephanie J Sawhill <i>et all</i>
91	Diamond – Dispersed Electroless Nickel Coatings	Central Electrochemical Research Institute, Karaikudi, India	G Sheela and M Pushpavanam
92	Characterisation of Electrical Performance of Anode Supported Micro-tubular Solid Oxide Fuel Cell with Methane Fuel	Journal of Power Sources 181 (2008) 195 – 198	Tae Jung Lee, Kevin Kendall
93	Effect of Surfactants on Codeposition of PTFE Particles with Electroless Ni-P Coating	Materials Chemistry and Physics 76 (2002) 38 – 45	Ming-Der Ger, Bing Joe Hwang
94	Manufacture of Electroless Nickel / YSZ Composite Coatings	Proceedings of World Academy of Science, Engineering and Technology Vol 37 January 2009 ISSN 2070-3740	N Bahiyah Baba, W Waugh and A M Davidson
95	Characterization of Chemically – Deposited NiB and NiWB Thin Films as a Capping Layer for ULSI Application	Surface and Coatings Technology 169 – 170 (2003) 124 – 127	Tetsuya Osaka <i>et al</i>
96	Electroless Deposition of Amorphous Ni-Re-P Alloys from Acidic Hypophosphite Solutions	Journal of Alloys and Compounds 306 (2000) 158 – 162	D Mencer
97	Deposition and Properties of Electroless Ni-P-B ₄ C Composite Coatings	Surface & Coatings Technology 168 (2003) 259 - 262	S M Moonir-Vaghefi <i>et al</i>

No.	TITLE	PUBLICATION	AUTHORS
98	Comparison of Electrical Conductivity Data Obtained by Four-Electrode and Four-Point Probe Methods for Graphite-Based Polymer Composites	Polymer Testing 26 (2007) 547 – 555	V S Mironov <i>et al</i>
99	Kinetics of Electroplating Process of Nano-sized Ceramic Particle / Ni Composite	Materials Chemistry and Physics 78 (2003) 574 – 580	Sheng-Chang Wang, Wen-Cheng J. Wei
100	Improving the Adhesion of Electroless Nickel Coating Layer on Diamond Powder	Surface and Coatings Technology 201 (2006) 3793 – 3796	J G Ahn <i>et al</i>
101	Fabrication of Magnetic Nickel – Tungsten – Phosphorus Particles by Electroless Deposition	Journal of Magnetism and Magnetic Materials 305 (2006) 342 - 347	Ming-Kai Chang <i>et al</i>
102	Effect of Plating Parameters on the Intrinsic Stress in Electroless Nickel Plating	Surface and Coatings Technology 167 (2003) 170 – 176	Zhong Chen <i>et al</i>
103	Microstructures and Electrical Conductivity of Nanocrystalline Ceria – based Thin Films	Solid State Ionics 177 (2006) 2513 - 2518	Jennife L M Rupp and Ludwig J Gauckler
104	Investigation on the Corrosion and Oxidation Resistance of Ni-Al ₂ O ₃ Nano-composite Coatings Prepared by Sediment Co-deposition	Surface and Coatings Technology (2008) 202 [17] 4137 – 4144	Quynan Feng <i>et al</i>
105	Effect of Surfactants Addition on the Suspension of PTFE Particles in Electroless Plating Solutions	Trans. Institute of Metal Finishing 1995, 73 (1) 16	H Matsuda <i>et al</i>
106	Morphological Control of Electroless Plated Ni Anodes: Influence on Fuel Cell Performance	Solid State Ionics 179 (2008) 2042 – 2046	Francesco Dalgrande <i>et al</i>
107	Fabrication and Properties of Anode – Supported Tubular Solid Oxide Fuel Cells	Journal of Power Sources 136 (2004) 66 – 71	Yanhai Du and N M Sammes
108	The Effects of Agitation on Electroless Nickel – Phosphorus – Molybdenum Disulphide Composite Plating	Metal Finishing June 1997 102 – 106	S M Moonir-Vaghefi <i>et al</i>

2. IMPEDANCE APPLICATION NOTES (see attached CD for copies)

Battery Research – impedance

Battery stack – impedance

Coatings adhesion – impedance tech

Corrosion – impedance

Electrochemical cells – impedance

Electrochemical methods – fundamentals and applications 2nd edition

Modulab user guide

Electrochemical impedance spectroscopy primer

Impedance spectroscopy

Impedance spectroscopy, theory, experiment and applications

Impedance spectroscopy of undoped BaTiO₃ ceramics

Modulab pages

Modulab getting started

3. STANDARDS (see attached CD for copies)

1. BS EN ISO 4527 : 2003 Metallic Coatings – Autocatalytic (electroless) nickel – phosphorus alloy coatings – specification and test methods.
2. ASTM B733-97 Standard specification for autocatalytic (electroless) nickel – phosphorus coatings on metal.
3. ASTM B244-97 Standard test method for measurement of thickness of anodic coatings on aluminium and of other nonconductive coatings on nonmagnetic basis metals with eddy-current instruments.
4. ASTM E376-06 Standard practice for measuring coating thickness by magnetic – field or eddy-current (electromagnetic) examination methods.
5. BS EN ISO 6507 : 2005 Metallic materials – Vickers hardness test – Part 1: test method.
6. ASTM B765-03 Standard guide for selection of porosity and gross defect tests for electrodeposits and related metallic coatings.
7. ASTM E156-68 Standard photometric method for determination of phosphorus in high-phosphorus brazing alloys.
8. ASTM E60-80 Standard practice for photometric methods for chemical analysis of metals.
9. ASME PTC 50-2002 Fuel cell power systems performance – Performance test codes.
10. BS EN 62282-3-3 Fuel cell technologies – Stationary fuel cell power systems – Installation
11. BS EN 62282-6-200 Fuel cell technologies – Micro fuel cell power systems – Performance test methods.
12. BS EN 62282-5-1 Fuel cell technologies – Portable fuel cell power systems – Safety.
13. BS EN 62282-3-1 Fuel cell technologies – Stationary fuel cell power systems – Safety
14. BS EN 62282-3-2 Fuel cell technologies – Stationary fuel cell power systems – Performance and test methods.

15. DD IEC TS 62282-1 Fuel cell technologies – Terminology.
16. BS EN 62282-2 Fuel cell technologies – Fuel cell modules.
17. BS EN 50465 Gas appliances. Fuel cell gas heating appliance. Fuel cell gas heating appliance of nominal heat input inferior or equal to 70kW.
18. ANSI Z39-18 Scientific and Technical reports – Elements, organisation and design.
19. MIL-STD-883F Test Method Standard – Microcircuits.
20. BS EN ISO 4287 Geometrical Product Specification – Surface Texture : Profile Method – Terms, Definitions and Surface Texture Parameters.

4. ELECTROLESS PLATING SOLUTION FORMULATIONS.

FAI Electroless Nickel

Nickel acetate	25 g.l ⁻¹
Acetic acid (glacial)	25 ml.l ⁻¹
Sodium hypophosphite	25 g.l ⁻¹
Sodium lactate	20 g.l ⁻¹
Sodium tellurate	0.005 g.l ⁻¹
pH	4-5
Temperature	87-92°C

Alkaline Electroless Nickel

Nickel chloride	30 g.l ⁻¹
Ammonium citrate	47 g.l ⁻¹
Sodium hypophosphite	10 g.l ⁻¹
Citric acid	18 g.l ⁻¹
pH (with ammonia)	8.5-9.5
Temperature	86-92°C
Deposition rate	~2.5µm.hour ⁻¹

Nickel-Boron Electroless Nickel

Nickel chloride	30 g.l ⁻¹
Ammonium hydroxide (0.88sg)	340 ml.l ⁻¹
Sodium borohydride	3.2 g.l ⁻¹
pH	11.6
Temperature	45°C
Deposition rate	0.5µm.hour ⁻¹

Immersion Gold

Potassium gold cyanide	35 g.l ⁻¹
Potassium dihydrogen citrate	10 g.l ⁻¹
EDTA disodium salt	30 g.l ⁻¹
pH (with ammonia)	5.2-5.6

Electroless Copper

Solution A

Copper sulphate	35 g.l ⁻¹
Sodium carbonate (anhydrous)	30 g.l ⁻¹
Rochelle salt	170 g.l ⁻¹
Sodium hydroxide	50 g.l ⁻¹
Sequestrene CS	20 ml.l ⁻¹

Solution B

40% W/V formaldehyde

Mix 5 parts A, 5 parts water and 1 part B

Chromium

Westhouse, process claiming deposition rate 5 μ m.hour⁻¹ on ferrous and non-ferrous metals. Published: Electroplating and metal finishing 1962, 15, No3, 99 deposit contains some phosphorus and also a small amount of nickel which is present in the solution as an activator to initiate the reaction.

Chromium acetate	3pt/wt
Sodium citrate	4
Glycolic acid	4
Sodium hypophosphite	1-3
Sodium acetate	2
Nickel acetate	0.1
Water	84-86
Temperature	100°C
pH	4-6

Palladium

Recommended Rhoda *et al.* Transactions Institute of Metal Finishing 1959, 36, 82

Palladium amine complex	5.4 g.l ⁻¹
Ammonium hydroxide	350 g.l ⁻¹
EDTA disodium salt	33.6 g.l ⁻¹
Hydrazine	0.3 g.l ⁻¹
Temperature	80°C
Deposition rate	5µm.hour ⁻¹

Electroless Cobalt – Tungsten Phosphorus

CoSO ₄ .7H ₂ O	0.082M
Na ₃ C ₅ H ₅ O ₇ .7H ₂ O	0.492M
H ₃ BO ₃	0.502M
NaH ₂ PO ₂ .2H ₂ O	0.169M
Na ₂ WO ₄ .2H ₂ O	0.03M
pH (with KOH)	8.8-9.0
Temperature	85-95°C
Deposition rate	1.51mg.hour ⁻¹ .cm ⁻¹

Ref: Journal of Electrochemical Society, 149(4)C187-C194(2002)

Alkaline Electroless Chrome

Chromic bromide	16 g.l ⁻¹
Chromic iodate	1 g.l ⁻¹
Sodium citrate	10 g.l ⁻¹
Sodium hypophosphite	10 g.l ⁻¹
Sodium oxalate	9 g.l ⁻¹
pH	8-10
Temperature	75-90°C
Rate of deposition	0.3mil.hour ⁻¹

Electroless Cobalt

Cobalt chloride	30 g.l ⁻¹
Sodium hypophosphite	20 g.l ⁻¹
Sodium citrate	35 g.l ⁻¹
Ammonium chloride	50 g.l ⁻¹
pH	9.5
Temperature	95°C

Electroless Chromium

Cr ₂ (SO ₄) ₃ .6H ₂ O	0.1M
NaH ₂ PO ₂ .H ₂ O	0.1M
K CNS	0.1-0.2M
NaCl	10 g.l ⁻¹
H ₃ BO ₃	20 g.l ⁻¹
Na NO ₂	5mM
Temperature	50°C
pH	3.0

Alkaline Electroless Nickel

Nickel Sulphate	30 g.l ⁻¹
Sodium Hypophosphite	30 g.l ⁻¹
Sodium Pyrophosphate	60 g.l ⁻¹
Triethanolamine	100 ml.l ⁻¹
pH	10.0
Temperature	30 -35°C

Sodium Borohydride Reduced Electroless Nickel

Nickel Chloride	31 g.l ⁻¹
Sodium Hydroxide	42 g.l ⁻¹
Ethylenediamine, 98%	52 g.l ⁻¹
Sodium Borohydride	1.2 g.l ⁻¹
Thallium Nitrate	0.022 g.l ⁻¹
pH	>13
Temperature	93 – 95°C

Low Phosphorus Electroless Nickel (Crystalline Deposit)

Nickel Sulphate Hexahydrate	50 g.l ⁻¹
Sodium Hypophosphite	100 g.l ⁻¹
Tetrasodium Pyrophosphate	100 g.l ⁻¹
Ammonium Hydroxide (38%)	45 ml.l ⁻¹
Temperature	64 – 66°C
Plating Rate	15 – 17 µm.hour ⁻¹
Nickel Content	96.66% wt
Phosphorus Content	3.34% wt
pH	10

Medium Phosphorus Electroless Nickel (Microcrystalline Deposit)

Nickel Sulphate Hexahydrate	21.2 g.l ⁻¹
Sodium Hypophosphite	12 g.l ⁻¹
Lactic Acid	28 ml.l ⁻¹
Propionic Acid	2.2 ml.l ⁻¹
Thiourea	0.8 ppm
Temperature	89 – 91°C
pH	4.5
Plating Rate	18 – 20 µm.hour ⁻¹
Nickel Content	93.3% wt
Phosphorus Content	6.70% wt

High Phosphorus Electroless Nickel (Amorphous Deposit)

Nickel Sulphate Hexahydrate	21.2 g.l ⁻¹
Sodium Hypophosphite	24 g.l ⁻¹
Lactic Acid	28 ml.l ⁻¹
Propionic Acid	2.2 ml.l ⁻¹
Thiourea	0.8 ppm
Temperature	89 – 91°C
pH	4.5
Plating Rate	24 – 26 µm.hour ⁻¹
Nickel Content	86.7% wt
Phosphorus Content	13.3% wt

Electroless Gold

Gold Hydrochloride Trihydrate	0.01 M
Sodium Potassium Tartrate	0.014 M
Dimethylamine Borane	0.013 M
Sodium Cyanide	400 mg.l ⁻¹
pH (adjusted with NaOH)	13.0
Temperature	60°C

Electroless Palladium

Palladium Chloride	10 g.l ⁻¹
Rochelle Salt	19 g.l ⁻¹
Ethylenediamine	25.6 g.l ⁻¹
Cool Solution to 20°C, then Add:	
Sodium Hypophosphite	4.1 g.l ⁻¹
pH (adjusted with HCl)	8.5
Temperature	68 – 73°C

Nickel – Rhenium – Phosphorus

Potassium Rhenium Oxide (KReO ₄)	0.0075 M
Nickel Sulphate 6 H ₂ O	0.1 M
Sodium Hypophosphite	0.2 M
Succinic Acid (C ₄ H ₆ O ₄)	0.2 M
Sodium Succinate	0.2 M
pH (adjusted with ammonia)	4.51
Temperature	90 – 95°C
Deposit Mass % Ni 82 : Re 11 : P7	
Deposit Atomic % Ni 83.5 : Re 3.5 : P13	

Nickel – Boron Electroless Nickel

Nickel Sulphate	25 g.l ⁻¹
Sodium Acetate	15 g.l ⁻¹
DMAB	4 g.l ⁻¹
Lead Acetate	0.002 g.l ⁻¹
pH	5.9
Temperature	65 – 77°C

The deposit typically contains 0.1 – 4.0% boron by weight depending on the bath composition which can be varied. DMAB (n – dimethylamine borane) is used as a reducing agent and the deposits have a melting temperature of 1350°C.

5. ETCHING SOLUTION FORMULATIONS

Solution 1	Hydrofluoric acid	20ml.l ⁻¹	
	Sodium fluoride	2 g.l ⁻¹	
Solution 2	Ammonium fluoride	4 parts	30-60 secs
	Hydrofluoric acid	1 part	
	Glycerine	2 parts	
Solution 3	Hydrofluoric acid	1 part	
	Ammonium fluoride	5 parts	
Solution 4	Hydrofluoric acid	100ml.l ⁻¹	15 min
	Sulphuric acid	100ml.l ⁻¹	
Solution 5	Sodium fluoride	6 g.l ⁻¹	10 – 20 mins @ room temp
	Hydrofluoric acid	100 ml.l ⁻¹	

6. ELECTRICAL RESISTANCE RESULTS

I = 50mA	Temperature °C	Resistivity ρ (x 10 ⁻⁴ Ω .cm)	Conductivity σ (x 10 ⁴ S. cm ⁻¹)
	23	3.76	0.266
	30	3.89	0.257
	45	4.121	0.243
	50	4.238	0.236
	75	4.823	0.207
	100	5.174	0.193
	125	5.304	0.188
	140	5.538	0.18
	150	5.655	0.179
	160	5.772	0.173
	170	6.006	0.166
	180	6.123	0.163
	190	6.24	0.16
	200	6.357	0.157
	210	6.474	0.154
	220	6.591	0.152
	230	6.591	0.152
	240	6.708	0.149
	250	6.708	0.149
	260	6.591	0.152
	270	6.591	0.152
	280	6.708	0.149
	290	6.825	0.146
	300	6.942	0.144
	310	7.059	0.141
	330	7.306	0.137
	340	7.41	0.135
	350	7.54	0.133
	360	7.66	0.13
	380	7.891	0.127
	400	8.242	0.121
	420	8.476	0.118
	440	8.71	0.115
	450	8.827	0.113
	460	9.074	0.11
	470	9.191	0.109
	480	9.256	0.108
	500	9.66	0.103
	520	9.89	0.101
	540	10.24	0.0976

560	10.478	0.0954
595	11.06	0.09
615	11.43	0.0875
625	11.54	0.0866
635	11.79	0.0849
645	11.895	0.084
660	12.13	0.0824
680	12.48	0.08
695	12.714	0.079
700	12.831	0.078
710	12.961	0.077
720	13.065	0.076
740	13.65	0.0732
760	14.04	0.0712
780	14.482	0.069
800	14.84	0.0673

Table 14 – Initial electrical property results on samples heated to 850°C

7. TECHNICAL DATA SHEETS

01810-PE Alumenate process sequence

18810-PE Electroless nickel Slotonip 1850

18812-PE Electroless nickel Slotonip 1860 high phosphorus

18821-PE Electroless nickel Slotonip 2010

Alumina TDS

Ceria based electrolytes

CeSZ 14% C.o.C.

Chromium TDS

Cobalt TDS

Coors ceramics properties

DIL 402C e 1106

Fuel cell handbook 7

Fuel cell directory – ninth edition

Melting and boiling points of the elements

Melting points periodic table

Molybdenum TDS

Nickel TDS

Palladium TDS

Platinum TDS

Rhodium TDS

Ruthenium TDS

Slotonip C.o.C.

Tungsten TDS

Unitec Ceramics TDS

Unitec zirconia 001

Unitec zirconia 002

Unitec zirconia 003

Vanadium TDS

YSZ 8% C.o.C.

YSZ TDS

Zirconia based electrolytes

8. CONVERSION FACTORS

Common Conversion Factors

Quantity	SI Unit	Other Unit	Conversion Factor
Energy	joule	calorie erg	1 cal = 4.184 J 1 erg = 10^{-7} J
Force	newton	dyne	1 dyn = 10^{-5} N
Length	metre	ångström	1 Å = 10^{-10} m = 10^{-8} cm = 10^{-1} nm
Mass	kilogram	pound	1 lb = 0.453592 kg
Pressure	pascal	bar atmosphere mm Hg lb/in ²	1 bar = 10^5 Pa 1 atm = 1.01325×10^5 Pa 1 mm Hg = 133.322 Pa 1 lb/in ² = 6894.8 Pa
Temperature	kelvin	Celsius Fahrenheit	1°C = 1 K 1°F = 5/9 K
Volume	cubic metre	litre gallon (U.S.) gallon (U.K.) cubic inch	1 L = 1 dm ³ = 10^{-3} m ³ 1 gal (U.S.) = 3.7854×10^{-3} m ³ 1 gal (U.K.) = 4.5641×10^{-3} m ³ 1 in ³ = 1.6387×10^{-6} m ³

$$5\mu\text{m} = 0.03937 \times 5 = 1.9685 \text{ Mil}$$

$$25.4\mu\text{m} = 1 \text{ thousandth of an inch}$$

9. SI UNITS

SI Unit Prefixes

Factors	Prefix	Symbol
10^{12}	tera	T
10^9	giga	G
10^6	mega	M
10^3	kilo	k
10^2	hecto	h
10^1	deca	da
10^{-1}	deci	d
10^{-2}	centi	c
10^{-3}	milli	m
10^{-6}	micro	μ
10^{-9}	nano	n
10^{-12}	pico	p
10^{-15}	femto	f
10^{-18}	atto	a

Parameter	Units
Power density	mW.cm^{-2}
Current density	A.cm^{-2}
Electrical resistivity	$\Omega.\text{cm}$
Electrical conductivity	S.cm^{-1}
Deposition rate	$\mu\text{m.hour}^{-1}$
Concentration, grams per litre	g.l^{-1}
Gas flow, litres per hour	l.hour^{-1}
Density, weight to volume	g.cm^{-3}
Coefficient of thermal expansion	$\mu\text{m.}^\circ\text{C}^{-1}$

APPENDIX D

1. COPY OF PATENT – WO 2009/044144
2. PATENT SEARCH RESULTS
3. PUBLISHED PAPERS
4. TURIN POSTER PRESENTATION AND INFORMATION
5. DAYTONA 2009 CONFERENCE INFORMATION
6. ELECTROCHEMICAL IMPEDANCE SPECTROSCOPY COURSE
7. OTHER CONFERENCES ATTENDED
8. MARKETING INFORMATION

1. Copy of patent - WO 2009/044144

ALL DOCUMENTS IN ATTACHED CD

2. Patent Search Results

Searching 1976 to present...

Results of Search in 1976 to present db for:

((nickel AND YSZ) AND composite) AND electroless): 8 patents.

Hits 1 through 8 out of 8

Jump To

Refine Search

nickel and YSZ and composite and electroless

PAT. NO.	Title
1 6,969,565	Solid oxide fuel cell stack and method of manufacturing the same
2 6,936,367	Solid oxide fuel cell system
3 6,893,762	Metal-supported tubular micro-fuel cell
4 6,824,907	Tubular solid oxide fuel cell stack
5 6,750,169	Composite electrodes for solid state devices
6 6,692,855	Solid electrolyte type fuel cell and method of producing the same
7 6,420,064	Composite electrodes for solid state devices
8 6,326,096	Solid oxide fuel cell interconnector

RESULT LIST

6 results found in the worldwide database for:
YSZ nickel SOFC in the title or abstract
 (Results are sorted by date of upload in database)

- 1 Method and apparatus for electrostatic spray deposition for a solid oxide fuel cell**
 Inventor: SFLMAN JAR R (US); NONURA HIROSHI (JP), Applicant: (-1)
 EC: B05B5/025; H01M8/12/20H IPC: B05B5/025; H01M8/12; B05B5/025 (+4)
 Publication info: US2005095369 - 2005-05-11
- 2 MANUFACTURE OF NiO AND/OR Ni/YSZ COMPOSITE POWDER AND MANUFACTURE OF SOLID ELECTROLYTE FUEL CELL USING THEREOF**
 Inventor: HYOJU KOJI; HOSHIYAMA HARUO; (+1) Applicant: TOYO LTD
 EC: IPC: H01M4/86; H01M4/88; H01M8/12 (-6)
 Publication info: JP2000353530 - 2000-12-09
- 3 ELECTROCHEMICAL CELL**
 Inventor: FRIEDRICH SOPREN (DK); BAGGER CARSTEN (DK); (+3) Applicant: RISOE FORSKNINGSCENTER (DK); PRINDAL SOREN (DK); (+4)
 EC: H01M4/120264 IPC: H01M8/12; H01M8/12; (IPC1-7): H01M4/86 (-1)
 Publication info: WO0030194 - 2000-05-25
- 4 MANUFACTURE OF SOLID ELECTROLYTE FUEL CELL**
 Inventor: NAGATA MASAKATSU; OHNO MUKIYUKI; (+2) Applicant: FUJIKURA LTD
 EC: IPC: H01M4/86; H01M4/88; H01M8/02 (-10)
 Publication info: JP9274922 - 1997-10-21
- 5 FUEL ELECTRODE FABRICATION METHOD FOR FUEL CELL WITH SOLID ELECTROLYTE**
 Inventor: MATSUIEMA TOSIHO; NAKOHO SAO; (+1) Applicant: NIPPON TELEGRAPH & TELEPHONE
 EC: IPC: H01M4/86; H01M4/88; (IPC1-7): H01M4/88
 Publication info: JP6089729 - 1994-03-29
- 6 FUEL ELECTRODE MATERIAL**
 Inventor: SAWADA AKIHIRO Applicant: MITSUBISHI HEAVY IND LTD
 EC: H01M8/120264 IPC: H01M8/12; H01M8/12; (IPC1-7): H01M4/86 (+2)
 Publication info: JP7029574 - 1995-01-31

Data supplied from the esp@cenet database - Worldwide

Inventor: FISHIRUNA YUICHI, YASUDA ISAMU (+2) Applicant: TOKYO GAS CO LTD
EC: IPC: H01M8/02; H01M8/02; (IPC1-7): H01M8/02
Publication Info: JP11016585 - 1999-01-22

Data supplied from the esp@cenet database - Worldwide

RESULT LIST

14 results found in the Worldwide database for:
YSZ, nickel, composite in the title or abstract
(Results are sorted by date of upload in database)

- 11 PRODUCTION OF NICKEL MONO-OXIDE-YTTRIA STABILIZED ZIRCONIA COMPOSITE POWDER**
Inventor: KAGAYAMA HIROYUKI, AIZAWA MASANOBU Applicant: TOYO LTD
EC: IPC: C01G25/00; C04B35/46; C04B35/495 (+0)
Publication Info: JP8059347 - 1996-03-05
- 12 METHOD FOR FORMING FUEL ELECTRODE OF SOLID ELECTROLYTE TYPE FUEL CELL**
Inventor: KAWASHIMA TAKESHI Applicant: TOKYO GAS CO LTD
EC: IPC: H01M4/88; H01M8/02; H01M8/12 (-0)
Publication Info: JP5069883 - 1993-04-20
- 13 FUEL ELECTRODE MATERIAL**
Inventor: SAWADA AKIHIRU Applicant: MITSUBISHI HEAVY IND LTD
EC: H01M8/12B1 IPC: H01M8/12; H01M8/12; (IPC1-7): H01M4/86 (12)
Publication Info: JP7029574 - 1995-01-31
- 14 SOLID ELECTROLYTE FUEL CELL**
Inventor: MARUMOTO KENICHI, AYA A, SUGI I Applicant: MITSUBISHI ELECTRIC CORP
EC: H01M8/12B IPC: H01M8/12; H01M8/12; (IPC1-7): H01M8/02 (11)
Publication Info: JP3283267 - 1991-12-11

Data supplied from the esp@cenet database - Worldwide

RESULT LIST

2 results found in the Worldwide database for:
YSZ, ruthenium, composite in the title or abstract
(Results are sorted by date of upload in database)

- 1 Precious metal catalysts for emissions.**
Inventor: GANGULI PARTHA S DR (US), SUNDARESAN SANKARAN (US) Applicant: PCP CONSULTING AND RESEARCH IN (US)
EC: B01D53/94K20; B01J23/10; (+2) IPC: B01D53/94; B01J23/10; B01J23/46 (16)
Publication Info: EP0637461 - 1994-02-08
- 2 Precious metal catalysts utilizing composites of oxygen-ion conducting and inert support materials**
Inventor: GANGULI PARTHA S (US); SUNDARESAN SANKARAN (US) Applicant: PCP CONSULTING AND RESEARCH IN (US)
EC: B01D53/94K20; B01J23/10; (+2) IPC: B01D53/94; B01J23/10; B01J23/46 (-1)
Publication Info: US5275997 - 1994-01-04

Data supplied from the esp@cenet database - Worldwide

3. Published Papers

See reference 94 in references section.

4. Turin conference poster information.

ALL DOCUMENTS IN ATTACHED CD

5. Daytona 2009 conference and information.

ALL DOCUMENTS IN ATTACHED CD

6. Electrochemical Impedance Spectroscopy Course

ALL DOCUMENTS IN ATTACHED CD

7. Other conferences attended (see attached CD)

Hydrogen and Fuel cells agenda

Supergen 2007

8. Marketing information (see attached CD)

1. Frost and Sullivan - North American portable fuel cell market 007
2. UK Universities Research KTN
3. US National Laboratory Research
4. Supergen
5. SOFC Review by Nigel Brandon
6. Kilner UK Research Report
7. An Industry Perspective